

# The Messenger



No. 145 – September 2011

Studies for a massively-multiplexed spectrograph  
Spectroscopy of Pluto and Triton  
VISTA survey of Orion Belt region  
VLT FLAMES Tarantula Survey



# TRAPPIST: TRAnsiting Planets and Planetesimals Small Telescope

Emmanuël Jehin<sup>1</sup>  
 Michaël Gillon<sup>1</sup>  
 Didier Queloz<sup>2</sup>  
 Pierre Magain<sup>1</sup>  
 Jean Manfroid<sup>1</sup>  
 Virginie Chantry<sup>1</sup>  
 Monica Lendl<sup>2</sup>  
 Damien Hutsemékers<sup>1</sup>  
 Stéphane Udry<sup>2</sup>

<sup>1</sup> Institut d'Astrophysique de l'Université de Liège, Belgium

<sup>2</sup> Observatoire de l'Université de Genève, Switzerland

TRAPPIST is a 60-cm robotic telescope that was installed in April 2010 at the ESO La Silla Observatory. The project is led by the Astrophysics and Image Processing group (AIP) at the Department of Astrophysics, Geophysics and Oceanography (AGO) of the University of Liège, in close collaboration with the Geneva Observatory, and has been funded by the Belgian Fund for Scientific Research (F.R.S.-FNRS) and the Swiss National Science Foundation (SNF). It is devoted to the detection and characterisation of exoplanets and to the study of comets and other small bodies in the Solar System. We describe here the goals of the project and the hardware and present some results obtained during the first six months of operation.

## The science case

The hundreds of exoplanets known today allow us to place our own Solar System in the broad context of our own Galaxy. In particular, the subset of known exoplanets that transit their parent stars are key objects for our understanding of the formation, evolution and properties of planetary systems. The objects of the Solar System are, and will remain, exquisite guides for helping us understand the mechanisms of planetary formation and evolution. Comets, in particular, are most probably remnants of the initial population of planetesimals of the outer part of the protoplanetary disc. Therefore the study of their physical and chemical properties allows the conditions that prevailed during the formation of the four giant planets to be probed.



Figure 1. The TRAPPIST telescope in its 5-metre enclosure at the La Silla Observatory, Chile.

TRAPPIST is an original project using a single telescope that has been built and optimised to allow the study of those two aspects of the growing field of astrobiology. It provides high quality photometric data of exoplanet transits and allows the gaseous emissions of bright comets to be monitored regularly. The project is centred on three main goals: (1) the detection of the transits of new exoplanets; (2) the characterisation of known transiting planets, in particular the precise determination of their size; and (3) the survey of the chemical composition of bright comets and the evolution of their activity during their orbit.

## A dedicated robotic telescope

The basic project concept is a robotic telescope fully dedicated to high precision exoplanet and comet time-series photometry, providing the large amount of observing time requested for those research projects. Exoplanet transits typically last several hours, up to a full night. There are now many known transiting planets, and many more candidates found by transit surveys which need to be confirmed and characterised. Moreover these targets need to be observed at very specific times, during eclipses, putting even more constraints on telescope availability. Similarly a lot of observing

time is obviously needed to monitor the activity of several comets with a frequency of a few times per week. Some comets are known, but others appear serendipitously. For the latter, telescope availability is crucial if we want to react rapidly to observe those targets at the appropriate moment and for several hours or nights in a row; this strategy can provide unique datasets impossible to obtain otherwise.

## Telescope and instrumentation

For low cost operations and high flexibility, TRAPPIST (see Figure 1) had to be a robotic observatory. The observation programme, including the calibration plan, is prepared in advance and submitted daily to a specific software installed on the computer controlling the observatory. This computer controls all the technical aspects of the observations: dome control, pointing, focusing, image acquisition, astrometry and software guiding, calibrations, data storage... It is in sleep mode during daytime and wakes up one hour before sunset, opening the dome and starting to cool the CCD. This process is made possible thanks to a collection of computer programs working together and interacting with the telescope, dome, CCD camera, filter wheels and meteorological station. Such a complete and rapid integration, using mostly off-the-shelf solutions, would have been impossible a few years ago and



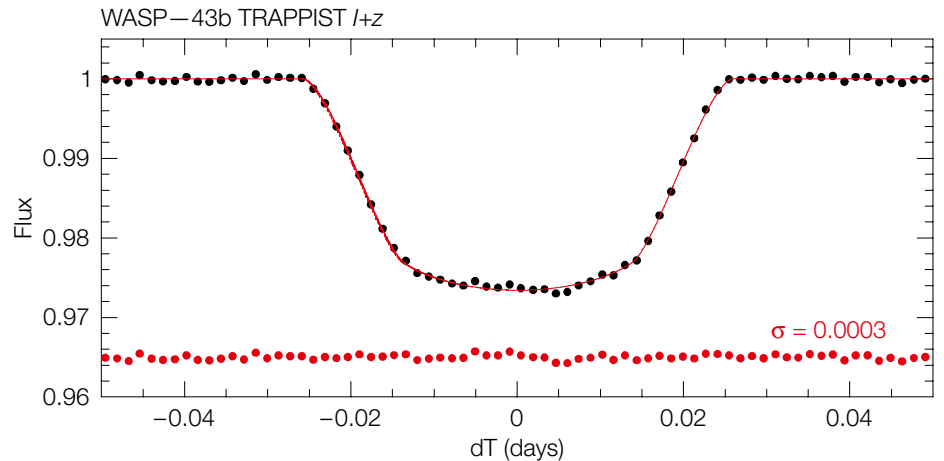
Figure 2. Close-up of the 60-cm TRAPPIST telescope.

allowed us to set up the experiment in less than two years.

The observatory is controlled through a VPN (Virtual Private Network) connection between La Silla and Liège University. The telescope and each individual sub-system can be used from anywhere in the world, provided an internet connection is available. In case of a low-level mechanical failure, we can count on the help of the Swiss technician on site or the La Silla staff.

Hundreds of images, amounting to 2–15 GB, are produced every night. Reduction pipelines run on a dedicated computer installed in the control room. For the exoplanet programme, only tables and plots with the final results are transferred to Liège, while for the comet programme, it is often necessary to transfer dozens of frames in order to perform more interactive tasks on the images. Every third month, a backup disk is sent to Belgium and transferred to the archive machine.

The telescope is a 60-cm f/8 Ritchey–Chrétien design built by the German ASTELCO company (see Figure 2). Owing to its open design with carbon fibre and



aluminium components, it weighs only 65 kg and was allied to a compact German equatorial mount, the New Technology Mount NTM-500, from the same company. This robust mount uses direct drive technology to avoid the well-known periodic errors found on the usual equatorial mounts for small telescopes and therefore permits accurate pointing and tracking. The accuracy of the tracking allows an exposure time of four minutes maximum, which is usually enough for our bright targets. Each frame is calibrated in right ascension and declination and software guiding runs continuously to keep the target centred on the same few pixels for the whole exposure sequence.

The CCD camera was built by Finger Lakes Instrumentation, with thermoelectric cooling and a CCD of the latest generation. This is a thinned broadband backside-illuminated Fairchild chip with  $2048 \times 2048$  15- $\mu\text{m}$  pixels providing a field of view of 22 by 22 arcminutes and a plate scale of 0.6 arcseconds per pixel. The sensitivity is excellent over all the spectral range, with a peak of 98% at 750 nm, declining to around 80% at 550 nm and 60% at 300 nm. It is optimised for low fringe level in the far red and achieves a sensitivity of 40% at 950 nm. The gain is set to 1.1  $e^-/\text{ADU}$ . There are three different readout modes: a low noise readout mode (readout noise [RON] 9.7  $e^-$  in 8s), a fast mode (RON 14  $e^-$  in 4s) and a very fast readout of 2s using two quadrants. The cooling is  $-55$  deg below ambient, usual operation being at  $-35$   $^\circ\text{C}$  with a dark count of 0.11  $e^-/\text{s}/\text{pixel}$ . Typical magnitudes reached in 20s with a  $2 \times 2$  binning

Figure 3. TRAPPIST *I + z* transit photometry of the planet WASP-43b, period-folded and binned per two minute intervals, with the best-fit transit model superimposed. The residuals of the fit, shifted along the *y*-axis for the sake of clarity, are shown below and their standard deviation is 300 parts per million (ppm). This light curve results from the global analysis of 20 transits observed by TRAPPIST for this exoplanet.

(1.3 arcseconds per pixel) and a 10% accuracy are *B*-band 16.2, *V*-band 16.4, *Rc*-band 16.4, *Ic*-band 15.5 and *I + z*-band 15.6; and in 200 seconds, *B*-band 19.7, *V*-band 19.4, *Rc*-band 19.2 and *Ic*-band 18.1.

The camera is fitted with a double filter wheel specifically designed for the project and allowing a total of 12 different  $5 \times 5$  cm filters and one clear position. One filter wheel is loaded with six broadband filters (Johnson-Cousins BVRclc, Sloan *z'*, and a special *I + z* filter for exoplanet transits) and the other filter wheel is loaded with six narrowband filters for the comet programme. The comet filters were designed by NASA for the international Hale–Bopp campaign (Farnham et al., 2000). Four filters isolating the main molecular emission lines present in cometary spectra (OH [310 nm], CN [385 nm],  $\text{C}_3$  [405 nm],  $\text{C}_2 + \text{NH}_2$  [515 nm]) are permanently mounted, while the two other filters of the set ( $\text{CO}^+$  [427 nm] and  $\text{H}_2\text{O}^+$  [705 nm]) are also available. In addition two narrowband filters, isolating “continuum windows” (BC [445 nm] and GC [525 nm]) for the estimation of the solar spectrum reflected by the dust of the comet, are mounted.

### Installation, first light and start of operations

The telescope was installed in April 2010 in the T70 Swiss telescope building belonging to Geneva University (Figure 1). This facility had not been used since the 1990s and was completely refurbished in early 2010. The old 5-metre dome (AshDome) was equipped with new azimuth motors and computer control. A Boltwood II meteorological station with a cloud sensor and an independent rain sensor was installed on the roof to record the weather conditions in real time. In case of bad conditions (clouds, strong wind, risk of condensation, rain or snow), the dome is automatically closed and the observations interrupted to guarantee the integrity of the telescope and equipment. An uninterruptible power supply (UPS) keeps the observatory running for 45 minutes during an electrical power cut and an emergency shutdown is triggered at the end of this period. Several webcams inside and outside the building help us to check what is going on in the observatory if needed. After two months of commissioning on site, TRAPPIST “first light” took place remotely on 8 June 2010, together with a press conference at Liège University<sup>1</sup>. Technical tests, fine tuning of the software as well as the first scientific observations were performed in remote control mode until November 2010. The fully robotic operation then started smoothly in December with several months of superb weather until the start of the winter.

The two scientific aspects of this dedicated telescope and the first results are described below.

### Survey of transiting exoplanets

The transit method used by TRAPPIST is an indirect technique, based on the measurement of the apparent brightness of a star. If a planet passes in front of the star, there is a slight observable decline in the apparent luminosity, as the planet eclipses a small fraction of the stellar disc. Recording this periodic event allows the radius of the planet to be measured. Combined with the radial velocity method, the transit method provides the mass and density of the planet,

allowing us to constrain its bulk composition. Furthermore, the special geometry of the orbit makes the study of important properties of the planet (e.g., atmospheric composition, orbital obliquity, etc) possible without the challenge of having to spatially resolve it from its host star. Transiting planets are thus key objects for our understanding of the vast planetary population hosted by the Galaxy.

Discovery of more transiting planets is important to assess the diversity of planetary systems, to constrain their formation and the dependence of planetary properties on external conditions (orbit, host star, other planets, etc.). TRAPPIST is participating in this effort through several different projects.

### Detection of new transiting planets

On account of its extended temporal availability and high photometric precision, TRAPPIST has very quickly become an important element for the transit surveys WASP<sup>2</sup> and CoRoT<sup>3</sup>. It is used to confirm the candidate transits detected by these surveys and to observe them with better time resolution and precision to discriminate eclipsing binaries from planetary transits. TRAPPIST observations have so far rejected more than 30 WASP candidates as being eclipsing binaries. It has confirmed, and thus co-discovered, ten new transiting planets (e.g., Triaud et al., 2011; Csizmadia et al., 2011; Gillon et al., 2011).

The search for transits of the planets detected by the radial velocity (RV) technique is another important science driver for TRAPPIST. RV surveys monitor stars significantly brighter than the transit surveys. The few RV planets that were revealed afterwards to be transiting, have brought improved knowledge of exoplanet properties because a thorough characterisation is possible (e.g., Deming & Seager, 2009). These planets thus play a major role in exoplanetology. In this context, TRAPPIST is used to search for the possible transits of the planets detected by the HARPS (Mayor et al., 2003) and CORALIE (Queloz et al., 2000) Doppler surveys. For the late M-dwarfs observed by HARPS, TRAPPIST is even able to detect the transit of a massive rocky planet.

### Characterisation of known transiting planets

Once a transiting planet is detected, it is of course desirable to characterise it thoroughly with high precision follow-up measurements. Assuming a sufficient precision, a transit light curve allows a number of parameters to be thoroughly constrained: (i) the planet-to-star radius ratio; (ii) the orbital inclination; (iii) the stellar limb-darkening coefficients; and (iv) the stellar density (assuming the orbital period is known). This last quantity can be used with other measured stellar quantities to deduce, via stellar modelling, the mass of the star, which leads finally to the stellar and planet radii (Gillon et al., 2007; 2009). So far, we have gathered many high precision light curves for two dozen transiting planets. These data will not only allow us to improve our knowledge of these planets (size, structure), but also to search for transit timing variations that could reveal the presence of other planets in the system. Since TRAPPIST is dedicated to this research project, it can monitor dozens of transits of the same planet, leading to an exquisite global precision, as shown in Figure 3.

### Transit search around ultra-cool dwarf stars (UCDs)

We have selected a sample of ten relatively bright late-M stars and brown dwarfs. For each of them, we have started an intense monitoring campaign (several full nights) to search for the transits of the ultra-short period (less than one day) terrestrial planets that are expected by some planetary formation theories. The photometric variability of these UCDs brings a lot of information on their atmospheric and magnetic properties, and the by product of this TRAPPIST project will thus be a significant contribution to the understanding of these fascinating UCDs that dominate the Galactic stellar population.

### Survey of the chemical composition of comets

TRAPPIST is the only telescope in the southern hemisphere equipped with the instrumentation to detect gaseous comet emissions on a daily basis. As recently outlined during a NASA work-

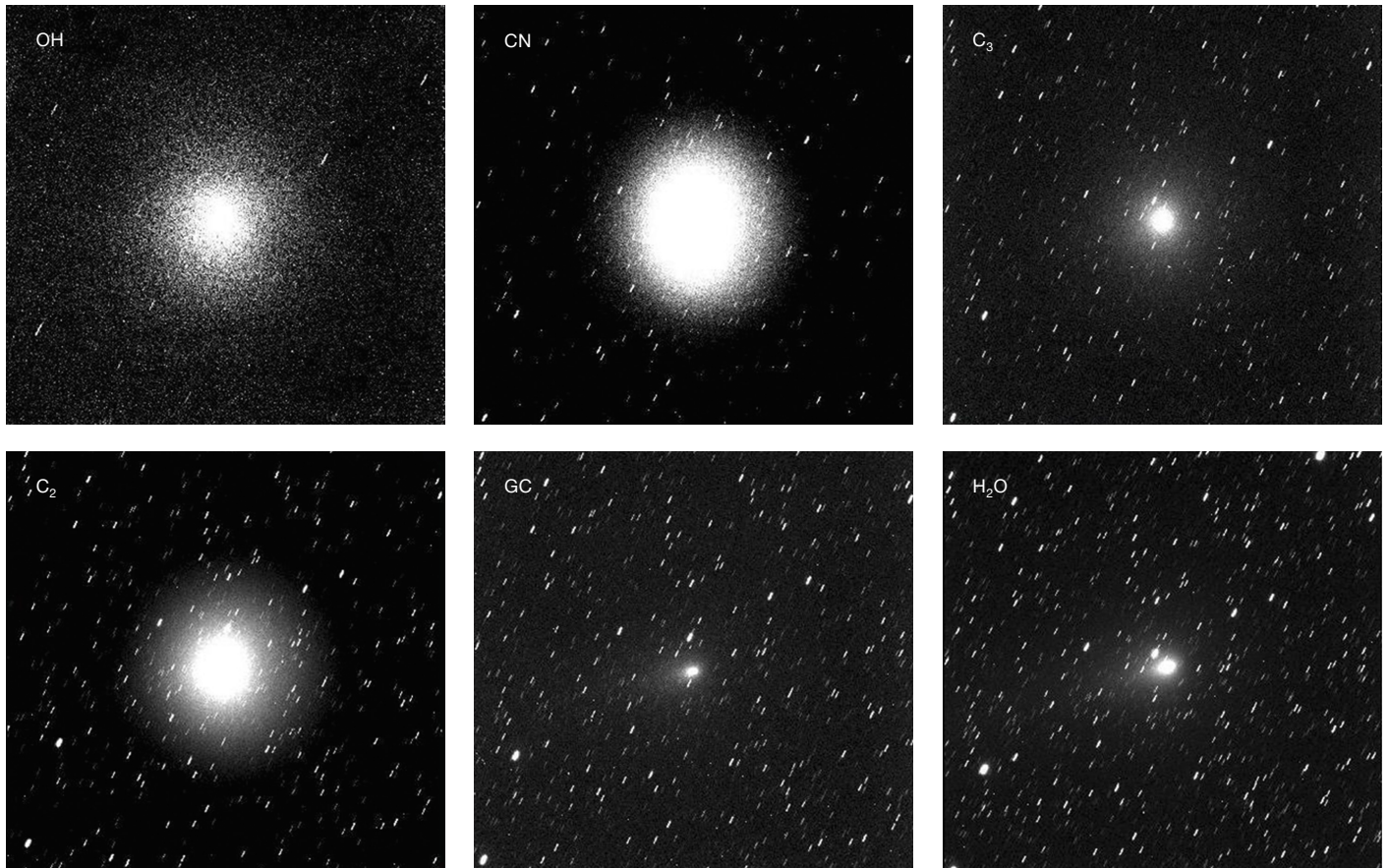


Figure 4. Comet 103P/Hartley 2 imaged with TRAPPIST through the different cometary filters on 5 November 2010: OH, CN, C<sub>3</sub>, C<sub>2</sub>, green continuum (GC) and H<sub>2</sub>O\*. Note the different shapes and intensities of the cometary coma in each filter.

shop<sup>4</sup>, the huge amount of data collected by TRAPPIST will bring crucial new information on comets and will rapidly increase statistics, allowing comets to be classified on the basis of their chemical composition. Linking those chemical classes to dynamical types (for instance short period comets of the Jupiter family and new long period comets from the Oort Cloud) is a fundamental step in understanding the formation of comets and the Solar System.

For relatively bright comets ( $V \leq 12$  mag), about twice a week, we measure gaseous production rates and the spatial distribution of several molecular species, including OH, CN, C<sub>2</sub>, and C<sub>3</sub> (see Figure 4 for an example). In addition to providing the production rates of the different species through a proper photometric

calibration, image analysis can reveal coma features (jets, fans, tails), that could lead to the detection of active regions and determination of the rotation period of the nucleus. Such regular measurements are rare because of the lack of telescope time on larger telescopes, yet are very valuable as they show how the gas production rate of each species evolves with respect to the distance to the Sun. These observations will allow the composition of the comets and the chemical class to which they belong (rich or poor in carbon chain elements for instance) to be determined, possibly revealing the origin of those classes. Indeed with about five to ten bright comets observed each year, this programme will provide a good statistical sample after a few years.

Broadband photometry is also performed once a week for fainter comets, usually far from the Sun, in order to measure the dust production rate from the *R*-band, to catch outbursts and find interesting targets for the main programme. Owing to the way the telescope is operated, the

follow-up of split comets and of special outburst events is possible very shortly after an alert is given and can thus provide important information on the nature of comets. Light curves from these data are useful to assess the gas and dust activity of a given comet in order, for instance, to prepare more detailed observations with larger telescopes, especially the southern ESO telescopes. Hundreds of photometric and astrometric measurements of all the moving targets in our frames are reported each month to the IAU Minor Planet Center. Two new asteroids were found during a laboratory session with students of Liège University. The observatory code attributed by the IAU is I40.

Our first target was periodic comet 103P/Hartley 2, which made a close approach to Earth in October 2010 and was observed in great detail during the NASA EPOXI spacecraft flyby on 4 November. We monitored this small (2 km) but very active comet roughly every other night for four months and collected ~ 4000 frames

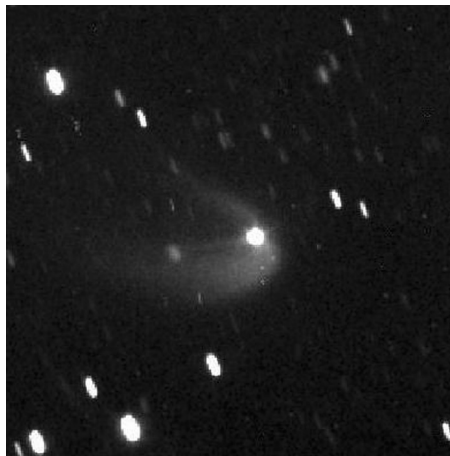


Figure 5. The TRAPPIST image of the activated asteroid (596) Scheila taken on 18 December 2010.

through ten different filters. Our contribution to the worldwide campaign on this comet was recently published in Meech et al. (2011). The quality of the data allowed us to observe periodic variations in the gaseous flux of the different species from which we could determine the rotation of the nucleus and show that the rotation was slowing down by about one hour in 100 days (Jehin et al., 2010). This behaviour had never been so clearly observed before. The long-term monitoring of the production rates of the different species is nearly completed and will be combined with high-resolution spectroscopic data in the visible and infrared that we obtained at the ESO Very Large Telescope (VLT) to provide a clear picture of the chemical composition of this unusually active comet from the Jupiter family.

On account of the fast reaction time (a few hours), TRAPPIST is an invaluable instrument for catching rare and short-term events. As an example, the night after the announcement that asteroid (596) Scheila was behaving like a comet and could be a new Main Belt comet (only five of them are known — Hsieh & Jewitt, 2006), we began a programme to monitor the expanding coma and the brightness of the nucleus every night during a period of three weeks (see Figure 5 for one of the images). From imaging with TRAPPIST and spectroscopy with the ESO VLT we concluded that this behaviour was the result of a collision with a smaller asteroid in the Main

Asteroid Belt and not the result of cometary activity (Jehin et al., 2010).

Among other related projects we joined an international collaboration whose goal is to catch rare stellar occultations by large trans-Neptunian objects (TNOs). This technique provides the most accurate measurements of the diameter of these very remote and poorly constrained icy bodies (provided at least two chords are observed). About one to two events per month are expected for a dozen big TNOs. On 6 November 2010, a unique observation was performed. A faint star was occulted by the dwarf planet Eris for 29 seconds. Eris is the most distant object known in the Solar System by far (three times the distance of Pluto) and supposedly the biggest TNO — it was even named the tenth planet for a few months in 2006. This was the third positive occultation by a TNO ever recorded and it allowed a very accurate radius for Eris (to a few kilometres) to be derived, providing a huge improvement in the determination of its size (previously known to within about 400 km). The surprise was to discover that Eris is a twin of Pluto and that it is not much bigger — remember that Pluto was demoted as a planet in 2006 because Eris was found to be bigger — both then received the new status of dwarf planets! A paper describing these results has been accepted for publication in *Nature* (Sicardy et al., 2011).

### Perspectives

After only six months of robotic operations, TRAPPIST is already recognised in the exoplanet and comet communities as a unique tool on account of, among other things, the large amount of telescope time available under photometric conditions for performing time-consuming research. In particular, TRAPPIST has very quickly become a key element in the follow-up effort supporting WASP. In future, TRAPPIST will play a similar role for the successor of WASP, the Next Generation Transit Survey (NGTS)<sup>5</sup>, a project led by Geneva Observatory and several UK universities, that will be installed at ESO Paranal Observatory in 2012. NGTS will focus on detecting smaller planets than WASP, and the high photometric precision of TRAPPIST will be a

key asset for confirming and characterising these planets.

Further information and the latest news about TRAPPIST can be found on our web page<sup>6</sup>.

### Acknowledgements

We would like to thank the following: Grégory Lambert of the Geneva Observatory for the continuous technical support on site and Vincent Megevand when he was in charge; Michel Crausaz, Nigel Evershed, Jean-Francois Veraguth, Francesco Pepe, Charles Maire, and Michel Fleury from Geneva Observatory for the refurbishment phase of the T70 building; Andrew Wright and Alexis Thomas from ESO and Pierre Demain from Liège University for the set-up of VPN at each site; Karina Celedon from ESO for the very efficient work and great help in the delivery of the many telescope parts to Chile and the La Silla Observatory; David Schleicher from Lowell Observatory for having recovered and lent one complete set of NASA cometary filters and Alain Gilliotte from ESO for the optical characterisation of those filters; Sandrine Sohy and Robert Sip from Liège University for setting up all the computers and backup procedures and Sandrine for being the webmaster.

We would finally like to pay special thanks to the whole staff of La Silla, and especially Gerardo Ihle and Bernardo Ahumada, for their constant help and support, most particularly during the installation phase.

M. Gillon and E. Jehin are FNRS Research Associates, J. Manfroid is an FNRS Research Director and D. Hutsemékers is an FNRS Senior Research Associate.

### References

- Csizmadia, Sz. et al. 2011, *A&A*, 531, 41
- Deming, D. & Seager, S. 2009, *Nature*, 462, 301
- Farnham, T. L. et al. 2000, *Icarus*, 147, 180
- Gillon, M. et al. 2011, *A&A* (accepted)
- Gillon, M. et al. 2007, *A&A*, 466, 743
- Gillon, M. et al. 2009, *A&A*, 496, 259
- Hsieh, H. & Jewitt D. 2006, *Science* 312, 561
- Jehin, E. et al. 2010, *CBET* #2589
- Jehin, E. et al. 2010, *CBET*, #2632
- Mayor, M. et al. 2003, *The Messenger*, 114, 20
- Meech, K. et al. 2011, *ApJL*, 734, L1
- Queloz, D. et al. 2000, *A&A*, 354, 99
- Sicardy, B. et al. 2011, *Nature*, accepted
- Triaud, A. et al. 2011, *A&A*, 513, A24

### Links

- <sup>1</sup> ESO PR on TRAPPIST: <http://www.eso.org/public/news/eso1023/>
- <sup>2</sup> Superwasp: <http://www.superwasp.org>
- <sup>3</sup> CoRoT: <http://smc.cnes.fr/COROT/index.htm>
- <sup>4</sup> Comet Taxonomy, NASA workshop held 12–16 March 2011, Annapolis, USA
- <sup>5</sup> Next Generation Transit Survey: <http://www.ngtransits.org/>
- <sup>6</sup> TRAPPIST web page: [http://www.ati.ulg.ac.be/TRAPPIST/Trappist\\_main/Home.html](http://www.ati.ulg.ac.be/TRAPPIST/Trappist_main/Home.html)

# CalVin 3 – A New Release of the ESO Calibrator Selection Tool for the VLT Interferometer

Markus Wittkowski<sup>1</sup>  
 Pascal Ballester<sup>1</sup>  
 Daniel Bonneau<sup>2, 3</sup>  
 Alain Chelli<sup>2, 4</sup>  
 Olivier Chesneau<sup>2, 3</sup>  
 Pierre Cruzalèbes<sup>2, 3</sup>  
 Gilles Duvert<sup>2, 4</sup>  
 Christian Hummel<sup>1</sup>  
 Sylvain Lafrasse<sup>2, 4</sup>  
 Guillaume Mella<sup>2, 4</sup>  
 Jorge Melnick<sup>1</sup>  
 Antoine Mérand<sup>1</sup>  
 Denis Mourard<sup>2, 3</sup>  
 Isabelle Percheron<sup>1</sup>  
 Stéphane Sacuto<sup>2, 5</sup>  
 Klara Shabun<sup>1</sup>  
 Stan Stefl<sup>1</sup>  
 Jakob Vinther<sup>1</sup>

<sup>1</sup> ESO

<sup>2</sup> Jean-Marie Mariotti Center, France

<sup>3</sup> Université Nice Sophia Antipolis, CNRS, Observatoire de la Côte d'Azur, Nice, France

<sup>4</sup> Université Joseph Fourier 1/CNRS-INSU, Institut de Planetologie et d'Astrophysique de Grenoble, France

<sup>5</sup> Department of Physics and Astronomy, Uppsala University, Sweden

Interferometric observations require frequent measurements of calibration stars of known diameter to estimate the instrumental transfer function. ESO offers the preparation tool CalVin to select suitable calibrators from an underlying list of calibrators. The latest version 3, first released in January 2011, offers major improvements in the number of available calibrators, the functionality of the search tool, as well as in terms of performance and ease of use. It has been developed in a collaboration between ESO and the French Jean-Marie Mariotti Center (JMMC).

The ESO VLT interferometer (VLTI) is an optical interferometer that is offered as a general user facility. It enables the community to conduct near-infrared (NIR) and mid-infrared (MIR) interferometric observations to obtain high spatial resolution measurements of celestial sources. The instruments of the VLTI that are offered to the community, currently including the

NIR instrument AMBER and the MIR instrument MIDI, are supported by ESO in the same way as any of the VLT instruments of the Paranal observatory (c.f. Wittkowski et al. [2005] for further general information on observing with the VLTI).

In particular, ESO supports the preparation of interferometric observations using the AMBER and MIDI instruments with the preparation tools VisCalc and CalVin<sup>1</sup>. VisCalc estimates visibility values for the expected intensity distribution of the science target and the chosen VLTI configuration to assess the feasibility of an observation. CalVin may be used to select calibration stars for a given science target based on an underlying list of calibrators and a number of user-defined criteria. Both tools are also offered in an expert mode for the use of any arbitrary observatory location, baseline configuration and spectral wavelength band (for CalVin *B*-, *V*-, *R*-, *I*-, *J*-, *H*-, or *K*-bands).

Optical interferometers measure the amplitude and phase of the interference pattern. When normalised these quantities are the amplitude and phase of the complex visibility function, which is related to the intensity distribution by a Fourier transform. An unresolved point source theoretically has a visibility amplitude of unity. However, the measured visibility amplitude of an infinitely small target, also called the interferometric transfer function, will be less than unity owing to losses introduced by the Earth's atmosphere and the instrument. These losses are time variable and need to be frequently monitored. For this purpose, the observer needs to select suitable calibration stars of known diameter, which will be observed close in time to the science targets.

With the growing capabilities of the VLTI, the increasing number of instrument modes, and the improving limiting magnitudes, it has become clear that CalVin's capabilities need to be improved beyond those available when it was first offered in ESO Period 73. Starting with a workshop on interferometric calibrators held in Nice, France, in March 2008, ESO and the French Jean-Marie Mariotti Center (JMMC) have been collaborating on developing a new version of CalVin. The two latest ver-

sions of CalVin, version 3.0 released in January 2011 and version 3.1 released in July 2011, now offer major improvements in terms of the number of available calibrators, the functionality of the search tool, as well as in performance and ease of use.

## Number of available calibrators

The underlying list of calibrators available with CalVin now incorporates the JMMC Stellar Diameter Catalog (JSDC<sup>2</sup>; Lafrasse et al., 2010). This catalogue is based on a search of catalogues available at the Centre de Données astronomiques de Strasbourg (CDS) using the bright mode of the JMMC calibrator search tool Search-Cal<sup>3</sup> (Bonneau et al., 2006) with the faintest limiting magnitudes that are offered for the VLTI. The angular diameter estimates and their errors given in the resulting table are based on statistical estimates and provide information on whether a star is a suitable calibration source for a certain instrument and baseline configuration.

The observer may need to study selected calibrators in more detail to obtain a more precise estimate of their diameters (c.f., for example, Cruzalèbes et al., 2010). Each calibrator is assigned a quality grade depending on whether it is only included in the JSDC catalogue or is also in the catalogues by Bordé et al. (2002), Mérand et al. (2005) or Verhoelst (2005), which were used as the core underlying catalogues of CalVin 2, and whose properties are studied in more detail.

The capacity of, for example, the NIR AMBER table is now 27 814 calibrators, of the MIR MIDI table 27 989 calibrators, and of arbitrary locations (expert version of CalVin) 38 472 calibrators. Figure 1 shows the sky coverage of the underlying list of calibrators available for AMBER, highlighting two typical use cases, a bright calibrator case and a faint calibrator case. The bright calibrator case highlights calibrators of *K* magnitudes  $K < 3$  as they are required for observations using the 1.8-metre auxiliary telescopes (ATs) and moderate conditions of 1.2-arcsecond seeing. The faint case highlights calibrators of *K* magnitudes  $5 < K < 7$  as they are typically required for observations using the 8-metre unit telescopes (UTs).



calibrator observation, visibility amplitudes are computed for the same time intervals at the wavelengths of observation and of the VLTI fringe tracker FINITO, and magnitudes are given at the wavelengths of the guiding camera IRIS and the Coudé guiding camera. Figure 2 shows for illustration some screenshots of a query using CalVin.

### Performance of CalVin

The performance of CalVin, in particular in terms of response time, has been optimised using a new database technology and JavaScript-based visualisation technology to display the plots. The ease of use has also been improved by optimising the layout of the query page, now including one single input page (Figure 2, left), compared to two pages in version 2.

### Future directions

The current underlying list of calibrators lacks MIR magnitudes for many calibra-

tors. We plan to add these using data from the AKARI/IRC mid-infrared all-sky survey (Ishihara et al., 2010). With upcoming fainter limiting magnitudes for the current VLTI instruments, and in particular for second generation VLTI instruments, the current underlying list may still not be sufficiently complete for the faintest magnitudes offered. The faint mode of SearchCal (Bonneau et al., 2011) may then be used to create a significantly larger underlying list of calibrators, which would also impose stronger requirements on the database technology. The additional use of the AKARI point source catalogue might then also allow a more robust selection of calibrator sources to be obtained. Astrometric observations using the upcoming VLTI facilities PRIMA and GRAVITY may require further selection criteria, such as a low proper motion of a phase reference calibrator, requiring additional information in the database as well as additional search criteria. An example of such a search for astrometric calibrators was recently described by Beust et al. (2011). Information on entries in the available bad calibrators' data-

bases<sup>4, 5</sup> as well as information on previous observations may be added to the output result of CalVin in a future release.

### References

- Beust, H. et al. 2011, MNRAS, 414, 108
- Bonneau, D. et al. 2006, A&A, 456, 789
- Bonneau, D. et al. 2011, to appear in A&A
- Bordé, P. et al. 2002, A&A, 393, 183
- Cruzalèbes, P. et al. 2010, A&A, 515, A6
- Ishihara, D. et al. 2010, A&A, 514, A1
- Lafrasse, S. et al. 2010, VizieR Online Data Catalog, 2300
- Mérand, A. et al. 2006, A&A, 447, 783
- Verhoelst, T. 2005, PhD thesis K. U. Leuven, Belgium
- Wittkowski, M. et al. 2005, The Messenger, 119, 14

### Links

- <sup>1</sup> VisCalc and CalVin are available from: <http://www.eso.org/observing/etc>
- <sup>2</sup> The JSDC catalogue: <http://cdsarc.u-strasbg.fr/cgi-bin/VizieR?-source=II/300>
- <sup>3</sup> SearchCal is available at: <http://www.jmmc.fr/searchcal>
- <sup>4</sup> The IAU Comm. 54 bad calibrators' registry (BCR) is available at: <http://www.eso.org/sci/observing/tools/catalogues/bcr.html>
- <sup>5</sup> The bad calibrators' database at JMMC: <http://apps.jmmc.fr/badcal>



One of the VLTI 1.8-metre Auxiliary Telescopes (ATs) being replaced on its tracks at Cerro Paranal after mirror re-aluminising. Each AT has its own transporter that lifts the telescope and moves it from one observing position to another on tracks. However the transfer by road to and from the coating plant at the base camp relies on a truck, as shown.

# A New Massively-multiplexed Spectrograph for ESO

Suzanne Ramsay<sup>1</sup>  
Peter Hammersley<sup>1</sup>  
Luca Pasquini<sup>1</sup>

<sup>1</sup> ESO

With the advent of many large-area imaging surveys in recent years, the need for a new facility for spectroscopic surveys has become apparent. Following a recommendation from the Science and Technical Committee, ESO made a call in 2010 for wide field spectroscopic instrument proposals among its community. Two of the ten proposals were selected for a competitive Phase A study. This article describes the selection process and two associated articles present the instrument concepts.

Large-scale observational surveys are powerful tools for advancing many astronomical fields, often opening up new directions of research, whether the goal is a statistical understanding of a particular class of source or the search for rare objects. In the optical and infrared many new ground-based imaging surveys are underway (e.g., WFCAM, VISTA, Pan-STARRS), are about to start (VST) or in the planning stages (Large Synoptic Survey Telescope, LSST). These imaging surveys will yield catalogues of hundreds of millions of sources and target scientific fields from gravitational lensing to the star formation history of the Galaxy, such as for VISTA and VST (Arnaboldi et al., 2007). In space, Gaia will provide an unprecedented catalogue of positional and radio-velocity information for about a billion stars and the eRosita mission will explore the nature of dark matter and dark energy with an all-sky X-ray survey. These survey projects will deliver new results in the second half of this decade which will demand spectroscopic follow-up. The requirement for a highly-multiplexed spectrograph was identified in the ASTRONET Infrastructure Roadmap (Bode, Cruz & Molster, 2008) as a high priority for exploiting these, and other, missions and as a standalone facility. The ESO Science and Technology Committee (STC) has recommended that steps be taken to improve the existing ESO capabilities in this field.

In 2010, ESO launched a call for proposals for the conceptual design of a multi-object spectroscopic (MOS) instrument/facility for carrying out public surveys. Up to two proposals were to be selected for a competitive Phase A study. The call for proposals was very broad and stated that the instrument should provide the ESO astronomical community with the ability to carry out original wide-field spectroscopic science. Beyond this requirement, the instrument concept and the detailed scientific goals were left open. Proposals were solicited for any ESO telescope: upgrades to existing instruments or completely new instrument concepts were both within the scope of the call. Even proposals for non-ESO telescopes were permissible. In total, ten letters of interest, describing in brief the proposal concept, were sent in by the community. Six teams were invited to submit full proposals consisting of a scientific and technical report and a management plan for the design study.

The final proposals were delivered on 1 March 2011 and included over 30 institutions and 160 contributors, demonstrating the wide interest in such an instrument. The quality of the submitted scientific and technical ideas was warmly appreciated by ESO and the panels involved in the evaluation of the instrument concepts.

The proposals were reviewed from a technical and scientific perspective by separate panels. The technical panel consisted of engineers and scientists from within ESO. The technical review addressed the quality of the technical case for the instrument concept, including the level of risk involved in the design, the quality of the management plan and the experience of the team. The important factors of the impact on the telescope and the operational model for the instrument were also considered.

The scientific panel was made up by a 50:50 split of astronomers from the community and from ESO. It commented on the major scientific questions to be answered by the instrument, whether the science case would be interesting and competitive on the timescales of 2016 and beyond and whether the instrument concept presented would address those goals.

Each panel was charged with commenting on the suitability of the proposals for further study. The proposals were for six very powerful and very different instruments. These included slit- and fibre-based spectrographs, covering the optical and near-infrared wavelength ranges and were for the VLT, VISTA and the NTT. Although some of the projects were judged to be very challenging and ambitious, no technical show-stoppers were identified. The scientific committee strongly endorsed the 2017 delivery timescale envisaged for the instrument as being required for Gaia and eROSITA follow-up. The requirement for high spectral resolving power ( $\lambda/\delta\lambda > 10\,000$ ) for optimal exploitation of Gaia was stressed. The possible selection of Euclid at the end of 2011 by ESA is expected to have an important influence, as the science goals of its spectroscopic instrument overlap with this project.

Overall, the science panel reached excellent agreement as to the most suitable proposals for further work. Finally, ESO management received the input from the two committees and selected the concepts for study. Their recommendation was presented to the Science and Technical Committee at its April 2011 meeting. The successful proposals are for MOONS — a fibre-fed infrared spectrograph designed for the VLT, led by Michele Cirasuolo from the UK Astronomy Technology Centre, and for 4MOST — a fibre-fed optical spectrograph, led by Roelof de Jong from the Leibniz-Institut für Astrophysik Potsdam. Conceptual designs for 4MOST on both the VISTA and NTT telescopes will be explored by the team before the selection is made at the midterm of the design study. In the following two articles the scientific and instrumental aspects of the two proposals are summarised.

The Phase A for the two instruments will finish in February 2013. It is expected that one of the instrument concepts will then be recommended to the STC for detailed design and construction. ESO's goal is to offer a new spectroscopic facility on one of its telescopes around 2017.

## References

Arnaboldi, M. et al. 2007, *The Messenger*, 127, 28  
Bode, M. F., Cruz, M. J. & Molster, F. J. 2008., *The ASTRONET Infrastructure Roadmap*, Astronet

# MOONS: The Multi-Object Optical and Near-infrared Spectrograph

Michele Cirasuolo<sup>1, 2</sup>  
 José Afonso<sup>3</sup>  
 Ralf Bender<sup>4, 5</sup>  
 Piercarlo Bonifacio<sup>6</sup>  
 Chris Evans<sup>1</sup>  
 Lex Kaper<sup>7</sup>  
 Ernesto Oliva<sup>8</sup>  
 Leonardo Vanzini<sup>9</sup>

- 1 STFC United Kingdom Astronomy Technology Centre, Edinburgh, United Kingdom
- 2 Institute for Astronomy, University of Edinburgh, United Kingdom
- 3 Observatorio Astronomico de Lisboa, Portugal
- 4 Universitäts-Sternwarte, München, Germany
- 5 Max-Planck-Institut für extraterrestrische Physik, München, Germany
- 6 GEPI, Observatoire de Paris, CNRS, Univ. Paris Diderot, France
- 7 Astronomical Institute Anton Pannekoek, Amsterdam, the Netherlands
- 8 INAF-Osservatorio Astrofisico di Arcetri, Italy
- 9 Centre for Astro-Engineering at Universidad Catolica, Santiago, Chile

## Team members:

Miguel Abreu<sup>1</sup>, Eli Atad-Etzedgui<sup>2</sup>, Carine Babusiaux<sup>3</sup>, Franz Bauer<sup>4</sup>, Philip Best<sup>5</sup>, Naidu Bezawada<sup>2</sup>, Ian Bryson<sup>2</sup>, Alexandre Cabral<sup>1</sup>, Karina Caputi<sup>6</sup>, Fanny Chemla<sup>3</sup>, Andrea Cimatti<sup>6</sup>, Maria-Rosa Cioni<sup>7</sup>, Gisella Clementini<sup>9</sup>, Emanuele Daddi<sup>9</sup>, James Dunlop<sup>5</sup>, Sofia Feltzing<sup>10</sup>, Annette Ferguson<sup>5</sup>, Andrea Fontana<sup>11</sup>, Johan Fynbo<sup>12</sup>, Bianca Garilli<sup>13</sup>, Adrian Glauser<sup>14</sup>, Isabelle Guinouard<sup>9</sup>, Francois Hammer<sup>3</sup>, Peter Hastings<sup>2</sup>, Hans-Joachim Hess<sup>15</sup>, Rob Ivison<sup>2</sup>, Pascal Jagourel<sup>3</sup>, Matt Jarvis<sup>7</sup>, Guinivere Kauffmann<sup>16</sup>, Andy Lawrence<sup>5</sup>, David Lee<sup>2</sup>, Gianluca Licausi<sup>11</sup>, Simon Lilly<sup>14</sup>, Dario Lorenzetti<sup>11</sup>, Roberto Maiolino<sup>11</sup>, Filippo Mannucci<sup>17</sup>, Ross McLure<sup>5</sup>, Dante Minniti<sup>4</sup>, David Montgomery<sup>2</sup>, Bernard Muschielok<sup>15</sup>, Kirpal Nandra<sup>16</sup>, Ramón Navarro<sup>19</sup>, Peder Norberg<sup>5, 21</sup>, Livia Origlia<sup>8</sup>, Nelson Padilla<sup>4</sup>, John Peacock<sup>5</sup>, Laura Pentericci<sup>11</sup>, Mathieu Puech<sup>3</sup>, Sofia Randich<sup>17</sup>, Alvio Renzini<sup>20</sup>, Nils Ryde<sup>10</sup>, Myriam Rodrigues<sup>3</sup>, Roberto Saglia<sup>15, 5</sup>, Ariel Sanchez<sup>18</sup>, Hermine Schnettler<sup>2</sup>, David Sobral<sup>5, 22</sup>, Roberto Speziali<sup>11</sup>, Eline Tolstoy<sup>23</sup>, Manuel Torres<sup>4</sup>, Lars Venema<sup>21</sup>, Fabrizio Vitali<sup>11</sup>, Michael Wegner<sup>15</sup>, Martyn Wells<sup>2</sup>, Vivienne Wild<sup>5</sup>, Gillian Wright<sup>2</sup>

<sup>1</sup> Centre for Astronomy & Astrophysics University of Lisboa; <sup>2</sup> United Kingdom Astronomy Technology Centre; <sup>3</sup> GEPI, Observatoire de Paris; <sup>4</sup> Centre for Astro-Engineering, Universidad Catolica; <sup>5</sup> Institute for Astronomy, Edinburgh; <sup>6</sup> Università di Bologna – Dipartimento di Astronomia; <sup>7</sup> University of Hertfordshire; <sup>8</sup> INAF-Osservatorio Astronomico

Bologna; <sup>9</sup> CEA-Saclay, Paris; <sup>10</sup> Lund Observatory; <sup>11</sup> INAF-Osservatorio Astronomico Roma; <sup>12</sup> Dark Cosmology Centre, Copenhagen; <sup>13</sup> IASF-INAF, Milano; <sup>14</sup> ETH Zürich; <sup>15</sup> Universitäts-Sternwarte München; <sup>16</sup> Max-Planck-Institut für Astrophysik; <sup>17</sup> INAF-Osservatorio Astrofisico di Arcetri; <sup>18</sup> Max-Planck-Institut für extraterrestrische Physik; <sup>19</sup> NOVA-ASTRON; <sup>20</sup> INAF-Osservatorio Astronomico Padova; <sup>21</sup> Durham University; <sup>22</sup> Leiden Observatory; <sup>23</sup> Kapteyn Astronomical Institute

**MOONS (Multi-Object Optical and Near-infrared Spectrograph) is a large field (500 square arcminutes), multi-object (500 object + 500 sky fibres) instrument with spectral resolution of 5000 and 20 000 proposed for the VLT Nasmyth focus. The science case for MOONS, covering Galactic structure and galaxy evolution up to the epoch of re-ionisation, is briefly outlined.**

MOONS<sup>1</sup> is a new conceptual design for a Multi-Object Optical and Near-infrared Spectrograph, which will provide the ESO astronomical community with a powerful and unique instrument that is able to serve a wide range of Galactic, extragalactic and cosmological studies. The grasp of the 8.2-metre Very Large Telescope (VLT) combined with the large multiplex and wavelength coverage of MOONS — extending into the near-infrared (NIR) — will provide the observational power necessary to study galaxy formation and evolution over the entire history of the Universe, from the Milky Way, through the redshift desert and up to the epoch of re-ionisation at  $z > 8-9$ . At the same time, the high spectral resolution mode will allow astronomers to study chemical abundances of stars in our Galaxy, in particular in the highly obscured regions of the Bulge, and provide the necessary follow-up of the Gaia mission.

## Science objectives

MOONS will be a versatile, world-leading instrument able to tackle some of the most compelling key questions in science: How do stars and galaxies form and evolve? Do we understand the extremes of the Universe? Here we briefly highlight some of the main science cases that are driving the design of MOONS.

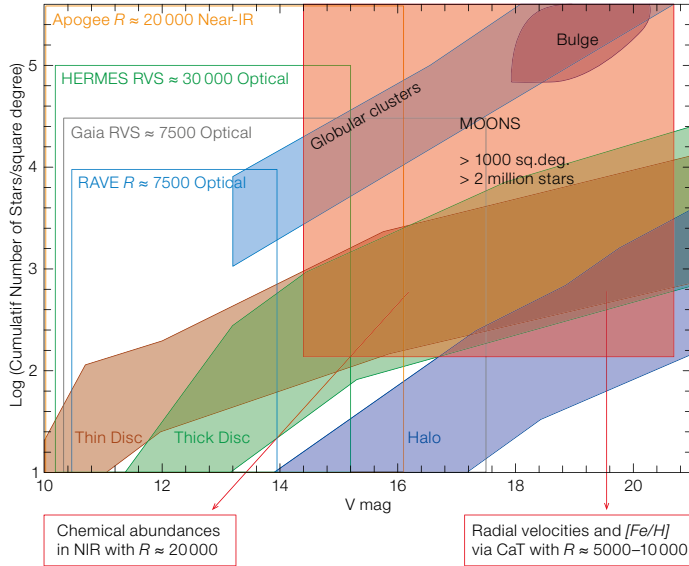
## Galactic archaeology

The study of resolved stellar populations of the Milky Way and other Local Group galaxies can provide us with a fossil record of their chemo-dynamical and star formation histories over many-gigayear timescales. Scheduled for launch in 2013, the ESA Gaia mission will deliver new insight into the assembly history of the Milky Way, but to exploit its full potential, ground-based follow-up is required. MOONS will provide this crucial follow-up for Gaia and for other ground-based surveys such as Pan-STARRS and UKIDSS, and the surveys with VISTA, by measuring accurate radial velocities, metallicities and chemical abundances for several million stars. Given the spectral resolutions ( $R \sim 5000$  and  $R \sim 20\,000$ ) and its ability to observe in the NIR, MOONS will perfectly complement the ongoing and planned surveys (see Figure 1) including the new large Gaia-ESO public spectroscopic survey. The unique features of MOONS will allow us in particular to clarify the nature of the extincted regions of the Bulge, but also to assess the chemo-dynamical structure of the Galactic thin and thick disc, understand the importance of satellites and streams in the halo, ultimately creating an accurate 3D map of our Galaxy to provide essential insight into its origin and evolution.

## The growth of galaxies

Tracing the assembly history of galaxies over cosmic time remains a primary goal for observational and theoretical studies of the Universe. Even though, in recent years, large spectroscopic surveys at optical wavelengths (0.3–1  $\mu\text{m}$ ) have provided key information on the formation and evolution of galaxies, NIR spectroscopy is now crucial to extend our knowledge beyond  $z \sim 1$ . In fact, at these redshifts almost all the main spectral features are shifted at  $\lambda > 1 \mu\text{m}$ . Exploiting the large multiplex and wavelength coverage of MOONS, it will be possible to create the equivalent of the successful Sloan Digital Sky Survey, but at  $z > 1$  (see Figure 2). This will provide an unparalleled resource to study the physical processes that shape galaxy evolution and determine the key relations between

**Figure 1.** Number density of stars in the various components of the Milky Way shown as a function of V-band magnitude (figure adapted from Recio-Blanco, Hill & Bienaymé, 2009). Gaia will provide astrometry for all stars with  $V < 20$ , however the onboard spectrometer (RVS) will deliver chemical abundance only for stars brighter than magnitude 13 and radial velocities for stars brighter than 17. MOONS will perfectly complement Gaia and the other spectroscopic surveys (e.g., Apogee, Hermes, RAVE) providing chemical abundances via high resolution spectroscopy in the NIR (e.g., observing Ca, Si, S, Fe, Ti lines) and radial velocities via the calcium triplet.



stellar mass, star formation, metallicity and the role of feedback. Filling a critical gap in discovery space, MOONS will be a powerful instrument to unveil “the redshift desert” ( $1.5 < z < 3$ , see Figure 2) and study this crucial epoch around the peak of star formation, the assembly of the most massive galaxies, the effect of the environment and the connection with the initiation of powerful active galactic nuclei. MOONS will also provide the essential deep spectroscopic follow-up of imaging surveys undertaken with facilities in optical and near-IR (VISTA, UKIDSS, VST, Pan-STARRS, Dark Energy Survey, LSST) and facilities operating at other wavelengths (ALMA, Herschel in the infrared, eRosita in the X-ray and LOFAR, WISE and ASKAP in the radio).

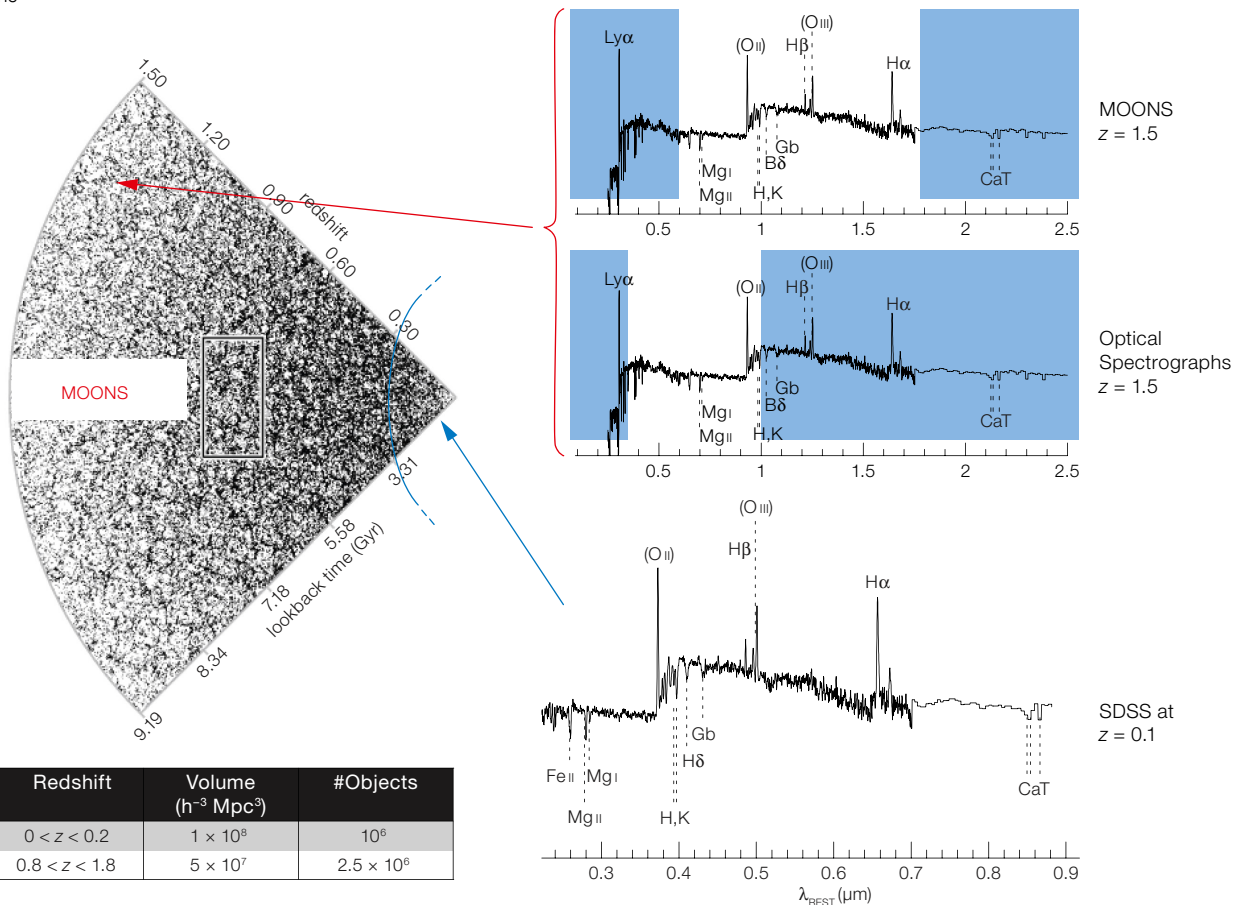


**Figure 2.** A medium-deep survey by MOONS at  $z > 1$  will provide a large number of spectra of similar quality and over the same restframe wavelength range and co-moving volume as the low-redshift SDSS

survey. As shown by the top right panels, the crucial redshift range  $1.5 < z < 2.5$ , encompassing the peak of star formation, has proved to be the hardest to explore spectrally (because the major features are

redshifted out of the optical range) and gained the nickname “redshift desert”. As shown MOONS will cover this gap and properly trace the evolution of galaxies throughout the redshift desert.

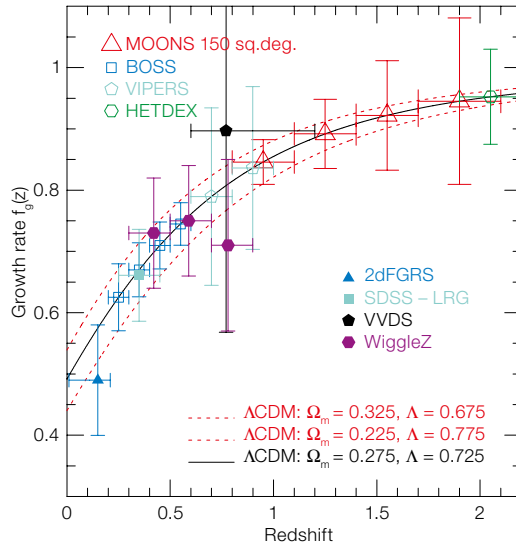
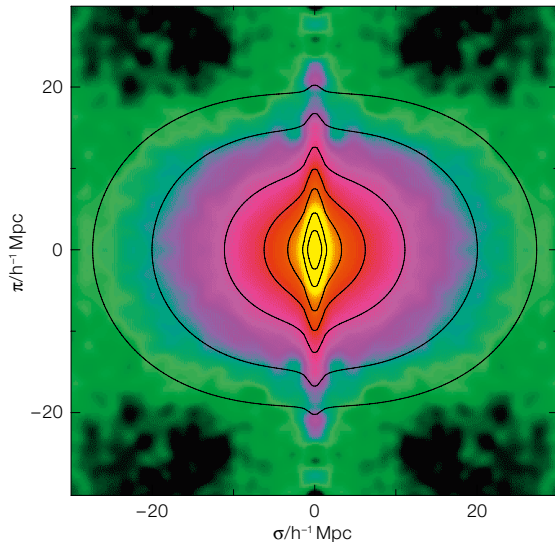


**Figure 3.** Left: The redshift-space correlation function for the 2dFGRS,  $\xi(\sigma, \pi)$ , plotted as a function of transverse ( $\sigma$ ) and radial ( $\pi$ ) pair separation at  $z < 0.3$  from the 2dF galaxy redshift survey (Peacock et al., 2001). This plot clearly displays redshift space distortions, with “fingers of God” elongations on small scales and coherent Kaiser flattening at large scales, the signature of the growth rate of structure on galaxy clustering measurements. Right: Comparison of growth rate measurements,  $f_g(z)$ , for currently available measurements (solid symbols, with 2dFGRS, SDSS-LRG, WiggleZ and VVDS) and to projected measurements (open symbols) of ongoing surveys (BOSS, VIPERS and HETDEX). Open triangles show the prediction for the growth rate measurement that will be obtained with MOONS using  $\sim 1$  million galaxies over 150 square degrees. No other ground-based survey is able to probe the redshift range considered by MOONS.

### The first galaxies

The shining of the first galaxies, just a few hundred million years after the Big Bang (at redshift  $7 < z < 12$ ) is of enormous importance in the history of the Universe since these first galaxies hold the key to furthering our understanding of cosmic reionisation. Although recent advances obtained by deep NIR imaging have been dramatic, very little is known about when and especially how this re-ionisation happened. The unique combination of 8-metre aperture, wide area coverage and NIR spectroscopy (key since at  $z > 7$  even the Ly $\alpha$  line is shifted to  $\lambda > 1 \mu\text{m}$ ) offered by MOONS, will provide accurate distances, relative velocities and emission line diagnostics, without which the power of these photometric surveys is severely limited. The capabilities of MOONS will give us the first realistic chance to perform a systematic, wide-area spectroscopic study of the very high redshift galaxies and establish the physics of reionisation.

### Cosmology

Over the last two decades several observational keystones have considerably changed our knowledge of the Universe. Measurements of the cosmic microwave background, high-redshift supernovae and large-scale structure have revealed that 96% of the density of the Universe

consists of currently unexplained dark energy and dark matter, and less than 4% is in the form of baryons. Understanding the nature of these dark components — which dominate the global expansion and large-scale structure of the Universe — is amongst the most fundamental unsolved problems in science. Complementary to other spectroscopic surveys at  $z < 1$  (e.g., Vipers, BOSS, WiggleZ, BigBOSS), the capabilities of MOONS will allow us to constrain the cosmological paradigm of the  $\Lambda$  Cold Dark Matter model by determining the dark matter halo mass function and obtain crucial constraints on the nature of dark energy and gravity via detailed measurements of the growth rate of structure at  $z > 1$ , extending previous determinations, such as that by the 2dF galaxy redshift survey at  $z < 0.3$  (Peacock et al., 2001) and shown in Figure 3.

### Instrument specifications

To address such fundamental science questions MOONS will exploit the full 500 square arcminute field of view offered by the Nasmyth focus of the VLT and will cover the wavelength range  $0.8 \mu\text{m} - 1.8 \mu\text{m}$ , with a possible extension down to  $0.5 \mu\text{m}$ . A new pick-off system will allow a fast positioning of the fibres and the observation of 500 targets simultaneously, each with its own dedicated sky fibre for optimal sky subtraction. MOONS will have

### MOONS INSTRUMENT PERFORMANCE

Telescope	VLT
Field of view	500 sq. arcmin.
Number of targets	500 objects + 500 sky
Wavelength	0.8(0.5)–1.8 $\mu\text{m}$
Resolutions	Medium = 5000 High = 20 000

both a medium resolution ( $R \sim 5000$ ) mode and a high-resolution ( $R \sim 20\,000$ ) mode to allow detailed dynamical and chemical studies. Such characteristics and versatility make MOONS the long-awaited workhorse NIR multi-object spectrograph for the VLT, which will perfectly complement the optical spectroscopy performed by FLAMES and VIMOS.

### References

Peacock, J. et al. 2001, *Nature*, 410, 169  
 Recio-Blanco, A., Hill, V. & Bienaymé, O. 2009, *Proc. French Society of Astron. & Astrophys.* SF2A-2009

### Links

<sup>1</sup> MOONS: <http://www.roe.ac.uk/~ciras/MOONS.html>

# 4MOST – 4-metre Multi-Object Spectroscopic Telescope

Roelof de Jong<sup>1</sup>

<sup>1</sup> Leibniz-Institut für Astrophysik Potsdam (AIP), Germany

Team members:

Svend Bauer<sup>1</sup>, Gurvan Bazin<sup>2</sup>, Ralf Bender<sup>2</sup>, Hans Böhringer<sup>3</sup>, Corrado Boeche<sup>1</sup>, Thomas Boller<sup>3</sup>, Angela Bongiorno<sup>3</sup>, Piercarlo Bonifacio<sup>4</sup>, Marcella Brusa<sup>3</sup>, Vadim Burwitz<sup>3</sup>, Elisabetta Caffau<sup>5</sup>, Art Carlson<sup>2</sup>, Cristina Chiappini<sup>1</sup>, Norbert Christlieb<sup>5</sup>, Mathieu Cohen<sup>4</sup>, Gavin Dalton<sup>6</sup>, Harry Enke<sup>1</sup>, Carmen Feiz<sup>5</sup>, Sofia Feltzing<sup>7</sup>, Patrick François<sup>4</sup>, Eva Grebel<sup>5</sup>, Frank Grupp<sup>2</sup>, Francois Hammer<sup>4</sup>, Roger Haynes<sup>1</sup>, Jochen Heidt<sup>5</sup>, Amina Helmi<sup>8</sup>, Achim Hess<sup>2</sup>, Ulrich Hopp<sup>3</sup>, Andreas Kelz<sup>1</sup>, Andreas Korn<sup>9</sup>, Mike Irwin<sup>10</sup>, Pascal Jagourel<sup>4</sup>, Dave King<sup>10</sup>, Gabby Kroes<sup>11</sup>, Georg Lamer<sup>1</sup>, Florian Lang-Bardl<sup>2</sup>, Richard McMahon<sup>10</sup>, Baptiste Meneux<sup>2</sup>, Shan Mignot<sup>4</sup>, Ivan Minchev<sup>1</sup>, Joe Mohr<sup>2</sup>, Volker Müller<sup>1</sup>, Bernard Muschelok<sup>2</sup>, Kirpal Nandra<sup>3</sup>, Ramon Navarro<sup>11</sup>, Ian Parry<sup>10</sup>, Johan Pragt<sup>11</sup>, Andreas Quirrenbach<sup>5</sup>, William Rambold<sup>1</sup>, Martin Roth<sup>1</sup>, Roberto Saglia<sup>3</sup>, Paola Sartoretti<sup>4</sup>, Olivier Schnurr<sup>1</sup>, Axel Schwöpe<sup>1</sup>, Matthias Steinmetz<sup>1</sup>, Jesper Storm<sup>1</sup>, Will Sutherland<sup>12</sup>, Rikter Horst<sup>11</sup>, David Terrett<sup>6</sup>, Ian Tosh<sup>6</sup>, Scott Trager<sup>8</sup>, Lars Venema<sup>11</sup>, Marija Vlahić<sup>1</sup>, Jacob Walcher<sup>1</sup>, Nicolas Walton<sup>10</sup>, Mary Williams<sup>1</sup>, Lutz Wisotzki<sup>1</sup>

<sup>1</sup> Leibniz-Institut für Astrophysik Potsdam, <sup>2</sup> Universitäts-Sternwarte München, <sup>3</sup> Max-Planck-Institut für extraterrestrische Physik, Garching, <sup>4</sup> GEPI, Observatoire de Paris, <sup>5</sup> Zentrum für Astronomie der Universität Heidelberg, <sup>6</sup> Rutherford Appleton Laboratory, Didcot, <sup>7</sup> Lund Observatory, <sup>8</sup> Kapteyn Astronomical Institute, Groningen, <sup>9</sup> Department of Physics and Astronomy, Uppsala University, <sup>10</sup> Institute of Astronomy, Cambridge, <sup>11</sup> NOVA-ASTRON, the Netherlands, <sup>12</sup> Queen Mary College London.

4MOST (4-metre Multi-Object Spectroscopic Telescope) is a very large field (goal > 5 square degrees) multi-object spectrograph with up to 3000 fibres and spectral resolutions of 5000 and 20 000, proposed for the New Technology Telescope (NTT) or the VISTA survey telescope. The science cases covering Gaia follow-up for chemistry and kinematics of the Galaxy and redshift surveys of targets from the eROSITA X-ray mission are briefly outlined.

The 4MOST consortium aims to provide the ESO community with a fibre-fed spectroscopic survey facility on either VISTA or the NTT with a large enough field of view (FoV) to survey a large fraction of the southern sky in a few years, a multiplex and spectral resolution high

enough to detect chemical and kinematic substructure in the stellar halo, bulge and thin and thick discs of the Milky Way, and enough wavelength coverage (> 1.5 octave) to secure velocities of extragalactic objects over a large range in redshift. Such an exceptional instrument enables many science goals, but our design is especially intended to complement two key all-sky, space-based observatories of prime European interest, Gaia and eROSITA. Such a facility has been identified as of critical importance in a number of recent European strategic documents (Bode et al., 2008; de Zeeuw & Molster, 2007; Drew et al., 2010; Turon et al., 2008) and forms the perfect complement to the many all-sky survey projects around the world.

## Science drivers

The Gaia satellite will provide distances from parallaxes and space kinematics from proper motions for more than one billion Milky Way stars down to  $m_V \sim 20$  mag. Gaia will also provide radial velocities and astrophysical characterisation for about 150 million stars, but its sensitivity is limited to  $m_V \sim 12\text{--}16$  mag, strongly dependent on stellar spectral type, because its spectrograph only covers the Ca II-triplet region at 847–874 nm. Figure 1 shows how, by covering the full optical wavelength region, the 4MOST instrument complements Gaia where it lacks spectroscopic capabilities, so that full 6D-space coordinate information can be obtained and objects throughout the Milky Way chemically characterised. Large-area surveys of faint Galactic stellar objects will enable us to elucidate the formation history of the Milky Way.

Models of hierarchical galaxy formation predict large amounts of dynamical substructure in the Milky Way halo that 4MOST can detect through measuring red giant branch (RGB) stars (see Figure 2). Furthermore, we will determine the three-dimensional Galactic potential and its substructure, discern the dynamical structure of the Milky Way disc and measure the influence of its bar and spiral arms, measure the Galactic assembly history through chemo-dynamical substructure and abundance pattern labelling, and find thousands of extremely

metal-poor stars to constrain early galaxy formation and the nature of the first stellar generations in the Universe.

eROSITA (extended ROentgen Survey with an Imaging Telescope Array, Predehl et al., 2010) will perform all-sky X-ray surveys in the years 2013 to 2017 to a limiting depth that is a factor 30 deeper than the ROSAT all-sky survey, and with broader energy coverage, better spectral resolution and better spatial resolution (see Figure 3). We will use 4MOST to survey the > 50 000 southern X-ray galaxy clusters that will be discovered by eROSITA, measuring 3–30 galaxies in each cluster. These galaxy cluster measurements determine the evolution of galaxy populations in clusters, yield the cluster mass evolution, and provide highly competitive constraints on dark energy evolution. 4MOST enables us to determine the nature of > 1 million active galactic nuclei (AGNs), thus constraining the cosmic evolution of active galaxies to  $z = 5$ . With 4MOST we will characterise several hundreds of thousands of dynamo- and accretion-powered Galactic X-ray emitters, thereby uncovering the active Milky Way and constraining evolutionary channels of stellar populations.

Other science cases that are fully feasible with 4MOST, but that will not drive the design, include the dynamic structure and content of nearby galaxies, follow-up of extragalactic radio and infrared surveys, and constraining dark energy properties through baryon acoustic oscillation (BAO) measurements.

## Instrument specification

The 4MOST facility consists of a wide-field corrector with atmospheric dispersion corrector, acquisition, guiding and wavefront sensing systems, a fibre-positioning system, and a fibre train feeding the light to an  $R > 20\,000$  spectrograph and several  $R \sim 5000$  spectrographs. The baseline and goal instrument specifications can be found in Table 1. We have preliminary wide-field corrector designs yielding 7 square degree FoV on the VISTA 4.1-metre telescope and 3 square degree FoV on the 3.58-metre NTT. We will study two fibre positioner designs, one based on a variation of

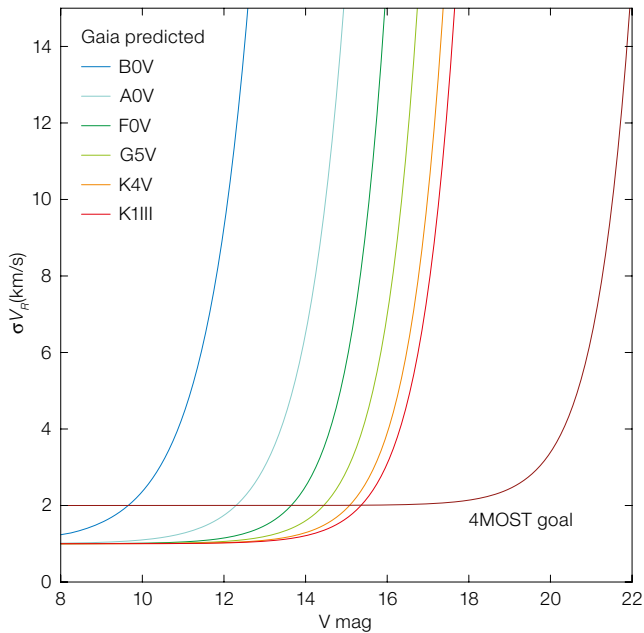
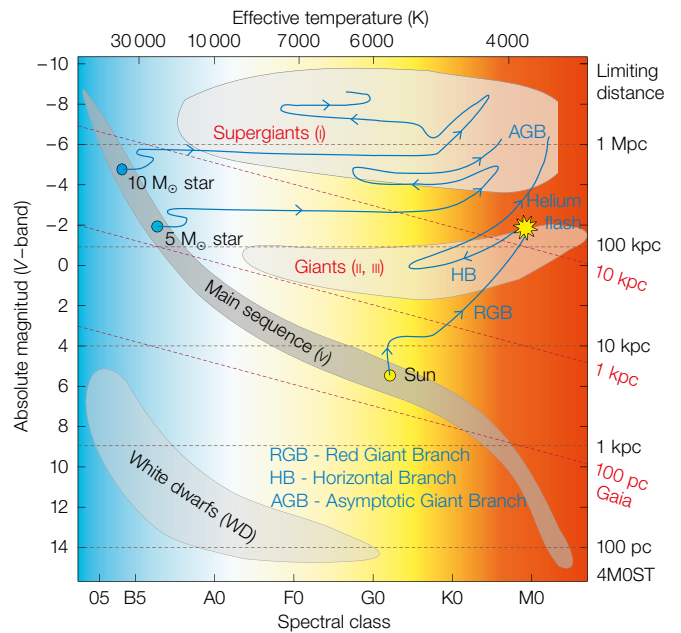


Figure 1. Left: The 4MOST goal for radial velocity accuracy compared to the Gaia end of mission accuracy as function of stellar apparent magnitude. Our aim is to match the spectroscopic magnitude limits of 4MOST to the astrometric limits of Gaia,



thereby enabling 6D-phase space studies to Gaia's limits. Right. Limiting distances for radial velocity measurements with Gaia (maroon diagonal) and 4MOST (black horizontal) overlaid on a Hertzsprung-Russell diagram. 4MOST can measure Sun-like stars

to nearly the centre of the Milky Way, RGB stars to 100 kpc, and massive stars throughout the Local Group, substantially expanding on Gaia's spectroscopic view. Distance limits for the 4MOST high resolution spectroscopy are about four times smaller.

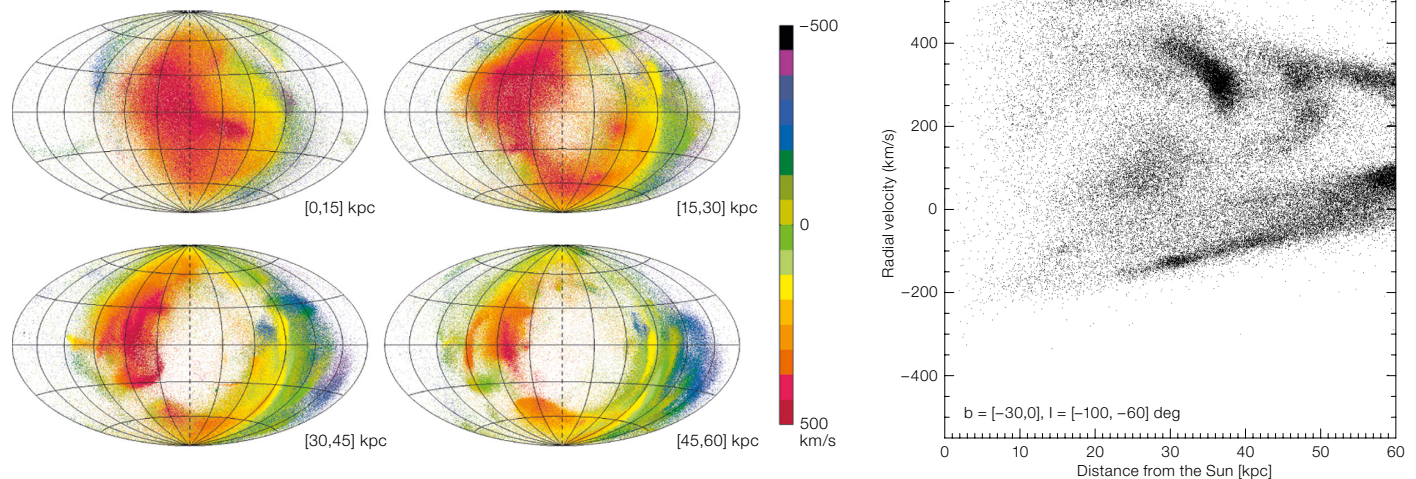
the Echidna design as developed by the Australian Astronomical Observatory (AAO) for FMOS (Akiyama et al., 2008) and another one based on the positioner design of the Guoshoujing (formerly LAMOST) Telescope (Hu et al., 2004).

Efficient full-sky surveying requires at least 1500 targets to be observed simultaneously, but our goal is to provide a multiplex of > 3000 to create a unique, world-class facility. Most fibres will lead to spectrographs with spectral resolution

of  $R \sim 5000$  covering the full optical wavelength range, but about 10% of the fibres will permanently go to a spectrograph with resolution of  $R > 20000$ . The facility will be complemented with a full array of software to enable target selection, scheduling, data reduction and analysis, and an archive. During the conceptual design phase we will perform a number of trade-off studies to find the

Figure 2. Spatial and radial velocity substructure distribution of RGB stars on the sky for a stellar halo formed in the Aquarius project cosmological simulations (Cooper et al., 2010; Helmi et al., 2011). The projection corresponds to stars located in the inner

halo in four distance bins (left) and in one direction on the sky (right) and clearly demonstrates the large amount of substructure that becomes apparent, consequent on the opening of a new phase-space dimension (in this case, line-of-sight velocity).



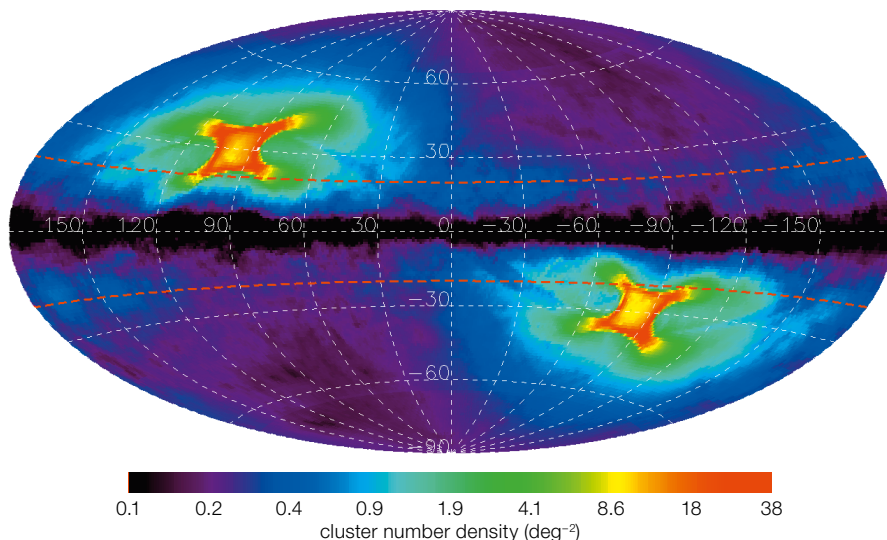


Figure 3. All-sky map (in Aitoff projection) of the predicted number density of eROSITA galaxy cluster detections (from Mühlegger, 2010). 4MOST enables efficient follow-up of the  $\sim 70\,000$  clusters detected in the southern hemisphere and provides dynamical mass estimates for a large fraction of them by measuring radial velocities of 5–30 galaxies in each cluster.

optimal designs for both the VISTA and the NTT telescopes, with ESO then making the final telescope selection about halfway through the study.

### Surveys with 4MOST

To reach maximum impact, we propose to use 4MOST continuously for a five-year Public Survey delivering  $\geq 7$  million (goal 25 million) spectra over  $10\,000$ – $20\,000$  square degrees, which is an order of magnitude larger than the Sloan Digital Sky Survey (SDSS) spectroscopic survey at  $> 2.5$  times the spectral resolution. The targets selected for this Public Survey could be determined through a combination of open calls to the ESO astronomical community and the consortium guaranteed time observations (GTO), with all surveys running in parallel. Observing objects from many survey catalogues simultaneously at each pointing enables surveys that require tens of thousands objects spread sparsely over the sky. Such surveys have too few targets to use all 4MOST fibres in one pointing, but are too large to be performed in standard observing modes with existing facilities.

The consortium will make all data, including high-level science products, available to the general public in yearly increments through a high-quality database system.

European astronomers have currently no access to a 4MOST-like facility, and frankly, such an instrument does not exist worldwide. Only the HERMES instrument currently under construction for the AAO in combination with the planned, but not yet funded, BigBOSS or SuMIRe prime focus instruments (for the 4-metre Kitt Peak and 8-metre Subaru telescopes respectively) would provide similar capabilities as those proposed for 4MOST. However, even if these instruments were successfully constructed,

European astronomers would not have direct access to them. For many science cases where spectral samples of more than a few 100 objects are required, 4MOST will outperform existing instrumentation on 8-metre-class telescopes like FLAMES and VIMOS. Running in permanent Public Survey mode, it will take observations for many science programmes simultaneously, enabled by its huge grasp in multiplex, field of view and wavelength coverage. The reduced photon-gathering power of a 4-metre-class telescope is thus easily compensated by the larger field of view and the increased time available per target. Therefore, if 4MOST is realised, the ESO community gains a facility that can be described as an 8-metre-class instrument on a 4-metre telescope.

### References

- Akiyama, M. et al. 2008, SPIE, 7018, 94  
 Bode, M., Cruz, M. & Molster, F. 2008, *The ASTRONET Infrastructure Roadmap*  
 Cooper, A. P. et al. 2010, MNRAS, 406, 744  
 de Zeeuw, P. & Molster, F. 2007, *A Science Vision for European Astronomy (ASTRONET)*  
 Drew, J. et al. 2010, *Report by the European telescope strategic review committee on Europe's 2–4m telescopes over the decade to 2020 (ASTRONET)*  
 Helmi, A. et al. 2011, ApJL, 733, L7  
 Hu, H. et al. 2004, SPIE, 5492, 574  
 Mühlegger, M. 2010, Ph.D. thesis, Technische Universität München  
 Predehl, P. et al. 2010, SPIE, 7732, 23  
 Turon, C. et al. 2008, *Report by the ESA-ESO Working Group on Galactic populations, chemistry and dynamics*, ST-ECF, ESO

Specification	Baseline	Goal
Field of view	3 degree <sup>2</sup>	$> 5$ degree <sup>2</sup>
Multiplex fibre positioner	1500	$> 3000$
Spectrographs – blue arm		
resolution @ 500 nm	$R \sim 3000$	$R \sim 5000$
passband	420–650 nm	370–650 nm
Spectrographs – red arm		
resolution @ 850 nm	$R \sim 5000$	$R \sim 7500$
passband	650–900 nm	650–1000 nm
HR spectrograph (10–20% of all fibres)		
resolution		$R > 20\,000$ ,
passbands		390–450 & 585–675 nm
Number of fibres in 2' circle	$> 3$	$> 7$
Reconfigure time	$< 8$ min	$< 4$ min
Area (5-year survey)	10000 deg <sup>2</sup>	$2 \times \sim 20\,000$ deg <sup>2</sup>
Objects (5-year survey)	$6 \times 10^6$	$> 20 \times 10^6$
Start operations		end 2017

Table 1. Baseline and goal instrument specification.

# ALMA Status and Science Verification Data

Leonardo Testi<sup>1</sup>  
Martin Zwaan<sup>1</sup>

<sup>1</sup> ESO

ALMA is rapidly progressing towards the end of the construction phase. At the beginning of August 2011, 17 antennas were interferometrically linked on the Chajnantor plateau at an altitude of 5000 metres. Twelve-metre antennas from all the vendors were used in this experiment, which is a major milestone towards the first Early Science guest observer observations, currently planned to begin soon. In the meantime, ALMA Science Verification datasets are becoming available on the ALMA webpages for users to download and gain familiarity with ALMA data reduction and analysis procedures.

The Atacama Large Millimeter/submillimeter Array (ALMA) is at an advanced stage of construction with 17 fully equipped antennas at the high site at the time of writing (see Figure 1). The current array consists of 12-metre antennas of different designs from all three providers (AEM, MELCO and Vertex); all have been tested, fully equipped with the ALMA components and linked together to work as an interferometer. Following

the achievement of closure phase at the beginning of 2010 (Testi, 2010) and the collection of test datasets on astronomical sources with the array consisting of a few antennas during the second half of 2010 (Testi et al., 2010; Randall & Testi, 2011), the successful execution of the first Science Verification test projects (see below) have been completed. These early demonstrations are an important step towards the scientific validation of the ALMA observatory for Early Science operation.

The ALMA Early Science Cycle 0 Call for Proposals was issued in March 2011 with deadline 30 June 2011. The array has been offered with very preliminary capabilities (sixteen antennas, four frequency bands, limited correlator flexibility and without either the full polarisation option or the solar observations), and for a small fraction of the time, as construction and commissioning efforts towards full science operations are still a priority. Nevertheless, the response from the community worldwide was phenomenal: 919 observing proposals were received, resulting in an over-subscription rate of approximately a factor of nine as compared to the expected time available for science during Cycle 0 of ALMA Early Science. The review process is in progress at the time of writing, and the expectation is that proposers will be notified in early September; the observations for

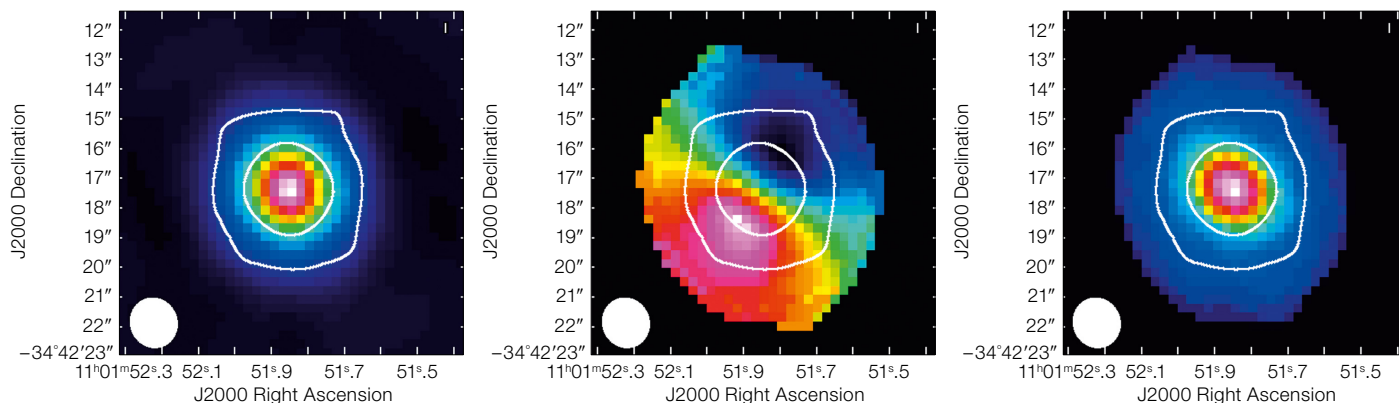
the scheduled proposals will then start in the autumn.

In the meantime, the Commissioning and Science Verification team, headed by Richard Hills and Alison Peck at the Joint ALMA Office in close collaboration with the ALMA Regional Centres (ARCs) in Europe, Japan and the USA and the ALMA science teams at ESO, National Astronomical Observatory of Japan (NAOJ) and the US National Radio Astronomy Observatory (NRAO), are testing the end-to-end system by taking Science Verification (SV) observations. The SV targets were chosen from a long list of suggestions provided by the community at the beginning of 2011. The current list of SV targets, along with a detailed description of the goals and constraints of the programme are posted on the ALMA observatory webpages<sup>1</sup>. The SV test data, once validated, are released publicly in raw and reduced format along with CASA scripts and tutorials to fully explain the data reduction procedures. The goal is to allow future users to look at scientifically validated ALMA data for sources already well known from previous (sub)millimetre observations. Astronomers from the community are encouraged to look at the data to learn the details of the data reduction and to publish any interesting scientific results that may come out of their analysis of the released datasets.

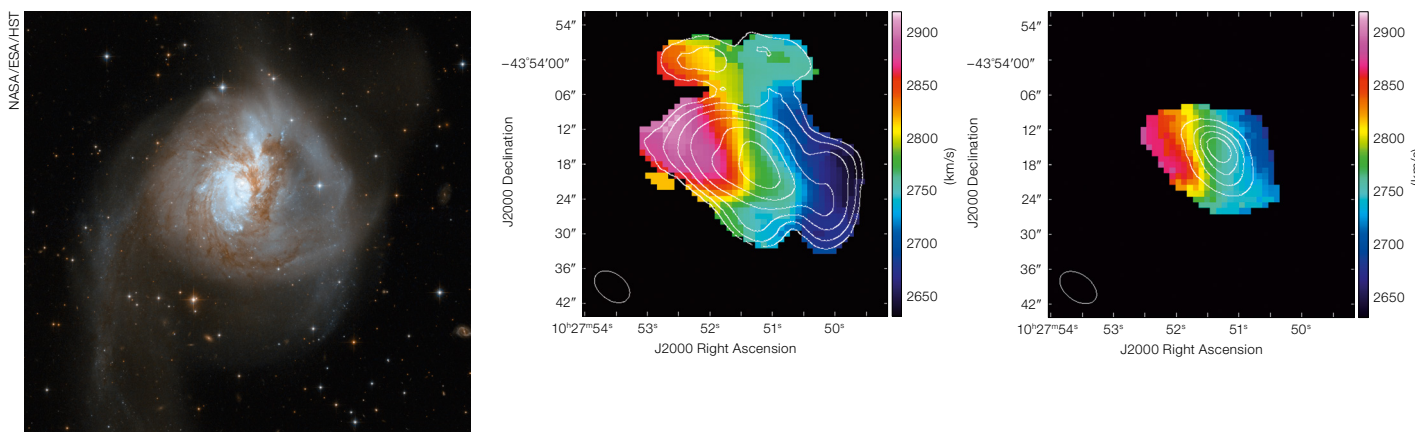


Figure 1. Seventeen ALMA antennas on the Chajnantor plateau, when fringes on 136 baselines (between the 17 antennas) were obtained for the first time. The first antenna to the high site produced by the AEM consortium was included in the array and is visible near the centre left of the picture.

R. Hills/ALMA (ESO/NAOJ/NRAO)



**Figure 2.** ALMA CO(3-2) and continuum SV test observations of the TW Hydrae protoplanetary disc. From left to right the colour-coded map of the molecular line total intensity, mean velocity and velocity dispersion respectively, with the contour plot of the continuum emission overlaid.



**Figure 3.** ALMA SV test observations of the luminous infrared galaxy NGC 3256. Left panel: optical HST image of the galaxy; Centre panel: contours of the CO(1-0) total intensity overlaid on the molecular gas mean velocity map; right panel: as the central panel but for the CN(1-0) line.

At the time of writing, on the ALMA Science Verification webpages<sup>1</sup>, users can download data released in June 2011 for the protoplanetary disc surrounding the young star TW Hydrae (see Figure 2) and for the luminous infrared galaxy NGC 3256 (Figure 3). The TW Hydrae dataset<sup>2</sup>, shown by the maps in Figure 2, includes continuum and spectral line observations in the molecular lines of CO(3-2) and HCO<sup>+</sup>(4-3) using ALMA Band 7. These data can be compared with published Sub-Millimeter Array (SMA) data for the continuum by Hughes et al. (2011) and for CO(3-2) by Qi et al.

(2008), who also presented HCO<sup>+</sup>(3-2) observations at a similar angular and spectral resolution as the ALMA SV data. The NGC 3256 dataset<sup>3</sup> consists of continuum data and CO(1-0) and CN(1-0) molecular line data obtained using ALMA Band 3, and is shown in Figure 3. No other high angular resolution observations of this galaxy are available in the CO(1-0) line, but the CO(2-1) line was observed with the SMA by Sakamoto, Ho & Peck (2006).

Additional data on TW Hya and on the NGC 4038/4039 (the Antennae) merging galaxies system are scheduled to be released in August 2011. The Antennae dataset will demonstrate the ALMA mosaicking capabilities that will be available during Early Science Cycle 0. Additional datasets are currently being worked on and will also be released soon.

## References

- Hughes, A. M. et al. 2011, *ApJ*, 727, 85
- Qi, C. et al. 2008, *ApJ*, 681, 1396
- Randall, S. & Testi, L. 2011, *The Messenger*, 144, 39
- Sakamoto, K., Ho, P. T. P. & Peck, A. B. 2006, *ApJ*, 644, 862
- Testi, L. 2010, *The Messenger*, 139, 52
- Testi, L. et al. 2010, *The Messenger*, 142, 17

## Links

- <sup>1</sup> ALMA Science Verification: <http://almascience.eso.org/alma-data/science-verification>
- <sup>2</sup> Access to TW Hydrae Science Verification data: <http://almascience.eso.org/alma-data/science-verification/tw-hya>
- <sup>3</sup> Access to NGC 3256 Science Verification data: <http://almascience.eso.org/alma-data/science-verification/ngc3256>

A color composite image of the Large Magellanic Cloud. The central focus is the star cluster NGC 1929, a dense field of blue and white stars. Surrounding this cluster is the nebula N44 (LHA 120-N44), which appears as a complex, multi-colored structure. It features prominent red filaments and clouds, interspersed with blue and purple regions. The overall scene is set against a dark background filled with numerous other stars of various colors.

The nebula N44 (LHA 120-N44) surrounding the star cluster NGC 1929 in the Large Magellanic Cloud, is shown in a FORS1 colour composite formed from images in the emission lines of He II 4686Å, [O III] 5007Å, He I 5876Å and H $\alpha$  6563Å. The stellar winds and subsequent supernova explosions from the hot young stars in NGC 1929 are blowing a superbubble into the interstellar medium. The image was created by ESO from FORS1 images identified by Manu Mejías, from Argentina, who participated in ESO's Hidden Treasures competition. See Release eso1125 for more details.

# The Tenuous Atmospheres of Pluto and Triton Explored by CRIRES on the VLT

Emmanuel Lellouch<sup>1</sup>  
 Catherine de Bergh<sup>1</sup>  
 Bruno Sicardy<sup>1</sup>  
 Hans-Ulrich Käuffl<sup>2</sup>  
 Alain Smette<sup>2</sup>

<sup>1</sup> LESIA-Observatoire de Paris, CNRS, UPMC Univ. Paris 06, Univ. Paris-Diderot, France

<sup>2</sup> ESO

The dwarf planet Pluto and Neptune's largest satellite, Triton, are two small icy bodies surrounded by tenuous and poorly known atmospheres. The high spectral resolution and high sensitivity of CRIRES on the VLT have permitted a major step forward in the study of these atmospheres, and especially of their composition. Absorptions due to methane and carbon monoxide in these atmospheres have been detected at 1.66 and 2.35  $\mu\text{m}$ , providing an insight into the way in which these atmospheres are maintained, the surface-atmosphere interactions, their seasonal evolution and thermal balance.

## Pluto and Triton: Frigid twins in the outer Solar System

Pluto and Triton are twins in the outer Solar System. Once the ninth planet and now classified as a dwarf planet, Pluto is a prominent member of the Kuiper Belt, the population of small primitive bodies orbiting the Sun beyond Neptune (e.g., Barucci et al., 2010). Its heliocentric orbit, fairly typical for a body in 3:2 resonance with Neptune, is elliptical (perihelion at 29.5 Astronomical Units [AU] and aphelion at 49.0 AU) and inclined (by 17° to the ecliptic plane). Pluto's axis of rotation is inclined by 120° to its orbital plane. Since its discovery in 1930, Pluto has covered only one third of its 248-year orbit and its most recent closest approach to the Sun occurred in 1989. With a diameter of about 2340 kilometres, Pluto is, along with Eris, one of the two largest members of the trans-Neptunian population.

At a mean distance of 30 AU from the Sun, Triton is the largest satellite of Neptune, with a diameter of 2707 kilometres.

Its orbit around the planet — retrograde and out of Neptune's equatorial plane — indicates that it is most likely a Kuiper Belt object that has been captured by Neptune. Triton's orbit and obliquity are such that at some time during the 165-year-long Neptune year, each of Triton's poles points almost directly toward the Sun — the obliquity of the current orbit is 50°, resulting in large seasonal effects in the insolation.

Beyond their similar sizes and dynamical kinship, Pluto and Triton have similar, albeit not identical, compositions. Earth-based near-infrared (NIR) observations indicate that both are covered by ices dominated by nitrogen, plus some methane and carbon monoxide. Ethane ice has also been detected on Pluto, while carbon dioxide and water ice are present on Triton. Detailed studies of ice band positions indicate that most of the ices are “diluted” by N<sub>2</sub> ice, i.e. are mixed with it in small proportions at the molecular level. The *Voyager 2* encounter with Triton in 1989 unveiled a frigid (38 K) but remarkably active world, with high surface diversity (see Figure 1). Until the *New Horizons* spacecraft gets to Pluto — the encounter is scheduled for July 2015 — and reveals how similar Pluto's appearance is to Triton's, Pluto will remain a crudely resolved 0.1-arcsecond dot. Yet even at the modest resolution of the Hubble Space Telescope (HST; see Figure 2), Pluto exhibits large brightness contrasts, up to 6:1 in reflectance. The

brightest areas are attributed to N<sub>2</sub> ice, while dark regions are thought to result from the irradiation of methane ice-rich areas, giving birth to tholins (heteropolymer molecules formed by UV radiation). The large surface variegation of Pluto is also responsible for a large heterogeneity in the surface temperature, varying from about 40 K in the bright areas to 60 K in the darkest regions.

## Tenuous and poorly understood atmospheres

Pluto and Triton both have tenuous atmospheres formed by the sublimation of the more volatile surface ices, whose composition, to first order, must reflect that of the surface and the relative volatility of the various ices. In spite of their large distance from the Sun, these atmospheres are strongly driven by solar heat. Given the large inclination of the rotation axes (and in Pluto's case the orbital eccentricity) they must also vary with time. Pluto's atmosphere is expected to completely collapse at aphelion — around 2113.

Triton's atmosphere was discovered by *Voyager 2*. Its main component, N<sub>2</sub>, was detected in the ultraviolet, with a ground pressure of 14  $\mu\text{bar}$ , and gaseous CH<sub>4</sub> could also be observed. On Pluto, N<sub>2</sub> must also be the major gas, but cannot be observed from Earth, and only a low signal-to-noise (S/N) detection of

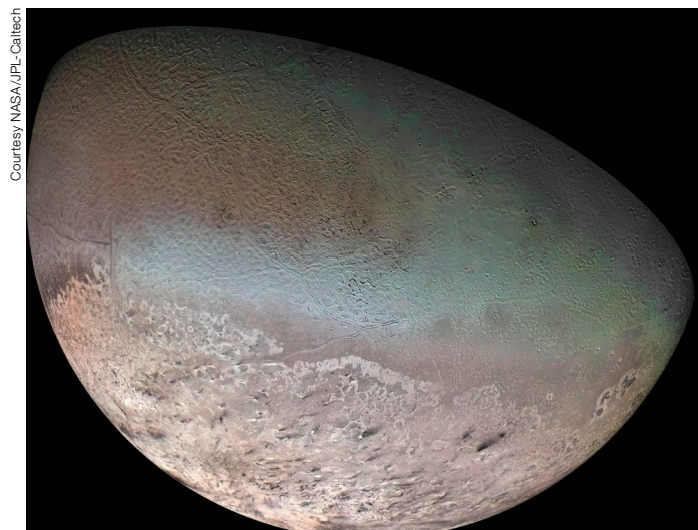


Figure 1. Image of Triton's South Polar cap, seen by *Voyager 2* in 1989.

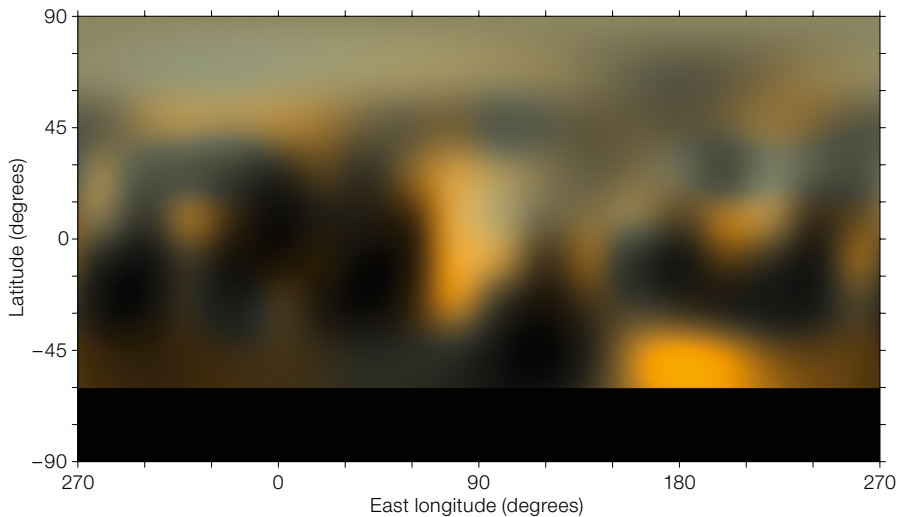


Figure 2. A map of Pluto from HST observations (from Buie et al., 2010). The brightest region near 180° longitude is suspected to be CO ice-rich.

atmospheric methane was achieved, using observations from the NASA Infrared Telescope at 1.67  $\mu\text{m}$  (Young et al., 1997). Pluto's atmosphere, on the other hand, has been much more studied from stellar occultations. Although these observations cannot identify a particular species and are also unable to probe the atmosphere down to the surface itself, occultations are an extremely powerful way of revealing the atmosphere's thermal structure. Pluto's upper atmosphere appears to be "warm"  $\sim 100$  K, as opposed to  $\sim 60$  K for Triton at the same pressure level), a likely effect of heating by methane (similar to ozone heating in the Earth's stratosphere). In contrast, Pluto's lower atmosphere and the way the upper atmosphere connects to the 40–60 K surface are poorly understood. Remarkably, repeated occultations showed that Pluto's atmosphere has expanded, roughly doubling in surface pressure, from 1988 to 2002, even though Pluto has started to recede from the Sun. Similarly, Triton's surface pressure has been shown to increase through the 1990s.

Despite these remarkable findings, the composition of the atmospheres of Triton

Figure 3. The spectrum of Pluto's atmosphere showing the fit to the  $2\nu_3$  band of methane, observed by CRIRES (from Lellouch et al., 2009).

and Pluto, and how they may change with time, remain very poorly characterised. Atmospheric methane was not re-observed and the search for additional compounds failed. In the last three years, however, CRIRES observations at the VLT have brought about very significant progress.

### CRIRES spectra of the atmospheres of Pluto and Triton

The unprecedented combination of sensitivity and spectral resolution in the NIR

offered by CRIRES makes it a very powerful instrument to study tenuous and distant atmospheres. During a first service run in August 2008, we obtained a high S/N detection of the  $2\nu_3$  band of methane at 1.67  $\mu\text{m}$  in Pluto's spectrum. As Pluto's atmospheric pressure is typically only  $\sim 15$   $\mu\text{bar}$ , lines are purely Doppler-broadened and the highest spectral resolution is desirable. We used a slit of 0.4 arcseconds, combined with the adaptive optics module MACAO, obtaining an effective spectral resolution of  $\sim 60\,000$ . This high resolution was also instrumental in separating the methane lines of Pluto from their telluric counterparts, so that methane lines from Pluto, interlinked within the Q-branch of the  $2\nu_3$  band of telluric methane (see Figure 3), could be observed. The quality of the spectrum (17 individual lines, including high- $J$  lines) made it possible to separate abundance and temperature effects in Pluto's spectrum (Lellouch et al., 2009). Pluto's mean methane temperature is 90 K, which implies that Pluto cannot have a deep and cold troposphere as had been proposed (otherwise the bulk of the methane would be at  $\sim 40$  K). By linking this to a re-analysis of occultation measurements, new constraints on the structure of Pluto's lower atmosphere and surface pressure could also be derived, indicating that Pluto's

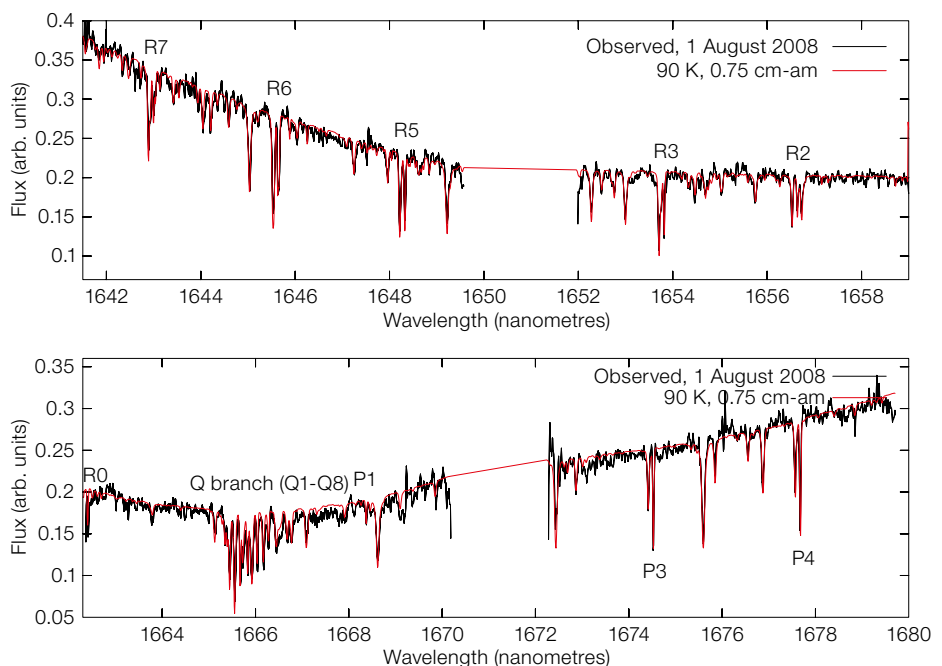
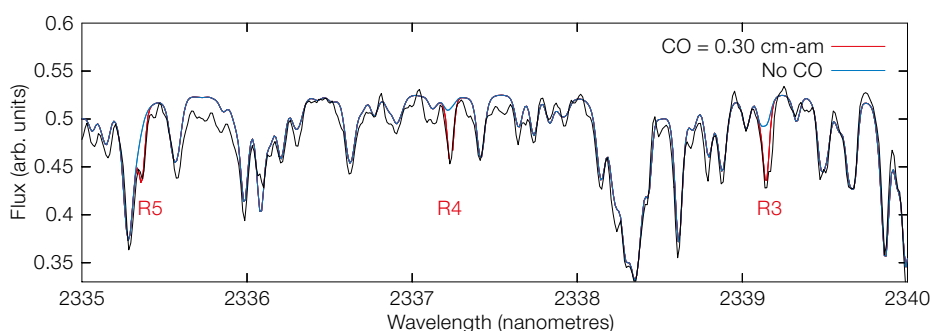


Figure 4. A section of Triton's spectrum in the 2.35  $\mu\text{m}$  range, as seen by CRIRES, showing the detection of CO in Triton's atmosphere (from Lellouch et al., 2010).

current pressure is between 6.5 and 24  $\mu\text{bar}$  (i.e. 40 000–150 000 less than on Earth), and that the  $\text{CH}_4$  atmospheric abundance ( $\text{CH}_4/\text{N}_2$  mixing ratio) is 0.5 %.

Encouraged by the instrument's capabilities, we decided to conduct a search for atmospheric CO on Triton and Pluto. The best spectral region to look for CO is the 2.35  $\mu\text{m}$  (2–0) band. In July 2009, after four hours of integration with CRIRES under excellent sky conditions, we detected a strong signal of this molecule in Triton's atmosphere (shown in Figure 4), indicating a  $\text{CO}/\text{N}_2$  abundance of about  $6 \times 10^{-4}$  (Lellouch et al., 2010). As a bonus, the spectrum, which has a S/N of  $\sim 80$ , showed many lines from the  $\nu_3 + \nu_4$  band of gaseous methane. This was the first time that methane had been observed at Triton since Voyager, and the data showed that the column density of methane had increased by a factor of about four since 1989. This is in line with the occultation results, and certainly results from a seasonal effect, with increased insolation on Triton's ice-covered Southern polar cap.

Obtaining a spectrum of similar quality for Pluto is very challenging, as Pluto is not only somewhat smaller than Triton, but very dark in  $K$ -band (geometric albedo  $\sim 0.2$  vs. 0.6 for Triton, due to strong methane ice absorption; see, for example, Figure 3 in Barucci et al., 2010). This warranted another dedicated run in July 2010, during part of which we experimented with the fast ("windowed") read-out mode of CRIRES. In this mode, only detectors 2 and 3 of CRIRES are read and windowed, resulting in a noticeable gain in sensitivity for faint targets. Overall, after 7 hours 20 minutes on source, we obtained a spectrum with a S/N of 15–20. This spectrum clearly showed the spectral signatures of methane, and hints for CO at the position of nine lines. When these lines are co-added, evidence for CO is obtained at  $6\sigma$  confidence (Lellouch et al., 2011), providing a likely detection — but not as obvious as on Triton. For completeness, let us add that the detection of CO in Pluto's atmosphere has been claimed independently by Greaves



et al. (2011) from James Clerk Maxwell Telescope observations, but their results are hard to understand and inconsistent with the CRIRES ones.

#### Surface–atmosphere interactions

Our results on the abundances of CO and  $\text{CH}_4$  in Pluto and Triton's atmospheres are summarised in Table 1, assuming current total pressures of 15 and 40  $\mu\text{bar}$ , respectively. They are compared to the abundances of these species measured in the surface. Note that the amounts of atmospheric  $\text{CH}_4$  and CO correspond to a few tens of nanobars only at 60–90 K. With hindsight, it is fascinating to think that CRIRES is able to measure these quantities on 0.1-arcsecond-sized objects 4.5 billion kilometres away!

Pluto's atmosphere is thus much ( $\sim 20$  times) richer in  $\text{CH}_4$  than Triton's — this explains the warmer stratosphere on Pluto; in contrast the two atmospheres have similar CO abundances. The same is true for the surface abundances, and the striking result in Table 1 is that within the measurement uncertainties (which are about 20–40% for  $\text{CH}_4$ , but as much as a factor 2–3 for CO, due to the difficulty of determining abundances from unresolved, saturated lines) for both species, the atmospheric and surface abundances are the same.

This result looks remarkably simple, yet was not anticipated at all. Since for the most part ices on the surface of Pluto

and Triton are dissolved in  $\text{N}_2$  to form a solid solution, one would expect from simple thermodynamics (Raoult's law) that their atmospheric mixing ratio would be equal to the ratio of their vapour pressures to that of  $\text{N}_2$ , multiplied by their ice phase abundance. Because CO and especially  $\text{CH}_4$  are less volatile than  $\text{N}_2$ , this would lead to atmospheric abundances much lower than observed (by a factor of about seven for CO and over three orders of magnitude for  $\text{CH}_4$ ). Therefore, surface–atmosphere interactions or exchanges must proceed in a different way. Essentially there are two means to explain the enhanced atmospheric  $\text{CH}_4$  and CO abundances.

The first explanation is that the enhanced atmospheric abundances result from the sublimation of pure patches of  $\text{CH}_4$  and CO ices. This is probably what occurs for  $\text{CH}_4$ , whose much lower volatility compared to  $\text{N}_2$  is expected to lead, over the course of seasonal sublimation–condensation cycles, to geographically segregated (warmer than the  $\text{N}_2$  ice)  $\text{CH}_4$  ice patches. Evidence for pure methane ice, co-existing with diluted methane, is in fact present in the surface spectra of Pluto (Douté et al., 1999). On Triton the case for pure methane is not as clear, but the longitudinal distribution of methane ice is known to be different from that of  $\text{N}_2$ . This suggests that, in a similar way to Pluto, a region, or regions, of enhanced  $\text{CH}_4$  possibly controls the  $\text{CH}_4$  atmospheric abundance. Calculations indicate that pure or enhanced  $\text{CH}_4$  patches covering typically a percent of

	Pluto		Triton	
	Atmosphere	Surface	Atmosphere	Surface
$\text{CH}_4/\text{N}_2$	$5 \times 10^{-3}$	$4 \times 10^{-3}$ <sup>(a)</sup>	$2.4 \times 10^{-4}$	$5 \times 10^{-4}$
$\text{CO}/\text{N}_2$	$5 \times 10^{-4}$	$1 \times 10^{-4}$	$6 \times 10^{-4}$	$1 \times 10^{-3}$

Table 1. Comparison of surface and atmospheric molecular abundances on Pluto and Triton.

<sup>(a)</sup> Pure methane is also present

the surface are sufficient to maintain the high methane abundance in both objects.

This “pure ice” scenario is probably not valid for CO, which is thermodynamically not expected to segregate from N<sub>2</sub> and can stay mixed with it in all proportions, and an alternative situation is likely to occur. For this second explanation, it is thought that seasonal cycles form a very thin (a few molecules) surface upper layer enriched in CO (Trafton et al., 1998) that inhibits the sublimation of the underlying main ice layer. Exchanges between this thin layer (termed “detailed balancing layer”) and the atmosphere lead to an atmospheric composition reflecting that of the volatile reservoir, as observed. Yet a mystery remains, as it seems that at least one very bright area on Pluto’s surface (Buie et al., 2010; and Figure 2) is associated with a CO ice-rich region. It is hoped that data from *New Horizons* in 2015 will provide more information on this bright spot and its possible connection with CO’s atmospheric abundance.

Validating these scenarios will require additional observations. Direct spatial

resolution on the discs of Pluto and Triton is not possible, yet repeated observations, taking advantage of their rotation, would allow one to search for possible longitudinal variability of the CH<sub>4</sub> and CO atmospheric content. A correlation with the appearance of the surface features and the longitudinal distribution of ices would strongly advocate for the “pure ice” scenario. Monitoring the evolution of the minor compounds in the atmosphere over the upcoming years will also further reveal the nature of atmosphere–surface interactions. In the future, spatially-resolved observations with an instrument such as SIMPLE on the ELT (Origlia & Oliva, 2009; Origlia et al., 2010) will permit direct imaging, constraining, for example, the latitudinal distribution of these atmospheres.

Studying Pluto and Triton’s atmospheres is not only interesting in itself, but it opens a window on this class of tenuous atmospheres dominated by sublimation equilibrium (of which Io is another example). Other ice-covered trans-Neptunian objects, especially the largest of them (Quaoar, Eris, Makemake), may have retained their volatiles over the age of the

Solar System (Schaller & Brown, 2007) and be able to develop atmospheres near perihelion. While such atmospheres have not yet been detected, searches are underway, especially from stellar occultations. Should they be discovered, spectroscopy with the Extremely Large Telescope (ELT) could play a pivotal role in characterising them.

#### References

- Barucci, M. A. et al. 2010, *The Messenger*, 141, 15  
Buie, M. W. et al. 2010, *AJ*, 139, 1128  
Douté, S. et al. 1999, *Icarus*, 142, 421  
Greaves, J. S., Helling, C. & Friberg, P. 2011, *MNRAS*, 414, L36  
Lellouch, E. et al. 2009, *A & A*, 495, L17. See also ESO PR-0809.  
Lellouch, E. et al. 2010, *A & A*, 512, L8. See also ESO PR-1015.  
Lellouch, E. et al. 2011, *A & A*, 511, L4  
Origlia, L. & Oliva, E. 2009, *Earth, Moon & Planets*, 105, 123  
Origlia, L., Oliva, E. & Maiolino, R. 2010, *The Messenger*, 140, 38  
Schaller, E. L. & Brown, M. E. 2007, *ApJ*, 659, L61  
Trafton, L. M., Matson, D.L. & Stansberry, J. A. 1998. In *Solar System Ices*, Kluwer Academic Publishers, 773  
Young, L. et al. 1997, *Icarus*, 153, 148



The giant planet Saturn, as observed with the VLT NACO adaptive optics instrument on 8 December 2001 when the planet was at a distance of 1209 million kilometres. The image is a composite of exposures in the near-infrared *H*- and *K*-bands and displays well the intricate, banded structure of the planetary atmosphere and the details of the ring system. The dark spot close to the south pole is approximately 300 km across and is a polar vortex. More details can be found in Release eso0204.

# Molecular and Dusty Layers of Asymptotic Giant Branch Stars Studied with the VLT Interferometer

Markus Wittkowski<sup>1</sup>

Iva Karovicova<sup>1</sup>

David A. Boboltz<sup>2</sup>

Eric Fossat<sup>3</sup>

Michael Ireland<sup>4, 5</sup>

Keiichi Ohnaka<sup>6</sup>

Michael Scholz<sup>7, 8</sup>

Francois van Wyk<sup>9</sup>

Patricia Whitelock<sup>9, 10</sup>

Peter R. Wood<sup>11</sup>

Albert A. Zijlstra<sup>12</sup>

<sup>1</sup> ESO

<sup>2</sup> United States Naval Observatory,  
Washington, DC, USA

<sup>3</sup> Laboratoire d'Université  
d'Astrophysique de Nice, France

<sup>4</sup> Dept. of Physics and Astronomy,  
Macquarie University, Sydney, Australia

<sup>5</sup> Australian Astronomical Observatory,  
Epping, Australia

<sup>6</sup> Max-Planck Institut für Radioastronomie,  
Bonn, Germany

<sup>7</sup> Zentrum für Astronomie, University of  
Heidelberg, Germany

<sup>8</sup> School of Physics, University of  
Sydney, Australia

<sup>9</sup> South African Astronomical Observa-  
tory, Cape Town, South Africa

<sup>10</sup> Astronomy Dept., University of Cape  
Town, Rondebosch, South Africa

<sup>11</sup> Australian National University,  
Canberra, Australia

<sup>12</sup> Jodrell Bank Centre for Astrophysics,  
University of Manchester, United  
Kingdom

Mass loss from asymptotic giant branch (AGB) stars is the most important driver for the evolution of low to intermediate mass stars towards planetary nebulae. It is also one of the most important sources of chemical enrichment of the interstellar medium. The mass-loss process originates in the extended atmosphere, whose structure is affected by stellar pulsations, and where molecular and dusty layers are formed. Optical interferometry resolves the extended atmospheres of AGB stars and thereby enables us to obtain measurements of the intensity profile across this region. We present an overview of recent results from our spectro-interferometric observations of AGB stars using the near- and mid-infrared instruments AMBER and MIDI of the VLT Interferometer.

Low to intermediate mass stars, including our Sun, evolve to red giant stars and subsequently to asymptotic giant branch stars after the hydrogen and helium supplies in the core have been exhausted by nuclear fusion. An AGB star is in the final stage of stellar evolution that is driven by nuclear fusion, where a degenerate carbon–oxygen core is surrounded by hydrogen- and helium-burning layers, a huge convective envelope and a very extended and diluted stellar atmosphere. Mass loss becomes increasingly important during AGB evolution, both for stellar evolution, and for the return of material to the interstellar medium. It reduces the convective stellar envelope until the star begins to shrink and evolves at constant luminosity toward the hotter post-AGB and planetary nebula (PN) phases, and is thus the most important driver for the further stellar evolution (e.g., Habing & Olofsson, 2003). Mass loss from AGB stars is also one of the most important sources for the chemical enrichment of the interstellar medium and of galaxies.

Depending on whether or not carbon has been dredged up from the core into the atmosphere, AGB stars appear in observations to have an oxygen-rich or a carbon-rich chemistry. A canonical model of the mass-loss process has been developed for the case of carbon-rich chemistry, where atmospheric carbon dust has a sufficiently large opacity to be radiatively accelerated and driven out of the gravitational potential of the star and where it drags the gas along. For the case of oxygen-rich chemistry, the details of this process are not understood, and are currently a matter of vigorous debate. Questions remain also for the carbon-rich case, such as regarding the formation of the recently detected oxygen-bearing molecule water in the inner atmospheres of carbon-rich AGB stars by the Herschel space mission (Decin et al., 2010).

AGB stars experience stellar pulsations, from semi-regular variable stars (SRVs) on the early AGB to large-amplitude long-period variable stars on the more evolved AGB, including Mira variables and more dust-enshrouded stars at the tip of the AGB. Pulsations and the induced shock fronts are expected to play a crucial role for the structure of the extended atmospheres, but the details of these processes

and their effects on the mass-loss mechanism are also not well understood. Because of the extension of the atmosphere, temperatures are cool enough so that molecules form, leading to a scenario where molecular layers lie above the continuum-forming photosphere. Dust is formed and believed to be accelerated within this extended atmospheric region with a certain condensation sequence, where dust species of higher condensation temperatures form closer to the stellar surface and dust species with lower condensation temperatures form at larger distances. There is also a notion that different dust species may prevail at different stages along the AGB, along with increasing stellar luminosity and increasing mass-loss rate.

Optical interferometry at near-IR and mid-IR wavelengths has proved to be a powerful tool to study the extended atmosphere and dust condensation zones of AGB stars, because of its ability to spatially resolve these regions. Indeed, red giants and AGB stars have historically been prime targets for optical interferometry, because of their brightness and the match of their angular size to the typical spatial resolution of optical interferometers. However, despite the long history of such measurements, they still continue to provide important new constraints on the open questions discussed above. In particular, the near-infrared (NIR) instrument AMBER and the mid-infrared (MIR) instrument MIDI of the VLT Interferometer (VLTI) have been shown to be well suited for new measurements of AGB stars because of their unprecedented ability to provide *spectro-interferometric* observations with spectral resolutions of 35–12 000 (AMBER) and 30–230 (MIDI). Here, we report on very recent results (Karovicova et al., 2011; Wittkowski et al., 2011) from our ongoing programme to characterise molecular and dusty layers of AGB stars using the VLTI instruments.

## Recent VLTI observations

VLTI observations of AGB stars using the instruments MIDI and AMBER started with the measurements described by Ohnaka et al. (2005) and Wittkowski et al. (2008), respectively. These studies

demonstrated that the spectro-interferometric capabilities of MIDI and AMBER are well suited to characterise the dusty and molecular layers of AGB stars.

We obtained MIDI data of the Mira variable AGB stars S Ori, GX Mon, RR Aql, R Cnc, and X Hya between 2004 and 2009. Some of these observations were aimed at performing a mid-infrared monitoring of AGB stars in order to investigate intracycle and cycle-to-cycle variability, and others were designed to complement AMBER observations to provide a more complete picture of the dusty and molecular layers at the same time. Mid-infrared interferometric monitoring of the sources listed above has been performed by Iva Karovicova during her PhD thesis, together with theoretical simulations of the expected variability. For example, the observations of RR Aql described in Karovicova et al. (2011) include 52 observations obtained at 13 epochs between April 2004 and July 2007 covering three pulsation cycles (Figure 1).

Using the AMBER instrument, we secured data of the Mira variables R Cnc, X Hya, W Vel, RW Vel, and RR Aql between 2008 and 2010 using the medium resolution mode with a spectral resolution of 1500. First results from these campaigns have been presented by Wittkowski et al. (2011).

Some of these observations were coordinated with concurrent VLBA observations of the SiO, H<sub>2</sub>O, and OH maser emission (observation epochs shown in Figure 1), which provide complementary information on the kinematics and geometry of the molecular layers in which the maser emissions originate.

### Structure of molecular layers

The medium resolution ( $R \sim 1500$ ) near-infrared AMBER observations of the Mira variables of our sample confirmed a characteristic wavelength-dependent shape of the visibility function that is consistent with earlier low resolution AMBER observations of S Ori and that can be understood within the molecular layer scenario. In this scenario, the opacity of molecular layers, at NIR wavelengths, most importantly H<sub>2</sub>O and CO, is larger at certain wavelengths

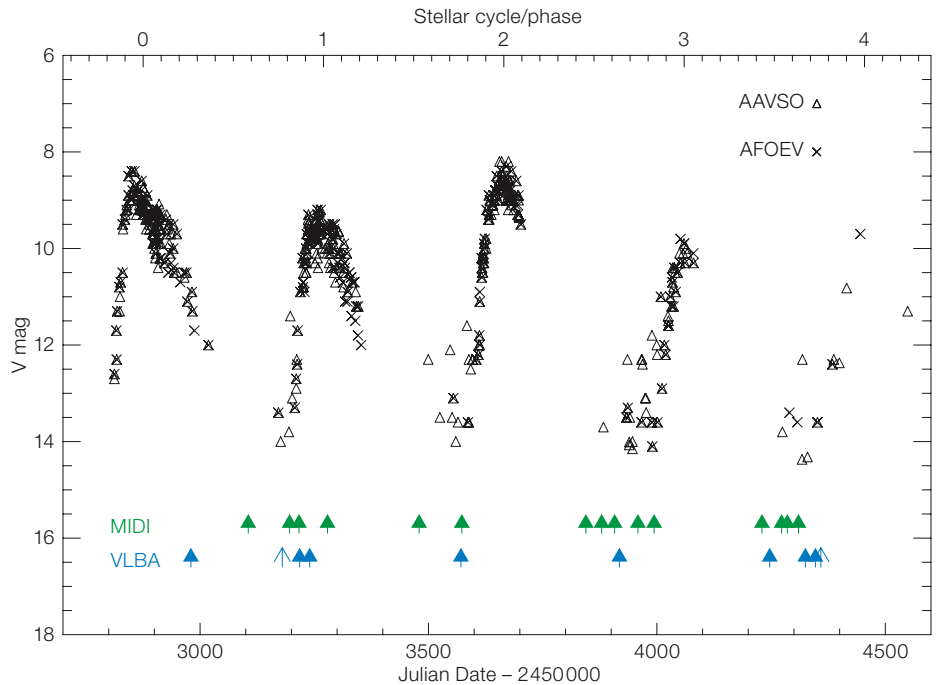
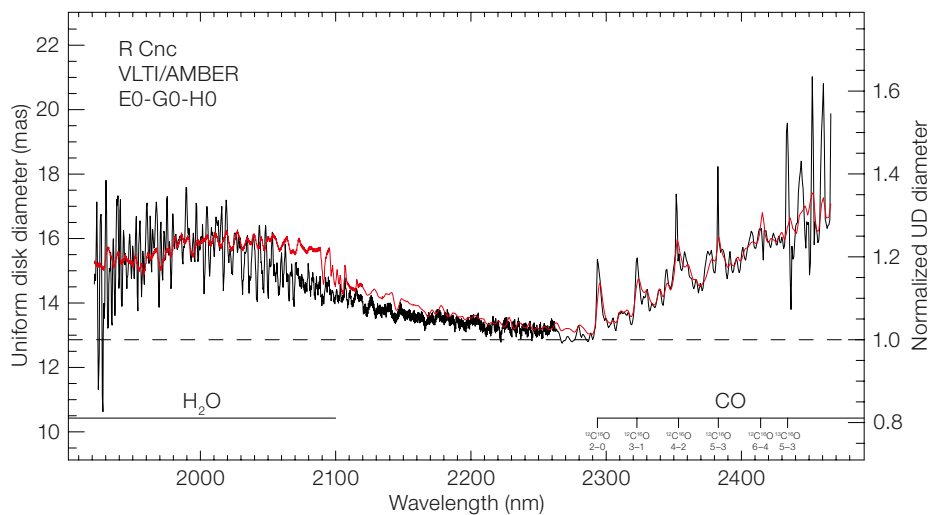


Figure 1. (Top) Visual light curve of RR Aql with our epochs of MIDI observations indicated in green. Epochs of Very Long Baseline Array (VLBA) observations are shown in blue. From Karovicova et al. (2011).

Figure 2. (Bottom) Uniform disc diameter as a function of wavelength obtained from VLT/AMBER observations of the Mira variable AGB star R Cnc. The red line denotes the best-fit prediction from the recent dynamical atmosphere model series CODEX. From Wittkowski et al. (2011).



so that the source appears larger and the visibility smaller, and lower at other wavelengths so that the source appears smaller and the visibility larger. Our observations confirm this effect, which has previously been detected by interferometric observations using a few narrowband filters. Hereby, the AMBER instrument has shown to be particularly well suited to further

study and to quantification of this effect because of its wide wavelength coverage with high spectral resolution. In our measurements, the corresponding wavelength-dependent uniform disc (UD) diameters show a minimum near the near-continuum bandpass at 2.25  $\mu$ m. They then increase by up to 30% toward the H<sub>2</sub>O band at 2.0  $\mu$ m and by up to

70% at the CO bandheads between 2.29  $\mu\text{m}$  and 2.48  $\mu\text{m}$ . Figure 2 shows the wavelength-dependent UD diameter for the example of the source R Cnc.

Recently, new dynamical model atmospheres for Mira variables were developed that are based on self-excited pulsation models and opacity-sampling radiation treatment (CODEX model series; Ireland et al., 2008; 2011), and which became available at the time of our data analysis. These models predict intensity profiles that are in excellent agreement with our visibility data and thus the uniform disc diameters, as also indicated in Figure 2. In order to estimate the effective temperatures of the sources at the time of our observations, we coordinated simultaneous near-infrared photometry at the South African Astronomical Observatory (SAAO). The effective temperature values obtained are consistent with those of the model atmospheres, as are the distances obtained from the radii and bolometric magnitudes. Altogether, the agreement of our observations with the CODEX model atmosphere series increases the confidence in the model approach, and thus in the scenario where the stratification of the extended atmosphere is largely determined by the pulsation that originates in the stellar interior and in which the molecular layers lie above the continuum-forming photosphere.

### Inhomogeneities in molecular layers

The AMBER closure phase functions of our targets exhibit significant wavelength-dependent non-zero values at all wavelengths (Figure 3 shows the example of R Cnc). Non-zero values of the closure phase are indicative of deviations from point symmetry. Our data confirm non-zero closure phase data of Mira variables that have been previously observed by other interferometers. Again, the AMBER data provide additional information, thanks to their spectro-interferometric nature, that helps to constrain where within the atmosphere the asymmetric structure originates. In fact, we observe a complex wavelength-dependent closure phase signal that correlates with the features of the molecular layers, most importantly  $\text{H}_2\text{O}$  and CO. This indicates a complex non-spherical stratification of the extended

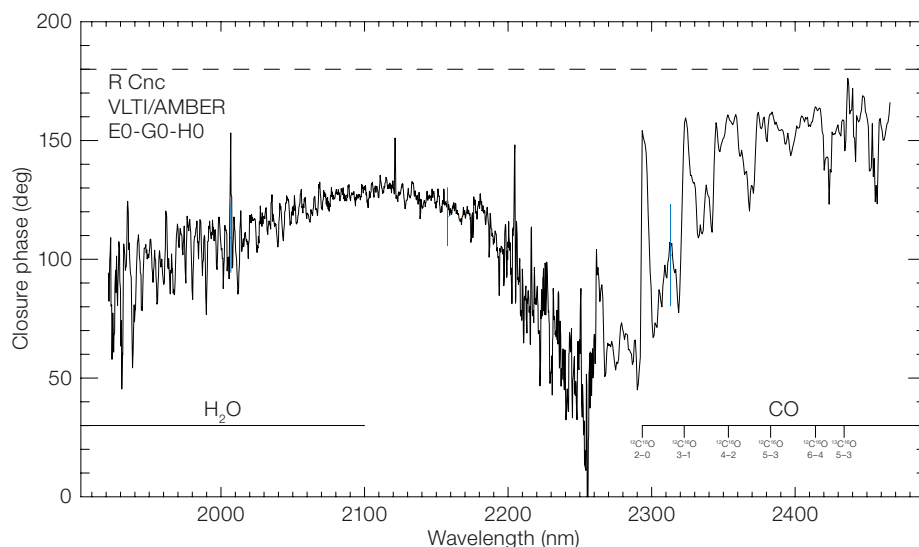


Figure 3. Closure phase as a function of wavelength for the example of the Mira variable AGB star R Cnc obtained with VLT/AMBER. From Wittkowski et al. (2011).

atmosphere, where inhomogeneities are present at distances where molecules are formed and where molecular emission originates.

With the limited amount of visibility data that we currently have, we cannot reconstruct the full morphology of the molecular layers. It would thus be important to conduct an interferometric imaging campaign of AGB stars at high spectral resolution. However, since the visibility data are overall well consistent with spherical models, we can already estimate that the deviation from point symmetry originates from substructure at a relatively low flux level for an overall spherical intensity distribution. For example, the values of R Cnc in the water vapour band shown in Figure 3 could be explained by an unresolved (up to 3 milliarcseconds [mas]) spot contributing 3% of the total flux at a separation of about 4 mas (for comparison, the photospheric diameter is estimated to 12 mas).

There are several physical mechanisms that may lead to asymmetric stellar surface structures. For our targets, we favour a scenario where the pulsation in the stellar interior induces chaotic motion in the outermost mass zones of the extended atmosphere that leads to different extensions of the mass zone on different sides

of the star, and thus to the observed inhomogeneities. An inhomogeneous or clumpy molecular environment in the extended atmosphere may have important implications for the non-LTE chemistry in this region and may help to understand the formation of certain molecules such as water in carbon-rich AGB stars (Decin et al., 2010). It may also be the source of observed clumpy molecular features in the circumstellar environment at larger distances.

### Variability of dusty layers

The observed MIDI visibility curves of RR Aql show significant wavelength dependence with a steep decrease from 8–9.5  $\mu\text{m}$  and a slow increase in the 9.5–13  $\mu\text{m}$  range. The shape of the 8–13  $\mu\text{m}$  flux spectrum with a maximum near 9.8  $\mu\text{m}$  is known to be a characteristic silicate emission feature. Our rich sample of MIDI data of RR Aql cover pulsation phases between 0.45 and 0.85, i.e. minimum to pre-maximum phases, for a total of three cycles. For many different pulsation cycles and phases, we obtained data at similar projected baseline lengths and position angles. This gives us a unique opportunity to perform a meaningful direct comparison of interferometric data obtained at different pulsation phases and cycles. An example of such a direct visibility comparison is shown in Figure 4.

We concluded that our data do not show any evidence of intracycle or cycle-to-

cycle visibility variations within the probed range of pulsation phases ( $\sim 0.45\text{--}0.85$ ) and within our visibility accuracies of about 5–20%. This implies either that the mid-infrared sizes of the molecular and dusty layers of RR Aql do not significantly vary within our phase coverage or that the conducted observations are not sensitive enough to detect such variations. The MIDI photometry exhibits a  $1\text{--}2\sigma$  signature of intracycle and cycle-to-cycle flux variations which are most pronounced toward the silicate emission feature at  $9.8\ \mu\text{m}$ . Additional observations with a dedicated mid-infrared spectrograph, such as the instrument VISIR at the VLT, are recommended to confirm the flux variations.

We performed a number of model simulations in order to investigate the visibility and photometry variations that are theoretically expected in the 8–13  $\mu\text{m}$  wavelength range for the typical parameters of RR Aql. We used a radiative transfer model of the dust shell where the central source is described by the dust-free dynamic model atmosphere series, as they were used to model the near-IR AMBER data. We varied model parameters such as the phase of the central atmosphere model and the opacity and inner radius of the dust shell to investigate the expected photometry and visibility variations during a pulsation cycle. An example of such a simulation is shown in Figure 5.

These model simulations show that visibility variations are indeed not expected for the parameters and observational settings of RR Aql at wavelengths of 8–13  $\mu\text{m}$  within the uncertainties of our observations. Variations in the flux spectra may in some cases just be detectable. Thus, our observational result of a constant visibility curve and only slightly varying flux spectra at wavelengths of 8–13  $\mu\text{m}$  are consistent with, and not contradicting, theoretical expectations of a pulsating atmosphere. We used our simulations as well to determine the best baseline configurations for the parameters of certain targets in order to optimise future interferometric observing campaigns that aim at characterising the small expected visibility variations.

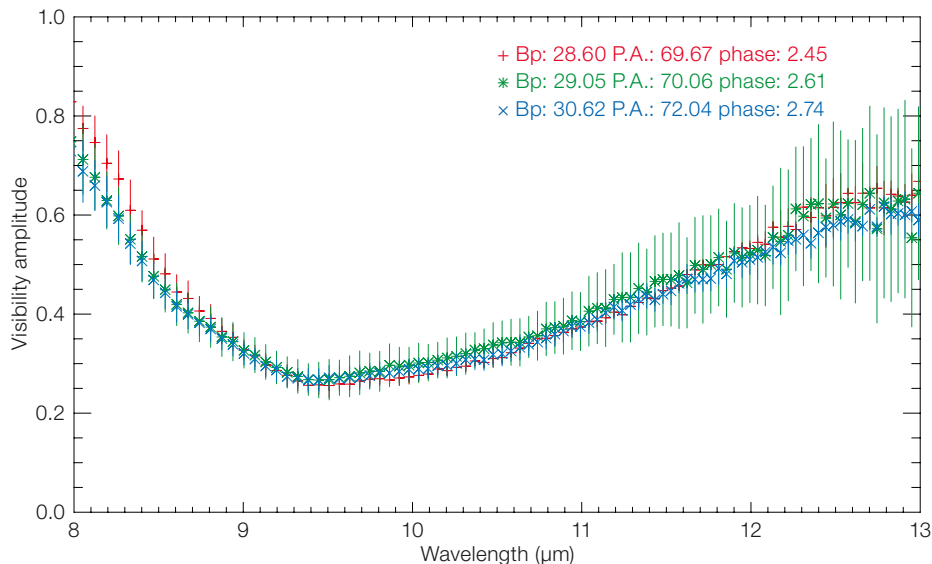


Figure 4. MIDI visibility amplitudes of RR Aql for different pulsation phases (indicated by different coloured points) within the same cycle, chosen to investigate intracycle visibility variations. From Karovicova et al. (2011).

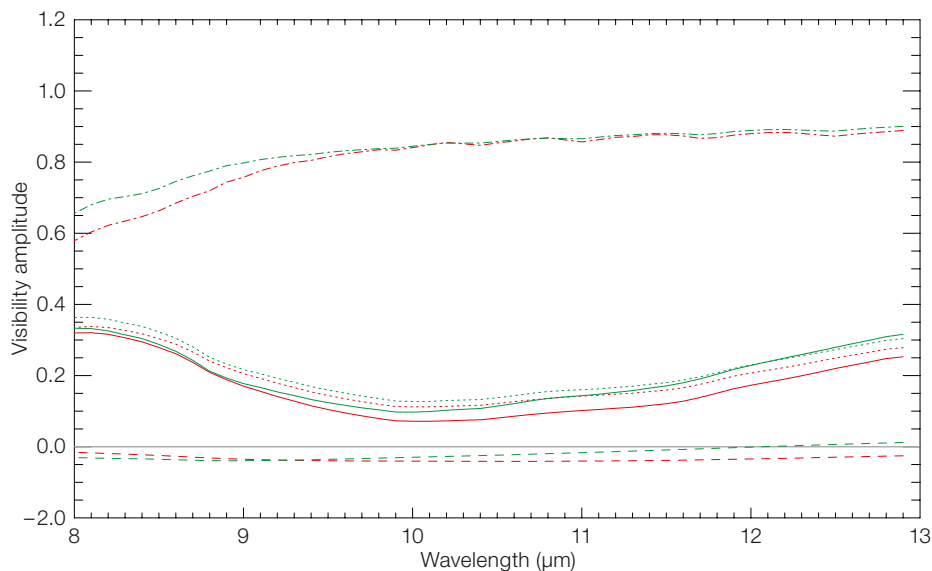


Figure 5. An example of expected intracycle visibility variation based on a simulation using two atmosphere models with a phase difference of 0.2 and a dust shell that is located closer to the star with a higher optical depth toward stellar minimum compared to stellar maximum. The solid green and red lines denote the two global models of this simulation, the dash-dotted lines the unattenuated stellar contribution, the dotted lines the attenuated stellar contribution and the dashed lines the dust shell contribution. From Karovicova et al. (2011).

### Characteristics of dusty layers

We characterised RR Aql's dust shell by using radiative transfer models of shells of  $\text{Al}_2\text{O}_3$  and/or silicate grains with independent inner radii and opacities, following earlier such attempts in the literature. We obtained best-fit results for RR Aql with a silicate shell alone. The addition of an  $\text{Al}_2\text{O}_3$  shell did not result in any improvement in the model fits. The best-fit model for our average pulsation phase of  $\Phi_V = 0.64 \pm 0.15$  includes a silicate dust shell with an optical depth of  $\tau_V = 2.8 \pm 0.8$  and an inner radius of  $R_{in} = 4.1 \pm 0.7 R_{phot}$  (where  $R_{phot}$  is the photospheric radius) and uses a central intensity profile corresponding to an atmosphere model with an effective temperature of 2550 K. Figure 6 shows a comparison of our radiative transfer model to the RR Aql visibility data of one of our epochs. We conclude that a radiative transfer model of the circumstellar dust shell that uses dynamical model atmospheres representing the central stellar source can reproduce well the spectral shape of both the visibility and the photometry data (not shown).

In addition to RR Aql, we determined best-fit dust shell parameters for other sources of our sample (S Ori, GX Mon, and R Cnc). The mid-IR visibility and spectra of each star can be described by an  $\text{Al}_2\text{O}_3$  dust shell with a typical inner

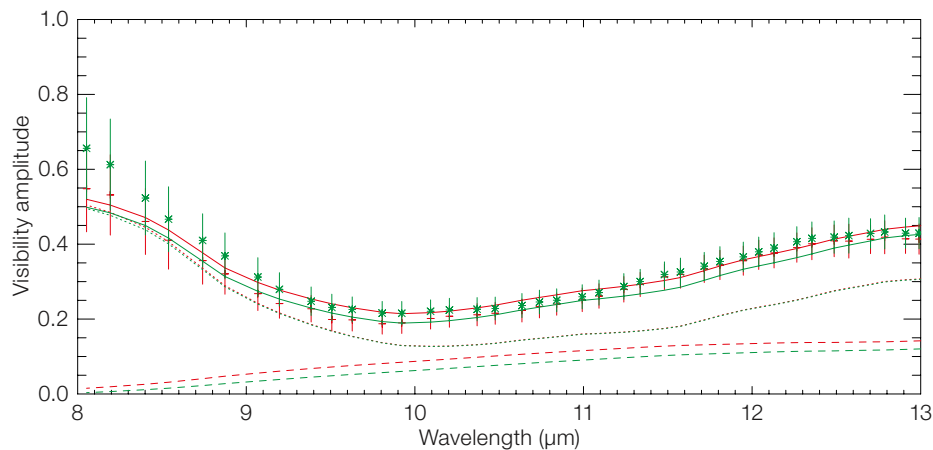


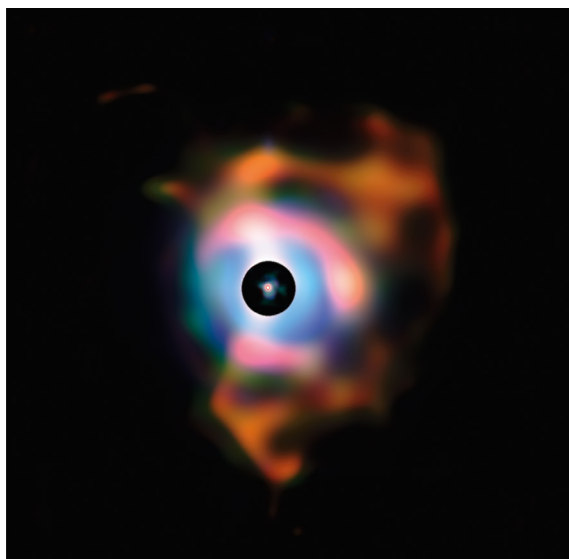
Figure 6. Radiative transfer model of RR Aql (solid lines) compared to the visibility data of one of our epochs including two observations. The solid lines indicate our best-fit model, while the contributions of the attenuated stellar and dust components alone are denoted by the dotted and dashed lines, respectively. From Karovicova et al. (2011).

radius of 2–2.5 stellar radii and/or a silicate dust shell with a typical inner radius of 4–5 stellar radii. This result is consistent with the scenario of a dust condensation sequence where  $\text{Al}_2\text{O}_3$  grains form closer to the stellar surface and silicate grains at larger radii, which is as well consistent with the condensation temperatures. Our best-fit values of the optical depths of the  $\text{Al}_2\text{O}_3$  and silicate dust shells together with the mass loss rates adopted from the literature may

confirm earlier suggestions of a sequence where the dust content of stars with low mass-loss rates is dominated by  $\text{Al}_2\text{O}_3$  grains, while the dust content of stars with high mass-loss rates predominantly exhibit substantial amounts of silicates.

### References

- Decin, L. et al. 2010, *Nature*, 467, 64
- Habing, H. J & Olofsson, H. 2003, *Astronomy and astrophysics library*, New York, (Berlin: Springer)
- Ireland, M. et al. 2008, *MNRAS*, 391, 1994
- Ireland, M. et al. 2011, *MNRAS*, in press (arXiv 1107.3619)
- Karovicova, I. et al. 2011, *A&A*, 532, A134
- Ohnaka, K. et al. 2005, *A&A*, 429, 1057
- Wittkowski, M. et al. 2008, *A&A*, 479, L21
- Wittkowski, M. et al. 2011, *A&A*, 532, L7



A composite of images from VISIR and NACO of the red supergiant star Betelgeuse. The image is 5.63 by 5.63 arcseconds in extent and shows the extension of the nebula around the star to be some 26 milli-parsec (550 AU). The supergiant star itself is resolved by interferometry at 44 milli-arcseconds (3.4 AU). The larger image is taken with VISIR in thermal-infrared filters sensitive to dust emission and the compact image (inside the occulting spot) is taken with NACO in *J*-, *H*- and *K*-band filters. Some of the non-spherically symmetric eruptions close to the star in the NACO image can be traced to much larger distances in the VISIR image. More details can be found in Kervella et al., *A&A*, 531, 117, 2011 and in Release eso1121.

# Science Results from the VISTA Survey of the Orion Star-forming Region

Monika Petr-Gotzens<sup>1</sup>  
 Juan Manuel Alcalá<sup>2</sup>  
 Cesar Briceño<sup>3</sup>  
 Eduardo González-Solares<sup>4</sup>  
 Loredana Spezzi<sup>5</sup>  
 Paula Teixeira<sup>1</sup>  
 María Rosa Zapatero Osorio<sup>6</sup>  
 Fernando Comerón<sup>1</sup>  
 Jim Emerson<sup>7</sup>  
 Simon Hodgkin<sup>4</sup>  
 Gaitée Hussain<sup>1</sup>  
 Mark McCaughrean<sup>5</sup>  
 Jorge Melnick<sup>1</sup>  
 Joanna Oliveira<sup>8</sup>  
 Suzanne Ramsay<sup>1</sup>  
 Thomas Stanke<sup>1</sup>  
 Elaine Winston<sup>9</sup>  
 Hans Zinnecker<sup>10</sup>

<sup>1</sup> ESO

<sup>2</sup> INAF–Osservatorio di Capodimonte, Napoli, Italy

<sup>3</sup> Centro de Investigaciones de Astronomía (CIDA), Mérida, Venezuela

<sup>4</sup> Institute of Astronomy, Cambridge, United Kingdom

<sup>5</sup> European Space Agency (ESTEC), Noordwijk, the Netherlands

<sup>6</sup> Centro de Astrobiología, Instituto Nacional de Técnica Aeroespacial (CSIC-INTA), Madrid, Spain

<sup>7</sup> Astronomy Unit, Queen Mary, University of London, United Kingdom

<sup>8</sup> Astrophysics Group, Keele University, United Kingdom

<sup>9</sup> School of Physics, University of Exeter, United Kingdom

<sup>10</sup> SOFIA Science Center, NASA-Ames, Moffett Field, USA

As part of the VISTA Science Verification programme, a large set of images in Orion was obtained at five near-infrared wavelength bands, from 0.9 to 2.2  $\mu\text{m}$ . The resulting multi-band catalogue contains approximately three million sources, allowing investigation of various issues concerning star and brown dwarf formation, such as a) the difference in the shape of the substellar mass function in a cluster vs. non-clustered environment, b) the influence of massive OB stars on the process of brown dwarf formation, c) the size and morphology of dust envelopes around protostars, and d) the comparative role of mass and environment

on the evolution of circumstellar discs. The data from the VISTA Orion Survey, including catalogues, are available to the community. In this article we present an overview of selected science results that have emerged so far from this survey.

In order to fully understand the star formation history of a star-forming region, it is of the highest importance to obtain a complete census of its entire stellar and substellar populations since the earliest epoch of star formation. For the large majority of stars in our Galaxy the complex process of star formation takes place in giant molecular clouds (GMCs), from which typically several generations of stars are formed sequentially. Comparative observational studies across these populations of differing age are fundamental to elucidate issues such as the timescales for circumstellar (protoplanetary) disc evolution, environmental effects leading to possible non-universality of the low-mass end of the initial (sub-) stellar mass function (IMF) and the timescales for the dispersal of stellar ensembles. Wide-field imaging surveys in the infrared are the best means to accomplish such large-scale studies systematically and consistently homogeneously.

The Orion star-forming region is an ideal target for studying almost all aspects related to the physics of star formation, early stellar evolution or the interplay between OB associations and the ISM (c.f., Bally, 2008). It is the closest GMC, at an average distance of 400 parsecs (pc), and has been actively forming stars within at least the last  $\sim 10$  Myr, which is also the approximate timescale on which giant planets are thought to be formed. A particularly interesting region for the purpose of a wide-field survey, investigating stellar and substellar properties in different evolutionary stages and environments, is the region around the Orion Belt stars.

The Belt is a prominent part of the constellation of Orion and is marked by three luminous OB stars, namely  $\zeta$  Ori (Alnitak),  $\epsilon$  Ori (Alnilam) and  $\delta$  Ori (Mintaka), from east to west. To the east of  $\zeta$  Ori there are very young populous stellar clusters, like NGC 2024, which is still partly embedded

in the Orion molecular cloud (OMC) B and which has an age of one million years or less. Nearly one degree southwest of  $\zeta$  Ori there is the well-known intermediate-age cluster  $\sigma$  Ori (age  $\sim 3$  Myr), while members of the slightly older Ori OB 1b association ( $\sim 5$  Myr) populate a wide area around the Belt stars over a few degrees on the sky and are found “off” the main molecular clouds (Briceño, 2008). Only recently, yet another group of kinematically distinct young stars has been identified northwest of  $\delta$  Ori, which is the group of  $\sim 10$ -Myr-old stars around the B-type star 25 Ori (Briceño et al., 2007).

Using VISTA, the world’s largest near-infrared survey facility (Emerson et al., 2006), which provides a field of view of  $\sim 1$  by 1.5 degrees, we have carried out a deep multiwavelength survey of a large region around the Orion Belt stars. This survey has delivered a new census of very low-mass stars and brown dwarfs and detected new brown dwarf candidates down to  $\sim 3$ –4 Jupiter masses at an age of 3 Myr. The advantageous location of Orion below the Galactic Plane and almost in the direction of the Galactic anti-centre implies that the contamination by foreground and background stars is low.

## Survey strategy, observations and data reduction

The survey consists of  $Z$ ,  $Y$ ,  $J$ ,  $H$ ,  $K_s$  images obtained during 14 nights between 16 October and 2 November 2009. The survey area is a mosaic of 20 VISTA fields covering a total of 30 square degrees around the Orion Belt stars; the surveyed area is shown in Figure 1a. Whenever possible the observations in all filters were carried out sequentially for one field, before observing the next field. The one VISTA field that included the young stellar group 25 Ori was imaged up to 23 times at  $J$ - and  $H$ -bands with the aim of detecting the photometric variability among the very low-mass stars and brown dwarf members of the 25 Ori group. More details on the observing strategy, the exposure times per filter and particular observing patterns were described in Arnaboldi et al. (2010). Figure 1b shows as an example of the data, a colour-

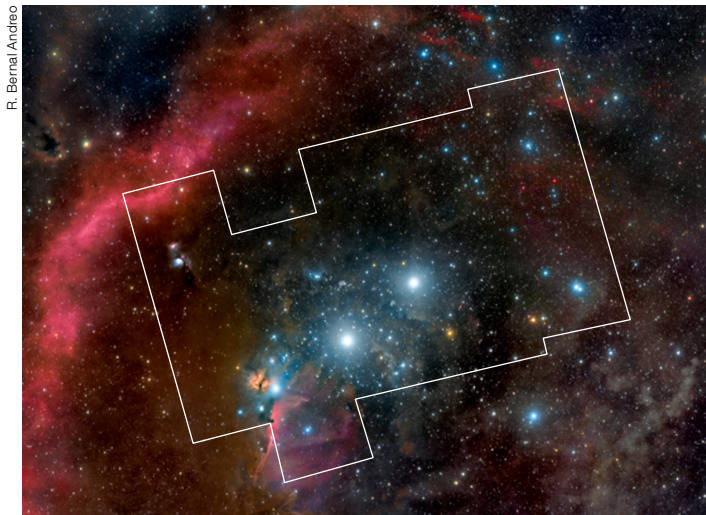


**Figure 1a.** The boundary of the VISTA Orion Survey is indicated in white, overplotted on an optical image. The size of the image is 10.5 by 8.4 degrees and the orientation is north up, east left.

composite image of the young cluster NGC 2071.

The amount of data collected for the VISTA Orion Survey was 559 Gigabytes, not including calibration data, clearly making data handling and reduction a challenge. The data reduction was performed by a dedicated pipeline, developed within the VISTA Data Flow System (VDFS), and run by the Cambridge Astronomy Survey Unit (CASU). The pipeline delivers science-ready stacked images and mosaics, as well as photometrically and astrometrically calibrated source catalogues. A total of 3.2 million sources was detected in the VISTA Orion Survey.

The photometric calibration was deduced from 2MASS photometry. The photometric errors are usually below 5% and the overall  $5\sigma$  limiting magnitudes of the survey are  $Z \sim 22.5$  mag,  $Y \sim 21.2$  mag,  $J \sim 20.4$  mag,  $H \sim 19.4$  mag,  $Ks \sim 18.6$  mag; different parts of the survey can have slightly better or poorer limits due to varying observing conditions. Additional data taken at  $Z$ - and  $J$ -bands for the field centred on the cluster  $\epsilon$  Ori significantly improved the sensitivity, and achieved  $5\sigma$  limits of  $Z \sim 22.9$  mag and  $J \sim 21.4$  mag. To further estimate the completeness, artificial stars of different magnitudes were added to the images and the statistics of the re-detected stars were used to estimate the completeness limits as a func-

tion of magnitude. In this way we find that the survey should have detected, for a population as young as 1 Myr, essentially all objects down to around six Jupiter masses in a region showing less than 1 mag of visual interstellar extinction.

### Selected science results

#### Young very low-mass stars and brown dwarfs close to $\epsilon$ Ori

The photometric identification of the lowest mass objects has greatly benefitted from the broad wavelength coverage of the survey. With inclusion of the  $Z$  and  $Y$  filters, the lowest-mass objects stand out in colour-magnitude diagrams involving those bands, appearing in a region inaccessible to other objects regardless of their reddening. This feature is caused by the appearance of small dust particles in the atmospheres of objects cooler than 2500 K, which causes a steep reddening of the colours involving wavelengths shorter than the  $J$ -band with decreasing temperature, while the spectral energy distribution at longer wavelengths remains nearly unchanged.

The photometric analysis of a  $\sim 1$  square degree region close to the B0 supergiant  $\epsilon$  Ori, in a  $Z$ - $J$  versus  $Z$  colour-magnitude diagram revealed a high number of potentially young substellar objects (Figure 2, shown as blue squares). These candidate brown dwarfs populate a



**Figure 1b.** VISTA colour image of the young stellar cluster NGC 2071 located in the Orion molecular cloud B (in the northeast of the surveyed area in Figure 1a). The size of the image is  $\sim 16 \times 16$  arc-minutes and shows a three colour composite ( $Z$  – blue,  $J$  – green,  $Ks$  – red). Orientation as Figure 1a.

sequence that clearly separates from the older main sequence objects of the surrounding general field. In the same figure the position of the spectroscopically-confirmed T Tauri stars, the higher mass counterparts to the brown dwarfs, are plotted (green diamonds in Figure 2), showing convincingly that the candidate brown dwarf sequence is an extension of the higher mass pre-main sequence stars. Note that the gap in between T Tauri stars and brown dwarfs is artificial and due to the selection criteria on one side and the spectroscopic sensitivity limit on the other side. A similar sequence of pre-main sequence objects in the  $\epsilon$  Ori cluster has previously been reported by some authors from an analysis of optical colour-magnitude diagrams (Caballero & Solano, 2008; Scholz & Eislöffel, 2005).

Employing the full wavelength range of the survey, it can be further tested whether the spectral energy distribution of the candidate brown dwarfs is indeed consistent with brown dwarf atmosphere models. One example is shown in Figure 3, where the 0.9 to 2.2  $\mu\text{m}$  fluxes of one of the brown dwarf candidates from Figure 2 is compared to the theo-

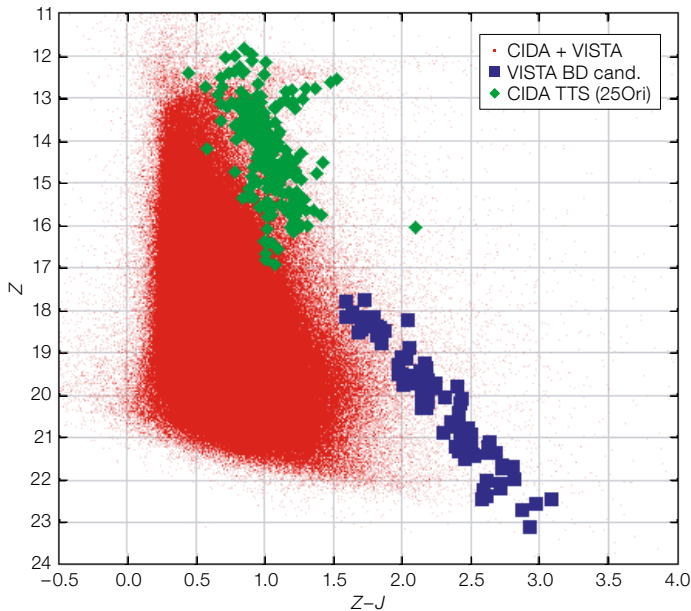


**Figure 2.** Colour–magnitude diagram of brown dwarf candidates (blue) close to  $\epsilon$  Ori. The red dots show field objects, mostly fore- and background dwarfs and giants, in the Orion Belt region, detected in the VISTA Orion Survey and having optical counterparts in the CIDA catalogue (Briceño et al., 2005; 2011). Spectroscopically confirmed T Tauri star (TTS) members of the 10-Myr-old group around 25 Ori are plotted as green points; the brown dwarf (BD) candidates may have a similar age.

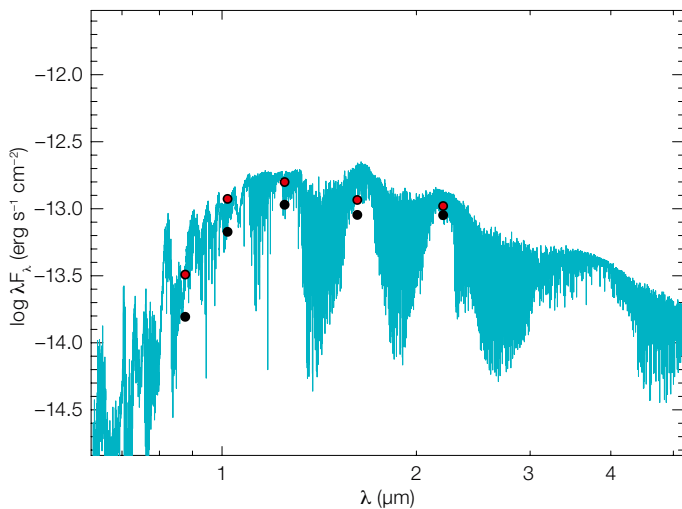


**Figure 3.** Spectral energy distribution of a candidate brown dwarf in the  $\epsilon$  Ori cluster. Black dots are the observed fluxes, while the red dots are the fluxes dereddened with  $A_V = 1.5$  mag. The spectral energy distribution model of a source with  $T_{\text{eff}} = 2500$  K,  $L = 7.9 \times 10^{-4} L_{\odot}$ , at a distance of 420 pc is shown in cyan (model from Allard et al., 2001).

retical flux distribution of a source with  $T_{\text{eff}} = 2500$  K,  $L = 7.9 \times 10^{-4} L_{\odot}$  — the overall agreement is quite good, supporting the brown dwarf nature of the candidate. A further step would be the assignment of masses to all the candidate brown dwarfs in order to extract the substellar IMF. This, however, is difficult from the colour–magnitude diagram alone, because the isochrones are very tightly bunched together in the low-mass regime and the age of the brown dwarf candidates are thus not well constrained. Hence assigning masses is very uncertain although future spectroscopy may help constrain them by probing surface gravity sensitive features.

### The $\sigma$ Ori cluster

The  $\sigma$  Ori cluster is one of the most studied clusters in Orion. It is essentially free of gas and dust, making the study of its stellar and substellar content little affected by interstellar extinction. Due to its youth ( $\sim 3$  Myr) substellar objects of  $\sigma$  Ori are relatively easy to detect, because they are brightest when they are young. The VISTA Orion Survey detected the well known T-dwarfs S Ori 70 and S Ori 73 (Peña Ramírez et al., 2011) and has been further explored to identify the lowest mass brown dwarfs, the L- and T-dwarfs, in a circular area of radius 30 arcmin around the bright, multiple star  $\sigma$  Ori. Photometric candidates were selected

from the  $Z$ - $J$  versus  $J$  colour–magnitude diagram (Figure 4). Out of 106 selected brown dwarf candidates, 37 are candidate free-floating planetary mass objects (6–13 Jupiter masses). Of the latter, 23 are new VISTA discoveries and have near-infrared colors compatible with spectral types L and T. All the new detections are fainter than  $J \sim 18.5$  mag, which indicates they are on the planetary mass boundary or below, assuming they are members of the 3-Myr-old  $\sigma$  Ori cluster.

### Scattered light images of protostellar envelopes

The youngest stellar objects are typically surrounded by large dusty discs and infalling envelopes and are located at or close to the cores of the molecular cloud. They represent the earliest phase of stellar evolution. About 350 such protostars (class 0 to class I sources), distributed all over the Orion molecular clouds A and B, have been identified by Spitzer imaging (Megeath et al., 2005; Allen et al., 2007). For several of the protostars located in parts of the Orion molecular cloud B which were covered by the VISTA Orion Survey, large extended scattered emission from protostellar envelopes was detected in the images.

One of the best examples is the edge-on disc and associated bipolar envelope of the source HOPS333 shown in Figure 5. The diameter of the envelope, as seen in the deep VISTA images, is roughly 2500 astronomical units (AU). The central protostellar source was detected with Spitzer in all IRAC bands, i.e. from 3.6 to 8.0  $\mu\text{m}$ , as well as with MIPS at 24  $\mu\text{m}$ . The 24  $\mu\text{m}$  flux of HOPS333 is 20 mJy, but it has not been detected in deep submillimetre continuum maps, suggesting that HOPS333 is a slightly more evolved protostellar object.

### A serendipitous re-discovery: Berkeley 20

Northeast of  $\delta$  Ori we detected a local stellar density enhancement, which turned out to be the Galactic old open cluster Berkeley 20. Most recently, Berkeley 20 has been studied at optical wavelengths by Andreuzzi et al. (2011) who determined an age of  $\sim 5$  Gyr and a distance of 8.7 kpc. In Figure 6 we plot the VISTA colour–magnitude diagram of Berkeley 20 for stars within one cluster

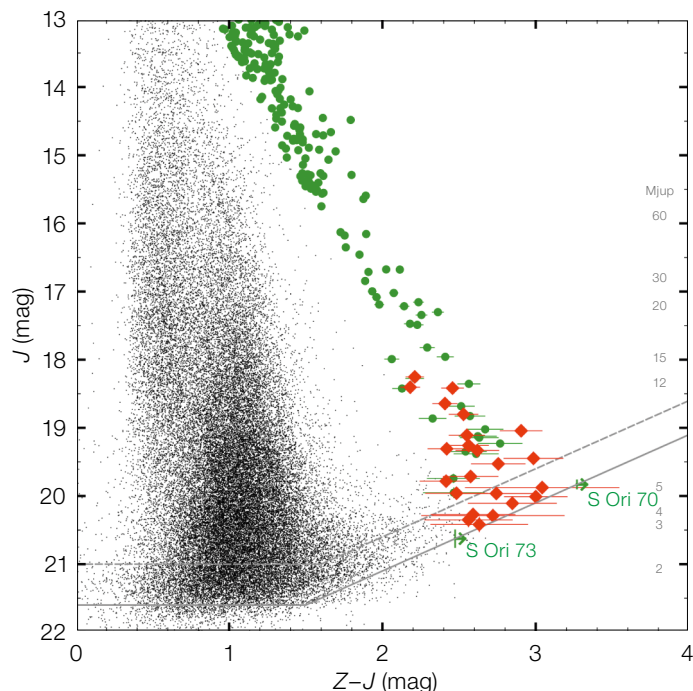


Figure 4. Colour-magnitude diagram of a 0.78 square degree field centred on  $\sigma$  Ori (Peña Ramírez et al. 2012, in prep.). Green dots are previously known very low-mass stars and red diamonds indicate new brown dwarf detections from the VISTA Orion Survey. The grey solid and dashed lines are the  $4\sigma$  and  $10\sigma$  detection limits. Object masses are labelled on the right of the diagram based on (sub-) stellar evolutionary models from the Lyon group (Chabrier et al., 2000; Baraffe et al., 2003).

radius (1.8 arcminutes) of the cluster centre; the cluster radius has been determined based on the  $K_s$ -band radial stellar density distribution. The 5 Gyr isochrones from the stellar evolutionary models of Girardi et al. (2002) are overplotted. Both isochrones, for metallicity  $[M/H] = -0.6$  as well as for  $[M/H] = -0.3$ , fit the stellar

sequence quite well. Spectroscopic observations of two cluster members confirm a metallicity of  $[M/H] = -0.45$  (Sestito et al., 2008). From isochrone fitting we derive a distance of 8.4 kpc for Berkeley 20 with an interstellar extinction of 0.32 mag, in agreement with previously published values.

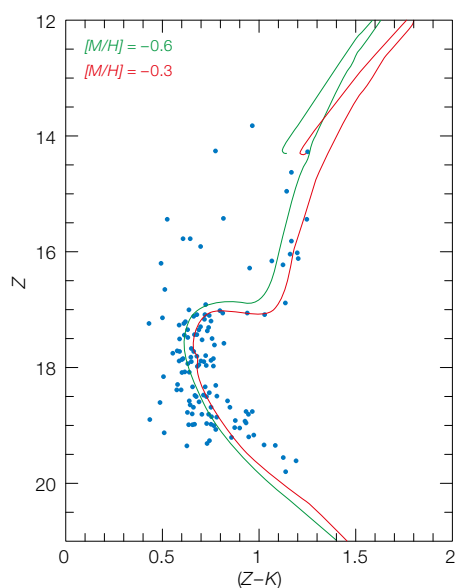


Figure 6. Colour-magnitude diagram of the Galactic old open cluster Berkeley 20, which was serendipitously re-discovered in the VISTA Orion Survey. Both isochrones represent a 5-Gyr population (Girardi et al., 2002), but at different metallicity, as indicated.

#### Outlook and data access

Further analysis of the full census of candidate very low-mass stars and brown dwarfs over the whole survey area is underway. Detailed investigations of the stellar and substellar content of the youngest stellar clusters imaged in the survey, e.g., NGC 2071, NGC 2068 and NGC 2024, will discuss their substellar IMFs out to large cluster radii. Spectroscopic follow-up of circumstellar discs surrounding cluster stars and brown dwarfs will allow the physical properties of these objects to be characterised in great detail. Complementary data from Spitzer and/or Chandra and XMM will help to distinguish young Orion sources from field stars. About one third of the sources, i.e. roughly one million objects, in the full area catalogue, have been classified as extended, suggesting that these are most likely background galaxies. All of these await scientific exploitation.



Figure 5. Three colour composite image ( $Z, J, K_s$ ) centred on the protostar HOPS333. Clearly visible is a dark central obscuration, indicating an edge-on disc, and a large bipolar envelope structure showing up in scattered near-infrared light. The full size of this image is  $\sim 18$  arcseconds, which corresponds to almost 8000 AU at the distance of the Orion B molecular cloud.

Access to the data products, including images and source catalogues, will be available via the ESO Archive Query Interfaces for Phase 3 ingested data products at: [http://archive.eso.org/wdb/wdb/adp/phase3\\_vircam/form](http://archive.eso.org/wdb/wdb/adp/phase3_vircam/form)

#### Acknowledgements

We gratefully thank Karla Y. Peña Ramírez and Victor J. Sanchez Bejar for providing Figure 4. We also very much appreciate the great work done by the VISTA consortium who built and commissioned the VISTA telescope and camera.

#### References

- Allard, F. et al. 2001, *ApJ*, 556, 357
- Allen, L. et al. 2007, in *Protostars and Planets V*. Eds. B. Reipurth, D. Jewitt, & K. Keil, Univ. Arizona Press, Tucson, p.361
- Andreuzzi, G. et al. 2011, *MNRAS*, 412, 1265
- Arnaboldi, M. et al. 2010, *The Messenger*, 139, 6
- Bally, J. 2008, in *Handbook of Star Forming Regions Vol. 1*, ed. B. Reipurth, ASP, p. 459
- Baraffe, I. et al. 2003, *A&A*, 402, 701
- Briceño, C. et al. 2005, *AJ*, 129, 907
- Briceño, C. et al. 2007, *ApJ*, 661, 1119
- Briceño, C. 2008, in *Handbook of Star Forming Regions Vol. 1*, ed. B. Reipurth, ASP, p. 838
- Briceño, C. et al. 2011, in preparation
- Caballero, J. A. & Solano, E. 2008, *A&A*, 485, 931
- Chabrier, G. et al. 2000, *ApJ*, 542, 464
- Emerson, J., McPherson, A. & Sutherland, W. 2006, *The Messenger*, 126, 41
- Girardi, L. et al. 2002, *A&A*, 391, 195
- Megeath, S. T. et al. 2005, *IAUS*, 227, 383
- Peña Ramírez, K. et al. 2011, *A&A*, 532, 42
- Scholz, A. & Eislöffel, J. 2005, *A&A*, 429, 1007
- Sestito, P. et al. 2008, *A&A*, 488, 943

# The VLT FLAMES Tarantula Survey

Chris Evans<sup>1</sup>  
 William Taylor<sup>2</sup>  
 Hugues Sana<sup>3</sup>  
 Vincent Hénault-Brunet<sup>2</sup>  
 Tullio Bagnoli<sup>3</sup>  
 Nate Bastian<sup>4</sup>  
 Joachim Bestenlehner<sup>5</sup>  
 Alceste Bonanos<sup>6</sup>  
 Eli Bressert<sup>7, 8, 9</sup>  
 Ines Brott<sup>10</sup>  
 Michael Campbell<sup>2</sup>  
 Matteo Cantiello<sup>11</sup>  
 Giovanni Carraro<sup>8</sup>  
 Simon Clark<sup>12</sup>  
 Edgardo Costa<sup>13</sup>  
 Paul Crowther<sup>14</sup>  
 Alex de Koter<sup>3, 15</sup>  
 Selma de Mink<sup>16, 17</sup>  
 Emile Doran<sup>14</sup>  
 Philip Dufton<sup>18</sup>  
 Paul Dunstall<sup>18</sup>  
 Miriam García<sup>19, 20</sup>  
 Mark Gieles<sup>21</sup>  
 Götz Gräfenor<sup>5</sup>  
 Artemio Herrero<sup>19, 20</sup>  
 Ian Howarth<sup>22</sup>  
 Rob Izzard<sup>11</sup>  
 Karen Köhler<sup>11</sup>  
 Norbert Langer<sup>11</sup>  
 Daniel Lennon<sup>23</sup>  
 Jesús Maíz Apellániz<sup>24</sup>  
 Nevena Markova<sup>25</sup>  
 Paco Najarro<sup>26</sup>  
 Joachim Puls<sup>27</sup>  
 Oscar Ramirez<sup>3</sup>  
 Carolina Sabín-Sanjulián<sup>19, 20</sup>  
 Sergio Simón-Díaz<sup>19, 20</sup>  
 Stephen Smartt<sup>18</sup>  
 Vanessa Stroud<sup>12, 28</sup>  
 Jacco van Loon<sup>29</sup>  
 Jorick S. Vink<sup>5</sup>  
 Nolan Walborn<sup>16</sup>

<sup>1</sup> United Kingdom Astronomy Technology Centre, STFC, Royal Observatory, Edinburgh, United Kingdom

<sup>2</sup> Scottish Universities Physics Alliance, Institute for Astronomy, University of Edinburgh, United Kingdom

<sup>3</sup> Astronomical Institute Anton Pannekoek, University of Amsterdam, the Netherlands

<sup>4</sup> Excellence Cluster Universe, Garching, Germany

<sup>5</sup> Armagh Observatory, Northern Ireland, United Kingdom

<sup>6</sup> National Observatory of Athens, Greece

<sup>7</sup> School of Physics, University of Exeter, United Kingdom

<sup>8</sup> ESO

<sup>9</sup> Harvard–Smithsonian Center for Astrophysics, Cambridge, USA

<sup>10</sup> Department of Astronomy, University of Vienna, Austria

<sup>11</sup> Argelander-Institut für Astronomie der Universität Bonn, Germany

<sup>12</sup> Department of Physics and Astronomy, The Open University, Milton Keynes, United Kingdom

<sup>13</sup> Departamento de Astronomía, Universidad de Chile, Santiago, Chile

<sup>14</sup> Department of Physics & Astronomy, University of Sheffield, United Kingdom

<sup>15</sup> University of Utrecht, the Netherlands

<sup>16</sup> Space Telescope Science Institute, Baltimore, USA

<sup>17</sup> Hubble Fellow

<sup>18</sup> Department of Physics & Astronomy, Queen's University Belfast, Northern Ireland, United Kingdom

<sup>19</sup> Instituto de Astrofísica de Canarias, La Laguna, Tenerife, Spain

<sup>20</sup> Departamento de Astrofísica, Universidad de La Laguna, Tenerife, Spain

<sup>21</sup> Institute of Astronomy, University of Cambridge, United Kingdom

<sup>22</sup> Department of Physics & Astronomy, University College London, United Kingdom

<sup>23</sup> European Space Agency, Space Telescope Science Institute, Baltimore, USA

<sup>24</sup> Instituto de Astrofísica de Andalucía-CSIC, Granada, Spain

<sup>25</sup> Institute of Astronomy with NAO, Smoljan, Bulgaria

<sup>26</sup> Centro de Astrobiología, CSIC-INTA, Madrid, Spain

<sup>27</sup> Universitäts-Sternwarte München, Germany

<sup>28</sup> Faulkes Telescope Project, University of Glamorgan, Wales, United Kingdom

<sup>29</sup> School of Physical & Geographical Sciences, Keele University, United Kingdom

**We introduce the VLT FLAMES Tarantula Survey, an ESO Large Programme from which we have obtained optical spectroscopy of over 800 massive stars in the spectacular 30 Doradus region of the Large Magellanic Cloud. A key feature is the use of multi-epoch observations to provide strong constraints on the binary fraction. This is the largest**

**high quality survey of extragalactic massive stars ever assembled, and is already providing exciting new insights into their evolution, multiplicity and formation.**

Massive stars and their descendants dominate the dynamics and chemical enrichment of young star-forming galaxies, through their intense winds, radiation fields and dramatic deaths as core-collapse supernovae. An overarching goal for studies of stellar evolution and resolved stellar populations is to develop realistic tools to analyse integrated-light observations of distant star clusters and galaxies; if we can understand the properties and behaviour of the stars on our own doorstep, we can be more confident of an accurate interpretation of unresolved populations far away.

## Background and motivations

A vibrant area of research has been the role of environment (metallicity) on the evolution of massive stars, often focusing on the properties of individual stars in the nearby metal-poor Magellanic Clouds compared to their Galactic cousins. These efforts culminated in a previous Large Programme, the VLT FLAMES Survey of Massive Stars (FSMS), which analysed tens of O-type stars and hundreds of early B-type stars, from observations centred on open clusters in the Galaxy and in the Clouds (Evans et al., 2008).

A major result from the previous survey was empirical evidence for weaker winds in massive O-type stars at lower metallicities, in agreement with theoretical predictions. This was a crucial test because evolutionary models employ theoretical scaling laws to account for the loss of mass and angular momentum in metal-poor stars. In lower metallicity systems stars therefore require a larger initial mass to progress to the Wolf–Rayet (W–R) phase than in the Galaxy, and will lose less angular momentum over their lifetimes. Consequences of this include reduced feedback of material from their winds and potentially different types of core-collapse explosions.

The O-type stars span a wide range of mass (upwards of  $\sim 20 M_{\odot}$ ), effective temperatures ( $\sim 30\,000$  to  $50\,000$  K) and wind properties, with a diverse range of morphological sub-groups. To understand the most massive stars as a population, including the evolutionary connections between those sub-groups, a much larger, homogeneous sample of high quality data was required. In particular, rotationally-induced mixing is thought to modify the surface chemistry of massive stars on the main sequence, with the most dramatic enhancements predicted for their nitrogen abundances. This is an important test of evolutionary models, where the benefits of large samples are highlighted by the puzzling results for some of the B-type stars from the FSMS (e.g., Brott et al., 2011; and references therein). Moreover, the progression of increasing wind strength along the evolutionary sequence of O–Of–Of/WN–WN types is not well known, yet these are the stars which truly dominate in terms of mechanical feedback and ionising photons.

To add to these factors, the catalyst for a new and ground-breaking survey was provided by recent results highlighting the prevalence of binarity in massive stars (e.g., Sana & Evans, 2011). Parts of the extragalactic community have begun to explore the consequences of this, with massive binaries argued to account for some of the integrated-light properties of low-redshift star-forming galaxies. However, an empirical description of the binary fraction of massive systems (and their distribution of mass ratios) has, to date, been poorly constrained in models of star formation and cluster evolution.

The VLT FLAMES Tarantula Survey (VFTS; Evans et al., 2011) was conceived to address these outstanding issues relating to the evolution, multiplicity and eventual fate of massive stars. By using the multi-object capability of FLAMES, combined with the light-gathering power of the VLT, we targeted the massive-star population of the Tarantula Nebula (30 Doradus, NGC 2070), the largest star-forming complex in the Local Group of galaxies, located in the Large Magellanic Cloud (LMC).

### A thriving stellar nursery

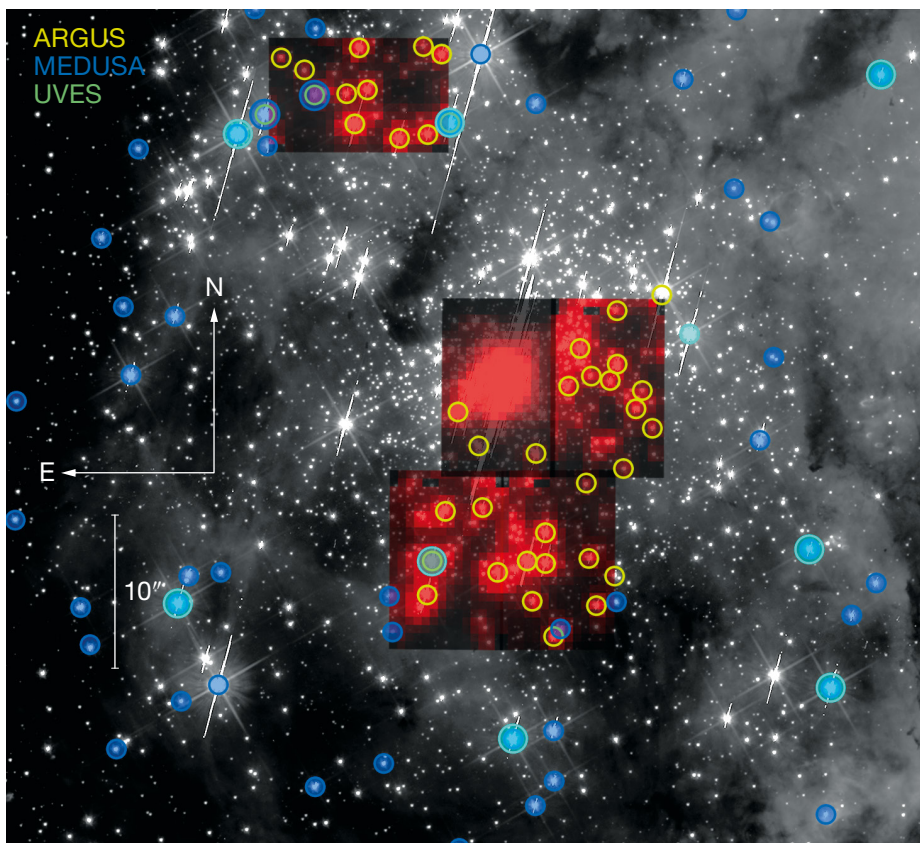
The 30 Doradus nebula is more than just a beautiful extragalactic H II region — it harbours one of the richest populations of massive stars in the local Universe and is our only opportunity to resolve the components of a young, small-scale starburst. The nebula spans 15 arcminutes on the sky, equivalent to over 200 parsecs (pc) and comparable in scale to regions of intense star formation observed in high-redshift galaxies. The engine at its core is the dense stellar cluster R136, home to some of the most massive stars known (with masses in excess of  $150 M_{\odot}$ ; Crowther et al., 2010). When combined with its well-constrained distance (by virtue of being in the LMC) and low foreground extinction, 30 Doradus provides us with a unique laboratory in which to compile a large spectroscopic sample of massive stars.

The VFTS observations primarily employed the Medusa mode of FLAMES, in which 132 fibres are positioned within a 25-arcminute field of view to feed targets

to the Giraffe spectrograph. Three of the standard Giraffe settings were used: LR02 (3960–4564 Å,  $R = 7000$ ), LR03 (4499–5071 Å,  $R = 8500$ ), HR15N (6442–6817 Å,  $R = 16\,000$ ). This provided intermediate resolution spectroscopy of the blue optical lines commonly used in classification and quantitative analysis of massive stars, combined with higher resolution observations of the H $\alpha$  line to provide a diagnostic of the stellar wind intensity. These settings also include important strong nebular lines (e.g., [O III] and [S II]), giving a useful tracer of the gas velocities along each line of sight. In addition, a small number of selected targets were observed at greater spectral resolution with the fibre-feed to UVES (see Figure 1).

One of the primary motivations of the VFTS was to detect massive companions

Figure 1. The FLAMES ARGUS integral field unit images (and extracted sources) overlaid on an HST WFC3 *F555W* image of R136. The location of Medusa and UVES targets in the central region are also shown.



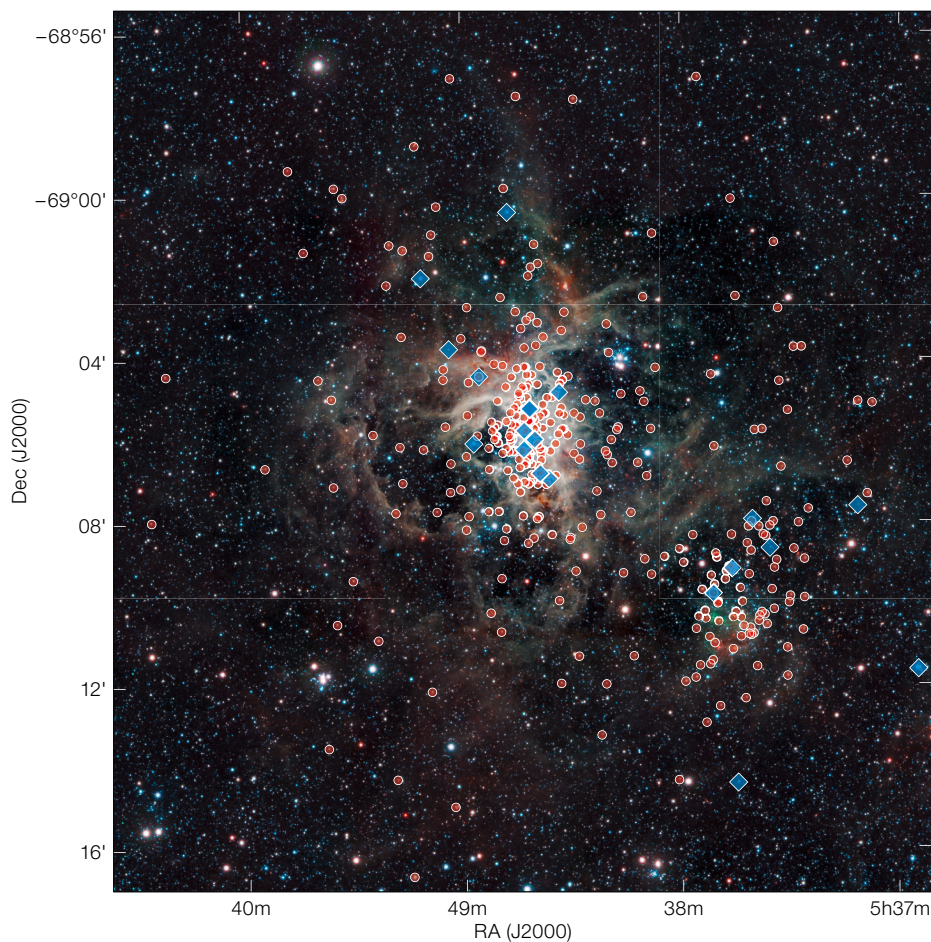


Figure 2. Combined *YJKs*-band image of 30 Doradus from the VISTA Magellanic Clouds (VMC) Survey (Cioni et al., 2011). The O-type (red circles) and W–R stars (blue diamonds) observed by the VFTS are overlaid.

if they are present. This search for “binaries” (both true binaries and multiple systems) shaped the observational strategy, which employed repeat observations at the LR02 setting to monitor for radial velocity variations. The majority of the data were obtained over the period October 2008 to February 2009, with constraints to ensure reasonable gaps (of 28 days or more) for the repeat LR02 observations. A final epoch of LR02 data was obtained in October 2009, which helps significantly with the detection of both intermediate- and long-period binaries.

A similar multi-epoch strategy was used to observe five pointings in the central region of R136 with the ARGUS integral field unit (Figure 1). The objective of this

part of the VFTS was to investigate if R136 is dynamically stable (i.e. in virial equilibrium) via a determination of its velocity dispersion. Rejecting detected binaries (which would otherwise inflate the result), preliminary results indicate a stellar velocity dispersion of less than 7.5 km/s, suggesting that the cluster is stable (Hénault-Brunet et al., in preparation).

In total, the VFTS has observed over 300 O-type stars and 20 W–R (and Of/WN) emission-line stars (see Figure 2) — a unique extragalactic sample in the high-mass domain of the Hertzsprung–Russell diagram. The VFTS has also observed over 500 B-type stars, which span the full luminosity range of main sequence dwarfs to bright supergiants. This gives a sample comparable in size to the B-type stars from the previous survey, but now with the benefit of multi-epoch data to investigate multiplicity. Lastly, there are 90 cooler-type stars with radial velocities consistent with them being members of

the LMC. We now summarise three discoveries which highlight the huge potential of the VFTS data.

### Discovery of a very massive star outside R136

There have been numerous narrowband imaging surveys in the Clouds to look for W–R stars and it is often presumed that we have a complete census of them. However, the VFTS has discovered a new hydrogen-rich W–R star, VFTS 682, located 29 pc northeast of R136 (Figure 3; Evans et al., 2011). The spectrum of VFTS 682, classified as WN5h, resembles those of the very luminous stars in the core of R136 (Crowther et al., 2010). No radial velocity shifts are seen between the individual epochs, suggesting that the star is single to a high level of confidence.

From analysis of the spectra and available optical/infrared photometry the star appears to be very luminous, with  $\log(L/L_{\odot}) = 6.5 \pm 0.2$  and with a current mass of  $\sim 150 M_{\odot}$  (Bestenlehner et al., 2011). It is optically faint ( $V \sim 16$ ) due to a line-of-sight visual extinction of  $\sim 4.5$  magnitudes, explaining why it had not been discovered by past narrowband imaging. To date, such massive stars have only been found in the cores of dense clusters (e.g., R136 and the Arches), whereas VFTS 682 appears to have either formed in relative isolation (asking important questions of theories of high-mass star formation) or was ejected from R136, which would pose an exciting challenge to models of cluster dynamics. Tantalisingly, its high effective temperature ( $52\,200 \pm 2500$  K) might be as a result of chemically-homogeneous evolution, a process suggested as an evolutionary channel for long-duration gamma-ray bursts.

### R139 revealed as an eccentric binary

One of the most luminous objects in 30 Doradus is R139 (VFTS 527;  $V \sim 12$ ). Located one arcminute to the north of R136 (Figure 3), it has been suggested in the past as the most massive star outside R136. In a conference proceedings from 2002, Virpi Niemela reminded us of an old adage that “the brightest star in each open cluster is (at least) a binary”

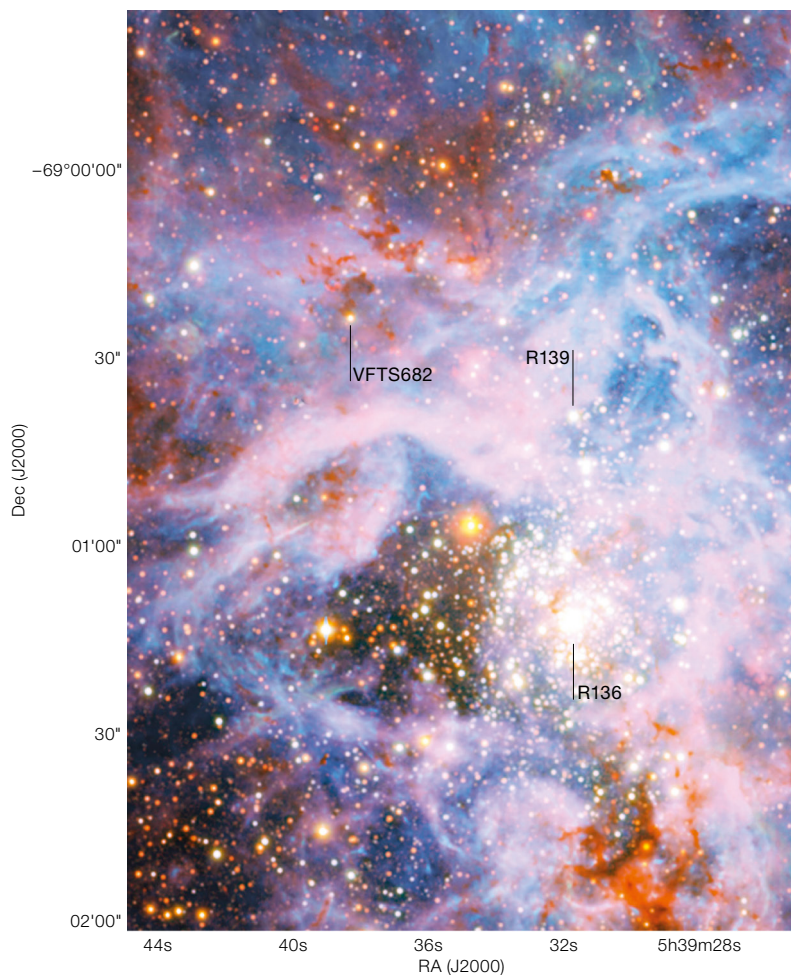


Figure 3. The central part of the Tarantula Nebula showing the locations of VFTS 682 and R139 with respect to the massive cluster R136. The image is a combination of the *YJKs* images from the VMC Survey with *V*- and *R*-band images from the MPG/ESO 2.2-metre telescope.

(Niemela, 2002). Her words ring true in 30 Doradus, as the VFTS data have revealed R139 as a double-lined binary comprising two luminous supergiants (Figure 4; Taylor et al., 2011), classified as O6.5 Iafc and O6 Iaf for the primary and secondary, respectively.

This discovery was only possible due to the high quality multi-epoch spectra from the VFTS. While the data are an excellent resource to *detect* binarity, characterisation of orbital parameters will necessitate additional spectroscopy (in the majority of cases) to determine periods and amplitudes. From follow-up observations of R139 with the MPG/ESO 2.2-metre telescope, Magellan and the VLT, its orbit appears to be highly eccentric with a period of 153.9 days. This gives lower mass limits for the components of  $M_1 \sin^3 i = 78 \pm 8 M_\odot$  and  $M_2 \sin^3 i = 66 \pm 7 M_\odot$ , making R139 one of the most massive binary systems known, and the most massive containing two O-type supergiants (i.e., both stars are relatively evolved).

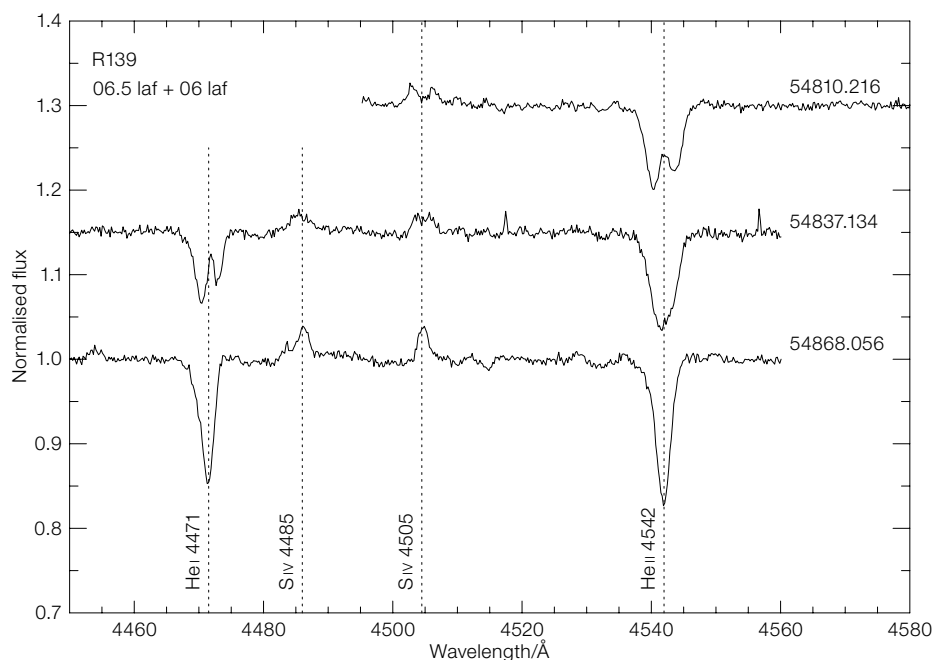


Figure 4. Illustrative FLAMES Giraffe spectra of R139 at minimum separation (lower spectrum) and with well-separated components (upper spectrum); each is labelled with the modified Julian Date (−2 400 000) of the exposure.

Mass estimates from comparisons with evolutionary models are in good agreement with the lower limits from the orbital analysis. This suggests a large inclination angle for the system, such that we might expect photometric eclipses. As part of a monitoring programme, we obtained 54 V-band images with the Faulkes Telescope South over an 18-month period, but found no evidence of photometric variations. An intensive photometric study near to the predicted periastron would determine conclusively if there is an eclipse, giving valuable constraints on the inclination of the system.

#### Identification of a massive runaway

A massive O2-type star, VFTS 016, on the western fringes of 30 Doradus provides an excellent illustration of how the multi-epoch VFTS data is also powerful in the case of *non-detections* of binarity. First observed with the 2-degree Field (2dF) instrument at the Anglo-Australian Telescope, its spectrum (classified as O2 III-if\*) had a radial velocity 85 km/s lower than the local systemic velocity. This could indicate a large-amplitude binary, but no variations were seen in any of the FLAMES data, from which a massive companion with a period of less than one year was excluded at the 98% level (Evans et al., 2010).

VFTS 016 is at a projected distance of 120 pc from R136, and 70 pc from the less massive cluster NGC 2060. Its

significant differential velocity when compared to nearby stars and gas suggest that it is a runaway star, ejected from its formation site by dynamical interactions in a cluster or by a kick from a supernova explosion in a binary system. Spectral analysis indicated a large evolutionary mass of  $\sim 90 M_{\odot}$ , suggesting interactions with the even more massive stars in R136. Considering R136 is thought to be too young to have undergone a supernova explosion, if VFTS 016 originated from there it would be one of the clearest cases to date for this ejection mechanism. Further investigation of the three-dimensional dynamics of VFTS 016 and other candidate runaways identified by the survey requires high quality proper motions; a recently approved imaging programme with the Hubble Space Telescope (HST; PI: Lennon) will provide the last piece of the puzzle in this regard.

#### Massive single stars are in the minority

These three results serve to illustrate the power of the multi-epoch approach. The full sample of O-type spectra from the survey has now undergone rigorous variability analysis, in which a target is considered a spectroscopic binary if it displays statistically-significant radial velocity variations (with an amplitude in excess of 15 km/s) or evidence of double-lined profiles. Absolute radial velocities have been obtained from this analysis for the apparently single stars which, when combined with spectral classifications, will be

used to explore the diverse populations in the region (Walborn et al., in preparation).

In the VFTS sample of 352 O-type stars (which includes some B0-type spectra), there are 125 with indications of binarity, giving a lower limit to the binary fraction of 36%. With informed assumptions about the intrinsic distribution of periods, eccentricities and mass ratios, the probability of detecting a spectroscopic binary (of a given period) from the VFTS observations can be calculated. Once corrected for completeness, the spectroscopic binary fraction rises to between 47 and 55% depending on the input period distribution (Sana et al., in preparation). This fraction is roughly comparable to results in young Galactic clusters (e.g., Sana & Evans, 2011). Compared to previous surveys of giant H II regions (e.g., Carina Nebula, NGC 346, etc.) the VFTS sample represents an order-of-magnitude increase in the number of O-type stars in a single environment. The significant number of B-type spectra from the VFTS have also been investigated for radial velocity variations. Preliminary results from cross-correlation analysis point to a binary fraction of greater than 33% (prior to correction for detection sensitivities), providing good evidence for a comparably large binary population in the lower-mass B-type regime (Dunstall et al., in preparation).

These preliminary values argue strongly that the *majority* of the most massive stars are in binary systems, and that the

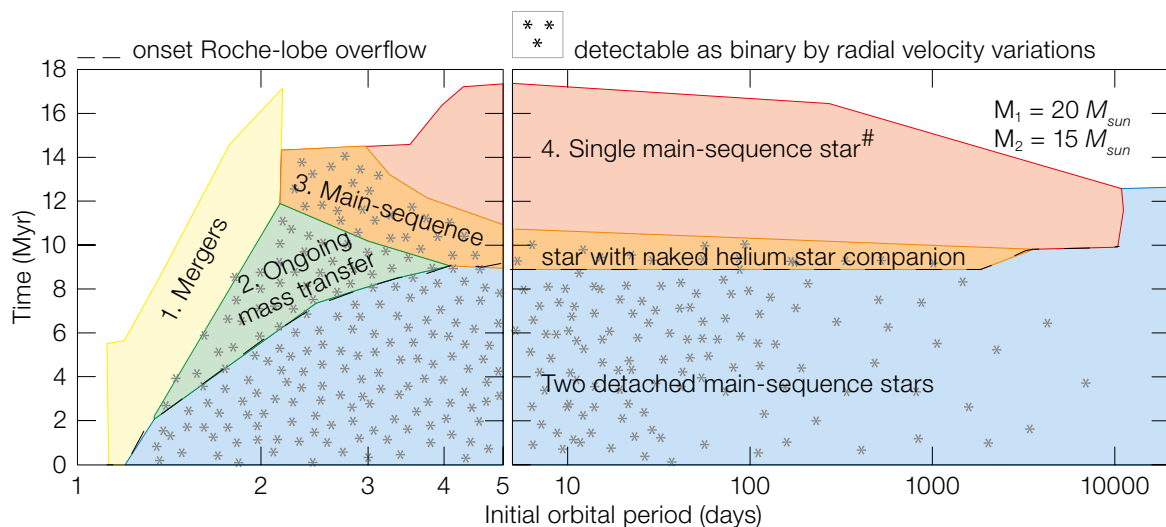


Figure 5. Evolutionary phases of a binary (initial masses of 20 and 15  $M_{\odot}$ ) as a function of initial orbital period and age (de Mink et al., 2011).

effects of binary evolution have to be explored thoroughly in the context of stellar evolutionary tracks and population synthesis models. Indeed, the development of new evolutionary models including the effects of rotation and binarity is an integral part of the VFTS collaboration. Extensive grids of evolutionary models of individual massive stars, including the effects of rotation, are being extended to include masses of up to  $300 M_{\odot}$  (Köhler et al., in preparation). In parallel, rapid evolutionary codes for population synthesis studies are being used to investigate the effects of binarity and stellar rotation, and how binaries can provide tests of the uncertain physics of binary interactions. For example, Figure 5 (de Mink et al., 2011) shows the effects of binarity, depicting the variety of stages (including mergers and spun-up accretors) during which one or both stars are on the main sequence. Figure 5 also illustrates the observational challenge posed by the apparently single stars that may well have experienced an interaction with a companion in the past, e.g., they may be the product of mergers or companions left after the explosion of the primary.

#### Candidates for isolated high-mass star formation

There were a number of O-type stars outside of R136 (and the lower-mass cluster NGC 2060) which appear to be single and have radial velocities consistent with the local systemic value. Rejecting stars which might have an associated cluster (from inspection of deep HST and VLT imaging), 15 of these appear to be unrelated to a cluster, leading to a similar question as that posed by VFTS 682, i.e. were these stars formed *in situ* or ejected from a cluster as runaways (in the plane of the sky)?

The two main theories of star formation, competitive accretion and monolithic collapse, predict different formation sites for the most massive stars in a young system. In the former, a cluster of low-mass stars provides a potential well to bring surrounding gas into the cluster, allowing some stars to accrete mass and to grow to become O-type stars — i.e.

every massive star should be associated with a cluster of (lower-mass) stars. In models of monolithic collapse, the stellar masses are set by the gas core from which they form, and star formation will trace the gas such that some form in a highly clustered distribution, whereas others can form in relative isolation (meaning that their formation is not strongly influenced by the gravitational potential of other nearby stars).

The spatial distribution of high-mass stars can also be used to constrain scenarios about how the stellar initial mass function is sampled, with a broad range of implications, from determinations of the star formation rate and mass of galaxies, to the chemical evolution of the Universe. The question is whether the mass of the most massive star is set by the mass of the host cluster, or if the mass of each star is simply set by stochastic sampling? The “isolated” O stars from the VFTS survey (Bressert et al., submitted) suggest the latter in at least some situations. Only with proper motions (HST and Gaia) and high resolution mm/sub-mm observations (e.g., ALMA) will the issue be settled for each candidate.

#### This is only the beginning...

The core set of results from the survey are yet to come — considerable work is now underway to analyse the W–R and OB-type stars from the VFTS to obtain full physical parameters (i.e., effective temperatures, gravities, mass-loss rates, rotational velocities, chemical abundances, and more). Given the scale of the dataset and the complexity of the theoretical model atmospheres we are using a combination of techniques, employing the genetic algorithm and the grid-searching methods developed in the course of the previous survey. The results of these quantitative analyses will provide us with an unparalleled view of the wind parameters for the full range of O- and WN-type stars, and enable the first study of the effects of rotation on surface abundances in the most massive stars. Knowledge of binarity will add a valuable parameter to the interpretation

of these results, enabling tests of evolutionary models which include the physical processes for both single stars and binary systems.

The physical parameters for each star will ultimately be combined to investigate the radiative and mechanical feedback beyond the confines of 30 Doradus, and will enable empirical tests of spectral synthesis techniques used to analyse distant, unresolved clusters/massive H II regions. The final piece of the picture will come from a new HST spectroscopic programme (PI: Crowther) to determine the physical properties of the large number of massive stars in the dense central parsec of R136, which can only be observed from space or with adaptive optics.

Remarkably, longer wavelength observations show that 30 Doradus is at the northern end of a large column of molecular gas which extends south for over 2000 pc. With such a reservoir of potential star-forming material, the region seems destined to become an even more impressive complex over the next few million years.

#### References

- Bestenlehner J. et al. 2011, A&A, 530, L14
- Brott, I. et al. 2011, A&A, 530, A116
- Cioni, M.-R. et al. 2011, A&A, 527, A116
- Crowther, P. et al. 2010, MNRAS, 408, 731
- de Mink, S., Langer, N. & Izzard, R. 2011, Bulletin Société Royale des Sciences de Liège, 80, 543
- Evans, C. et al. 2008, The Messenger, 131, 25
- Evans, C. et al. 2010, ApJ, 715, L74
- Evans, C. et al. 2011, A&A, 530, A108
- Niemela, V. 2002, Extragalactic Star Clusters, IAU Symp. 207, ASP, p202
- Sana, H. & Evans, C. 2011, Active OB stars, IAU Symp. 272, arXiv:1009.4197
- Taylor, W. et al. 2011, A&A, 530, L10

# The SINS and zC-SINF Surveys: The Growth of Massive Galaxies at $z \sim 2$ through Detailed Kinematics and Star Formation with SINFONI

Natascha M. Förster Schreiber<sup>1</sup>

Reinhard Genzel<sup>1, 2</sup>

Alvio Renzini<sup>3</sup>

Linda J. Tacconi<sup>1</sup>

Simon J. Lilly<sup>4</sup>

Nicolas Bouché<sup>5, 6, 7</sup>

Andreas Burkert<sup>8</sup>

Peter Buschkamp<sup>1</sup>

C. Marcella Carollo<sup>4</sup>

Giovanni Cresci<sup>9</sup>

Richard Davies<sup>1</sup>

Frank Eisenhauer<sup>1</sup>

Shy Genel<sup>1, 10</sup>

Stefan Gillessen<sup>1</sup>

Erin K. S. Hicks<sup>11</sup>

Therese Jones<sup>2</sup>

Jaron Kurk<sup>1</sup>

Dieter Lutz<sup>1</sup>

Chiara Mancini<sup>3</sup>

Thorsten Naab<sup>12</sup>

Sarah Newman<sup>2</sup>

Yingjie Peng<sup>4</sup>

Kristen L. Shapiro<sup>13</sup>

Alice E. Shapley<sup>14</sup>

Amiel Sternberg<sup>10</sup>

Daniela Vergani<sup>15</sup>

Stijn Wuyts<sup>1</sup>

Giovanni Zamorani<sup>15</sup>

Nobuo Arimoto<sup>16</sup>

Daniel Ceverino<sup>17</sup>

Andrea Cimatti<sup>18</sup>

Emanuele Daddi<sup>19</sup>

Avishai Dekel<sup>17</sup>

Dawn K. Erb<sup>20</sup>

Xu Kong<sup>21</sup>

Vincenzo Mainieri<sup>22</sup>

Claudia Maraston<sup>23</sup>

Henry J. McCracken<sup>24</sup>

Marco Mignoli<sup>15</sup>

Pascal Oesch<sup>25</sup>

Masato Onodera<sup>4, 19</sup>

Lucia Pozzetti<sup>15</sup>

Charles C. Steidel<sup>26</sup>

Aprajita Verma<sup>27</sup>

<sup>1</sup> Max-Planck-Institut für extraterrestrische Physik, Garching, Germany

<sup>2</sup> Dept. of Physics, University of California, Berkeley, USA

<sup>3</sup> INAF–Osservatorio Astronomico di Padova, Italy

<sup>4</sup> Institute of Astronomy, Eidgenössische Technische Hochschule Zürich, Switzerland

<sup>5</sup> Dept. of Physics, University of California, Santa Barbara, USA

<sup>6</sup> CNRS Institut de Recherche en Astrophysique et Planetologie, Université de Toulouse, France

<sup>7</sup> Université de Toulouse, UPS Observatoire Midi Pyrénées, Toulouse, France

<sup>8</sup> Universitäts Sternwarte München, Germany

<sup>9</sup> INAF–Osservatorio Astrofisico di Arcetri, Firenze, Italy

<sup>10</sup> Sackler School of Physics & Astronomy, Tel Aviv University, Israel

<sup>11</sup> Dept. of Astronomy, University of Washington, Seattle, USA

<sup>12</sup> Max-Planck-Institut für Astrophysik, Garching, Germany

<sup>13</sup> Northrop Grumman Aerospace Systems, Redondo Beach, USA

<sup>14</sup> Dept. of Physics and Astronomy, University of California, Los Angeles, USA

<sup>15</sup> INAF–Osservatorio Astronomico di Bologna, Italy

<sup>16</sup> National Astronomical Observatory of Japan, Tokyo, Japan

<sup>17</sup> Racah Institute of Physics, The Hebrew University, Jerusalem, Israel

<sup>18</sup> Dipt. di Astronomia, Università di Bologna, Bologna, Italy

<sup>19</sup> CEA Saclay, DSM/DAPNIA/SAP, Gif-sur-Yvette, France

<sup>20</sup> Dept. of Physics, University of Wisconsin, Milwaukee, USA

<sup>21</sup> Center for Astrophysics, University of Science and Technology of China, Hefei, China

<sup>22</sup> ESO

<sup>23</sup> Institute of Cosmology and Gravitation, University of Portsmouth, United Kingdom

<sup>24</sup> Institut d’astrophysique de Paris, France

<sup>25</sup> University of California Observatory/Lick Observatory, University of California, Santa Cruz, USA

<sup>26</sup> Caltech, Pasadena, USA

<sup>27</sup> Oxford Astrophysics, University of Oxford, United Kingdom

**In recent years, major advances have been made in our understanding of the early stages of galaxy formation and evolution. Remarkable progress has come from spatially– and spectrally–resolved studies of galaxies beyond  $z \sim 1$  with SINFONI at the VLT, when the Universe was less than 40 % of its present age. Here we report on key**

**insights from our SINFONI observations of over 100 massive  $z \sim 2$  star-forming galaxies, resolving the kinematics, physical, and star formation properties on scales of  $\sim 1$ –5 kiloparsecs.**

The  $z \sim 2$  Universe, at lookback times of  $\sim 10$  billion years, is now known to represent a critical epoch in the mass assembly of galaxies. During this era, both the cosmic star formation rate and the luminous quasar space density were at their peak. The assembly of galaxies is correspondingly rapid, with the total stellar mass density in galaxies increasing from  $\sim 15$  % of its current value at  $z \sim 3$  to  $\sim 50$ –75 % at  $z \sim 1$ . The multitude of multi-wavelength imaging surveys and large optical spectroscopic campaigns carried out over the past decade have set the stage for detailed spatially-resolved studies of individual galaxies. Such studies are essential to pin down the actual processes that drive early galaxy evolution and to address key questions such as: What is the relative importance of mergers versus smooth infall in the accretion of mass? What is the connection between bulge and disc formation? What is the interplay between angular momentum, dissipation and feedback processes? Is star formation at high redshift mostly driven by major mergers between galaxies of comparable mass, as in present-day galaxies with similarly high star formation rates?

Recent observational and theoretical findings indicate that the majority of  $z \sim 1$ –3 massive star-forming galaxies appear to be continuously fed by gas that promotes star formation, rather than occasionally undergoing starbursts as a result of major mergers. Some of the most convincing evidence has come from spatially-resolved ionised gas kinematics with SINFONI, which have revealed large clumpy rotating discs at  $z \sim 2$  with high star formation rates (SFR  $\sim 100 M_{\odot}/\text{yr}$ ), without any sign of ongoing merging (e.g., Förster Schreiber et al., 2009). In parallel, multi-wavelength galaxy surveys have shown that the star formation rate correlates tightly with stellar mass  $M_*$  and that the SFR versus  $M_*$  relation steadily declines from  $z \sim 2.5$  to  $z \sim 0$ , arguing against a

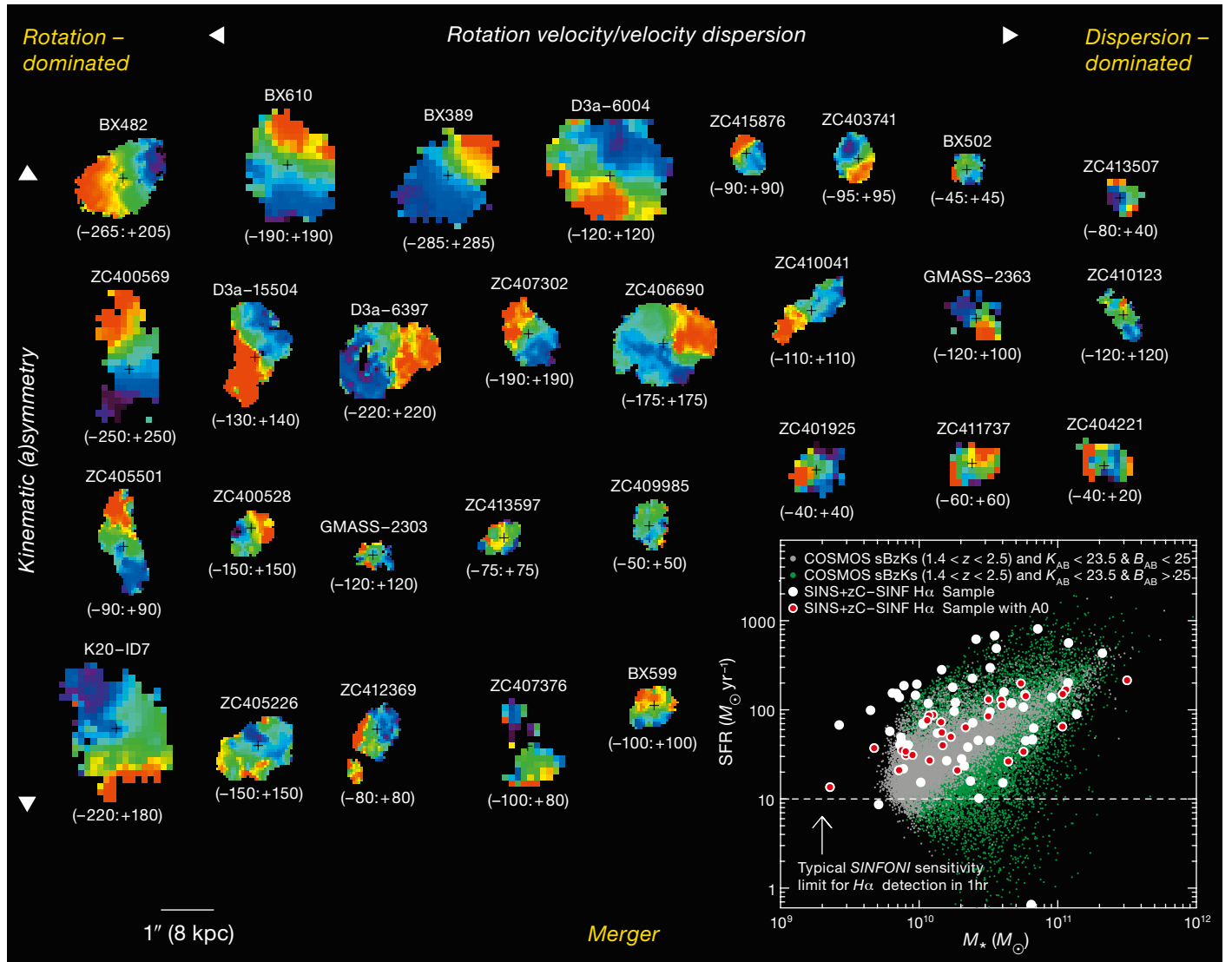


Figure 1. Velocity fields for 29 of the 110 galaxies observed with SINFONI as part of the SINS and on-going zC-SINF large programme. Blue to red colours correspond to regions of the galaxies that are approaching and receding relative to the systemic or bulk velocity of each galaxy as a whole. The minimum and maximum relative velocities are labelled for each galaxy (in km/s). All sources are shown on the same angular scale; the white bar at the bottom left corresponds to 1 arcsecond, or about 8 kpc at  $z = 2$ . The inset (adapted from Mancini et al., 2011) shows the distribution of all targets (white-filled circles) and the AO sample of 29 targets (red-filled circles) in the stellar mass versus star formation rate plane.

dominant bursty, major-merger-driven star formation mode (e.g., Daddi et al., 2007). Moreover, observations of (sub) millimetre CO line emission in non-major merging star-forming galaxies at  $z \sim 1-3$  have uncovered large molecular gas res-

ervoirs, implying gas-to-baryonic mass fractions of  $\sim 50\%$  and requiring continuous replenishment to maintain the observed star formation (e.g., Tacconi et al., 2010).

This new empirical evidence matches remarkably well with state-of-the-art cosmological simulations, within the now mature Cold Dark Matter paradigm, in which galaxies form as baryonic gas condensates at the centre of collapsing dark matter haloes. In these simulations, massive galaxies acquire a large fraction of their baryonic mass via steady gas accretion along narrow, cold streams and/or a rapid series of minor mergers. These mechanisms sustain elevated star formation rates over much longer timescales

than violent, dissipative major mergers. Under these conditions, the net angular momentum is largely preserved as matter is accreted onto galaxies, and discs can survive. Along with continuous replenishment of gas, dynamical processes within galaxies can drive the evolution of discs and the rapid formation of bulges.

#### The SINS and zC-SINF SINFONI surveys

Galaxies at  $z \sim 1-3$  are faint, their projected angular sizes are small, and important spectral diagnostic features that are emitted in the rest-frame optical are redshifted into the near-infrared bands, 1.0–2.5  $\mu\text{m}$ . The advent of cryogenic near-infrared integral field spectroscopy

on 8-metre-class telescopes, along with adaptive optics (AO), has opened up new avenues by making distant galaxies accessible to detailed spatially- and spectrally-resolved studies. The high sensitivity of SINFONI, mounted on Yepun (Unit Telescope 4; UT4) at the VLT, has allowed ground-breaking studies including those led by our team, providing unprecedented insights into the dynamical evolution of massive star-forming galaxies, the connection between bulge and disc formation, and the mechanisms driving star formation, angular momentum, feedback, and metal enrichment at  $z \sim 2$ .

Given the unique opportunities afforded by SINFONI, we have conducted the SINS survey to map the kinematic, star formation, and physical properties of high-redshift galaxies. SINS was the first and largest survey with full 2D mapping of the ionised gas kinematics and morphologies of 80 galaxies at  $z \sim 1.3$ – $2.6$  (Förster Schreiber et al., 2009). The SINFONI data were mostly collected as part of the Max-Planck-Institut für extraterrestrische Physik’s (MPE) SPIFFI and PARSEC Guaranteed Time Observations. The galaxies are resolved on typical seeing-limited angular scales of about 0.6 arcseconds, corresponding to 4–5 kiloparsecs (kpc) at  $z \sim 2$ , and as small as 0.1–0.2 arcseconds, or 1–1.5 kpc, for the dozen objects also observed with AO. We are continuing this effort through a SINFONI large programme (LP) in collaboration with zCOSMOS team members, capitalising on two major ESO VLT programmes: SINS with SINFONI and zCOSMOS, the VIMOS optical spectroscopic campaign in the 2-square-degree COSMOS field (Lilly et al., 2007; Lilly et al., 2008). With  $\sim 6000$  objects confirmed at  $1.4 < z < 2.5$  across the widest multi-wavelength cosmological survey field, zCOSMOS offers the best opportunity to significantly expand the SINS sample. SINFONI data have been taken in natural seeing for 30  $z \sim 2$  zCOSMOS targets, the “zC-SINF” sample (Mancini et al., 2011), out of which the best and most representative subset is now being observed with AO.

Together, the SINS and zC-SINF samples comprise 110  $z \sim 2$  galaxies with SINFONI integral field spectroscopy, which paral-

els existing near-infrared long-slit spectroscopic surveys. Once our LP is completed, the full AO sample will include nearly 30 objects, surpassing any other sample of this kind at  $z \sim 2$ . The galaxies cover roughly two orders of magnitude in stellar mass and star formation rate ( $\sim 3 \times 10^9$ – $3 \times 10^{11} M_{\odot}$  and  $\sim 10$ – $800 M_{\odot}/\text{yr}$ ), probing the bulk of massive, actively star-forming galaxies in the range  $1.4 < z < 2.5$  (Figure 1, inset). The samples shown in this figure cover well the region occupied by the bulk of the massive star-forming population at  $z \sim 2$ , here taken from photometrically-selected candidates in the COSMOS field (small green and white dots). For the vast majority of the galaxies, the  $H\alpha$  recombination line was the main feature of interest. The  $H\alpha$  line (and the neighbouring [N II] forbidden lines) predominantly trace star-forming regions. The SINFONI seeing-limited and AO datasets are highly complementary and provide, respectively, the overview of the kinematics and emission line properties on  $\sim 4$ – $5$  kpc scales and, for selected objects, a sharper view allowing the characterisation of the processes at play through  $\sim 1$  kpc-scale signatures (see Figure 1). In what follows, we highlight some of the key outcomes from SINS and initial results from our LP, with half the AO data taken to date.

### Kinematic diversity of $z \sim 2$ galaxies

One of the first and foremost results from SINS and zC-SINF is the kinematic diversity among massive star-forming galaxies at  $z \sim 2$ , illustrated in Figure 1. Velocity fields and velocity dispersion maps are measured from the shift in observed wavelength and the width of the  $H\alpha$  line across the sources. The galaxies shown in Figure 1 are approximately sorted from left to right according to whether their kinematics are rotation-dominated or dispersion-dominated, and from top to bottom according to whether they are disc-like or merger-like. All 29 objects have, or will have, SINFONI + AO observations. For 18 of the galaxies, the velocity fields are extracted from the existing AO data, with typical resolution of  $\sim 1$ – $2$  kpc; for the others, the seeing-limited data are shown, with resolutions of  $\sim 4$ – $5$  kpc. The classification in the

kinematic parameter space is based on: (1) the degree of symmetry of the kinematics: from regular kinematics characteristic of ordered disc rotation to irregular kinematics indicative of mergers, quantified for many objects through kinemetry (e.g., Shapiro et al., 2008); and (2) the dominant source of dynamical support, quantified through the ratio of rotational or orbital velocity  $v_{\text{rot}}$  to intrinsic velocity dispersion  $\sigma_0$ .

About one third of the galaxies are rotation-dominated yet turbulent discs, another third are major mergers with disturbed kinematics, and the remaining third are typically compact systems with velocity dispersion-dominated kinematics. The fraction of rotation-dominated discs appears to increase at higher masses and, among the larger, more luminous systems, discs account for around two thirds while major mergers represent a minority. The existence of large rotating discs among the massive actively star-forming  $z \sim 2$  population was a surprise, and is consistent with smoother but efficient mass accretion mechanisms playing an important role along with merging events.

### Properties and evolution of $z \sim 2$ discs

A remarkable finding from our studies is that  $z \sim 2$  discs are characterised by large intrinsic velocity dispersions  $\sim 30$ – $90$  km/s, implying low  $v_{\text{rot}}/\sigma_0 \sim 2$ – $6$ , and high gas-to-baryonic mass fractions of  $\sim 50\%$ . Although their sizes and specific angular momenta are comparable, the  $z \sim 2$  discs are thus geometrically thicker, more turbulent, and more gas-rich than their  $z \sim 0$  counterparts. Furthermore, many of the  $z \sim 2$  discs exhibit irregular  $H\alpha$  morphologies, and our SINFONI + AO observations resolve luminous kpc-sized clumps in several of the discs (Genzel et al., 2011). Similar clumps are also seen in the rest-optical continuum light tracing the bulk of stars in five discs for which we obtained sensitive Hubble Space Telescope (HST) NICMOS/NIC2  $H$ -band imaging (Förster Schreiber et al., 2011). The clumps have large inferred masses of  $\sim 10^8$ – $5 \times 10^9 M_{\odot}$ , typically a few percent and up to  $\sim 20\%$  of the mass of the host galaxy.

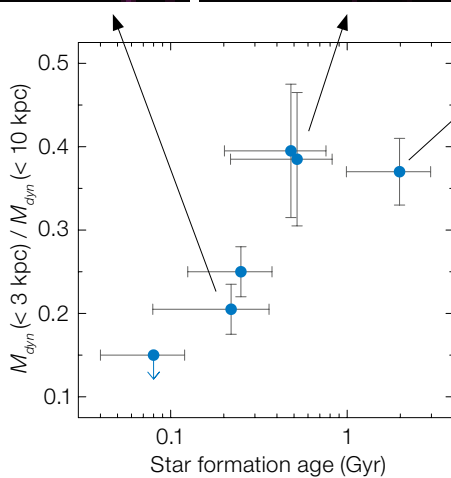
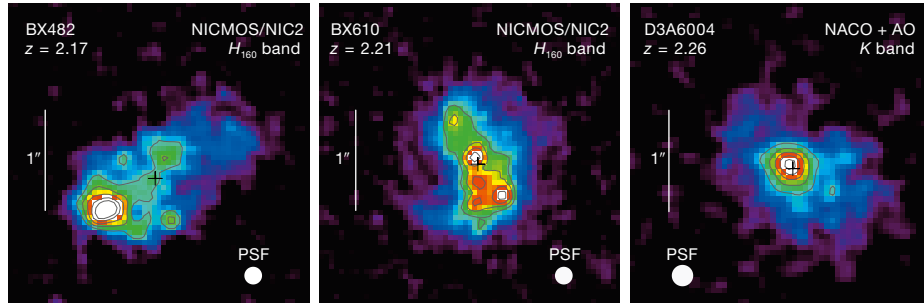


Figure 2. Trend of increasing central mass concentration (ratio of dynamical mass within a radius of 3 kpc and 10 kpc) with stellar age among six  $z \sim 2$  gas-rich turbulent SINS discs (adapted from Genzel et al., 2008). The rest-optical morphologies at  $\sim 1.5$  kpc resolution for three of the discs (upper) illustrate the evolutionary sequence: prominent clumps out to large radii at early stages and a progressively more concentrated distribution as clumps migrate inward and ultimately merge into a young bulge.

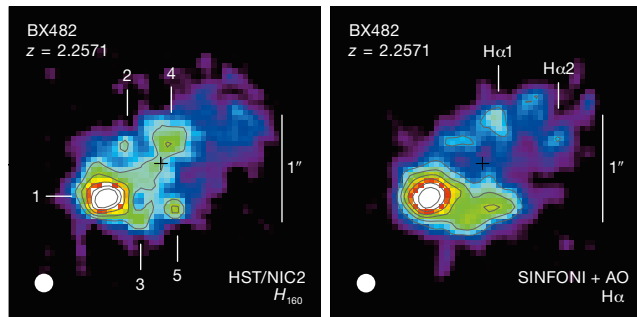
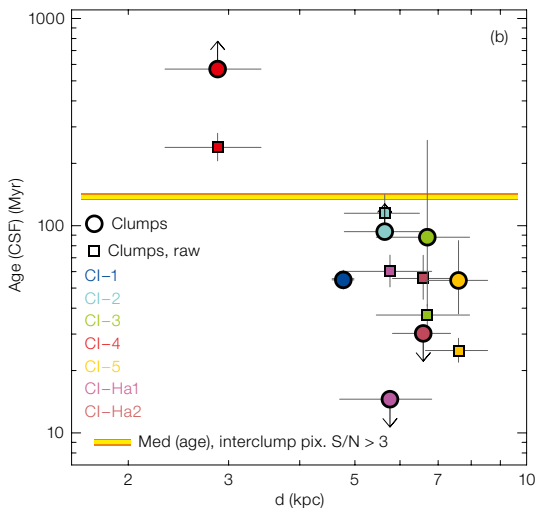


Figure 3. BX 482, a SINS disc galaxy at  $z \sim 2$ , for which both SINFONI + AO  $H\alpha$  and HST NIC2  $H$ -band observations at a resolution of  $\sim 1.5$  kpc are available (Förster Schreiber et al., 2011). For this galaxy, the sets of clumps identified in the optical continuum (upper left) and line (upper right) do not fully overlap, and the  $H\alpha$  line-to-continuum flux ratio (sensitive to age) reveals that the clump closest to the centre is the oldest (lower plot).



In a detailed study of several of our best-resolved SINS galaxies, our SINFONI data revealed the presence of turbulent rotating star-forming outer rings/discs and central bulge/inner disc components. The mass fractions of the central bulge/inner disc relative to the total dynamical mass appear to scale with the global stellar and chemical evolutionary stage of the galaxies (Figure 2; Genzel et al., 2008). This trend suggests a gradual buildup of the inner disc and bulge via internal processes that drive gas and stars inwards, without major mergers. For two of these discs, for which high-resolution Hubble Space Telescope (HST) imaging is available, radial variations in stellar age of individual clumps are inferred from age-sensitive indicators: the  $H\alpha$  line-to-continuum flux ratio for the one object with SINFONI + AO and HST NIC2 observations (Figure 3), and the restframe ultraviolet-to-optical colours for the other with HST NIC2  $H$ -band and ACS  $i$ -band imaging available (Förster Schreiber et al., 2011). The trends are such that the clumps closest to the centre of the galaxies appear older.

These results are in remarkable agreement with theoretical arguments and recent numerical simulations, which indicate that gas-rich turbulent discs as observed at  $z \sim 2$  can fragment via disc instabilities into very massive, kpc-scale star-forming clumps. These massive clumps can migrate inwards through dynamical friction and clump-clump interactions, and coalesce at the centre if they survive the disruptive effects of stellar feedback and tidal torques. Along with instability-driven inflow through the gas-rich discs, clump migration could contribute to the formation of nascent bulges. With the large intrinsic velocity dispersions and high gas mass fractions of  $z \sim 2$  discs, dynamical friction and viscous inflow processes proceed on timescales of less than one billion years, at least an order of magnitude faster than in present-day disc galaxies (e.g., Genzel et al., 2008).

### Vigorous star formation feedback in clumps

With our most recent SINFONI + AO datasets, we have discovered broad  $H\alpha$  (and

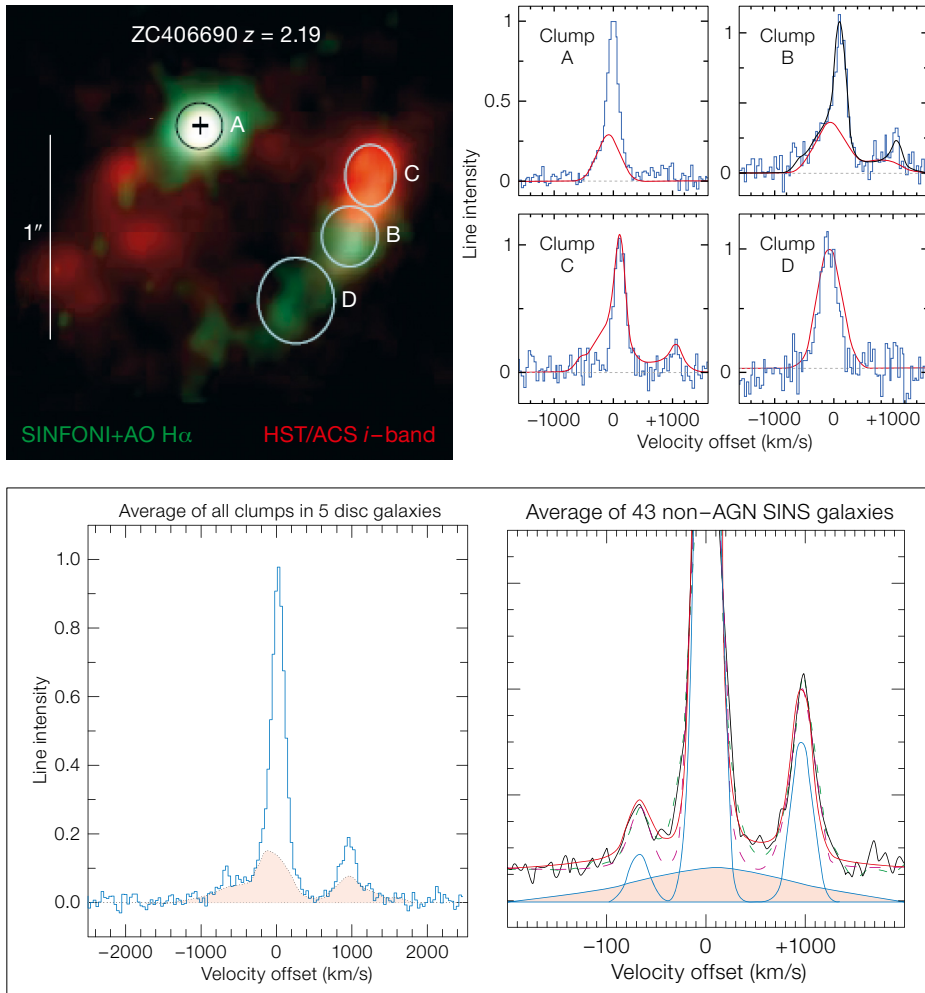


**Figure 4.** Another example of a kinematically-confirmed disc, for the galaxy ZC406690, with a clumpy star-forming ring in H $\alpha$  and rest-UV emission as revealed by SINFONI + AO and HST ACS *i*-band observations, respectively (colour-coded in green and red in the composite image, top left). The bright clumps A and B, and region D clearly show a broad emission line component in their spectrum (overplotted as red line in the top right panel), indicative of vigorous star formation driven gas outflows; such a component is undetected in clump C (the red line in this case is the scaled spectrum of clump B). The broad feature is also seen in the average SINFONI + AO spectrum of all clumps in five clumpy discs (bottom panel, left plot) but is undetected in the average of the interclump regions. It is moreover seen in the composite integrated spectrum of star-forming SINS galaxies with best S/N (bottom panel, right plot). Figure adapted from Genzel et al., 2011 and Shapiro et al., 2009.

[NII] emission components in the spectra of individual bright clumps across several disc galaxies, underneath the narrow component dominated by star formation (Figure 4; Genzel et al., 2011). This

$\sim 500$  km/s-wide component may trace gas outflows driven by the energy and momentum release from massive stars and supernova explosions in the star-forming clumps. In an earlier study, we had detected a similar broad H $\alpha$  + [NII] component in the high signal-to-noise (S/N) spectrum created by co-adding the spatially-integrated spectra of 43 star-forming SINS galaxies, for an equivalent integration time of about 180 hours (Shapiro et al., 2009). Now, our new SINFONI + AO data provide the first direct evidence for star-formation-driven feedback originating on the small scales of clumps within the discs, pinning down the origins of galactic-scale winds. These winds are ubiquitous at  $z \sim 2$ , but had so far only been observed on large ( $> 10$  kpc) scales.

The inferred clump mass outflow rates are comparable to or higher than the

clump star formation rates, echoing estimates derived from studies of galactic-scale winds at high redshift. Outflow rates largely exceeding the star formation rates suggest that some of the most actively star-forming clumps may lose a large fraction of their gas and be disrupted on very short timescales. Thus, while we found evidence that clumps may be able to migrate inwards and contribute to the early build-up of bulges, vigorous gas outflows could rapidly disrupt some of the more actively star-forming clumps before they reach the centre of the host disc.

### Outlook

As we pursue our SINFONI studies and exploit fully the rich SINFONI datasets, we can look forward to further new and exciting discoveries. In the short term, the remaining half of the AO observations planned as part of our SINFONI LP will be crucial to provide a more complete picture, notably: (i) filling in the missing bins in the stellar mass and star formation rate plane; (ii) probing better the different evolutionary stages of early discs; and (iii) unveiling the nature of the compact dispersion-dominated objects. In the longer term, future near-infrared integral field spectroscopic surveys with KMOS at the VLT (Sharples et al., 2010) will substantially augment the current SINFONI seeing-limited samples by factors of  $\sim 10$  or more. AO diffraction-limited capabilities at the VLT will remain essential for integral field spectroscopic as well as imaging follow-up of individual galaxies for more detailed investigations.

### References

Daddi, E. et al. 2007, ApJ, 670, 156  
 Förster Schreiber, N. M. et al. 2009, ApJ, 706, 1364  
 Förster Schreiber, N. M. et al. 2011, ApJ, 739, 45  
 Genzel, R. et al. 2008, ApJ, 687, 59  
 Genzel, R. et al. 2011, ApJ, 733, 101  
 Lilly, S. J. et al. 2007, ApJS, 172, 70  
 Lilly, S. J. et al. 2008, The Messenger, 134, 35  
 Mancini, C. et al. 2011, ApJ, submitted  
 Shapiro, K. L. et al. 2008, ApJ, 682, 231  
 Shapiro, K. L. et al. 2009, ApJ, 701, 955  
 Sharples, R. M. et al. 2010, The Messenger, 139, 24  
 Tacconi, L. J. et al. 2010, Nature, 463, 78



Yuri Beletsky



Gundolf Witsching

Photographs showing the appearance of the ESO sites after recent precipitation in the north of Chile during the southern winter. Upper left, the Paranal landscape on 8 August 2011 following a light snowfall and upper right, the road to the VISTA dome on the same day. At Paranal in early July there was also bad weather with high winds and heavy rainfall, leading to some flooding; see Announcement ann11049 for more details. The snowfall at the 5000-metre Altiplano de Chajnantor in July was much heavier and the lower image shows the scene at APEX and, left, one of the excavators from the ALMA project clearing snow around APEX.





Stephan Gaiser



Gundolf Wisching

## Multiwavelength Views of the ISM in High-redshift Galaxies

held at ESO Vitacura, Santiago, Chile, 27–30 June 2011

Jeff Wagg<sup>1</sup>  
Carlos De Breuck<sup>1</sup>

<sup>1</sup> ESO

Our knowledge of the formation and evolution of distant galaxies continues to advance dramatically with the advent of new facilities at most observable wavelengths. One of the outstanding questions related to this field is: How do galaxies get their gas? Over the next decade, radio and submillimetre facilities like the Expanded Very Large Array and the Atacama Large Millimeter/submillimetre Array will probe the chemistry, kinematics and obscured star formation properties of the interstellar medium in galaxies at high redshift, allowing this question to be addressed. We report on a timely workshop on the roles of theory and multi-wavelength observing facilities in furthering our understanding of interstellar medium physics in distant galaxies.

### Introduction

Observational tracers of the gas and star formation activity in high-redshift galaxies can be probed across the entire electromagnetic spectrum. Large optical/infrared telescopes like the ESO Very Large Telescope (VLT) and the Keck telescope allow us to observe emission lines like Ly $\alpha$ , H $\alpha$  and Mg II, which generally trace star formation and active galactic nuclei (AGN) activity. Far-infrared (FIR) lines like [C II] at 158  $\mu$ m, the dominant cooling line in the interstellar medium (ISM) of galaxies, are now being surveyed in large samples of galaxies with Herschel, building on the pioneering work of the ISO satellite. These FIR lines are redshifted to the Atacama Large Millimeter/submillimetre Array (ALMA) bands for high-redshift galaxies, and with early ALMA science now about to begin, such observations will become routine. In the mm- and cm-wavelength regime, the redshifted emission lines of molecules like CO, HCN and HCO<sup>+</sup> trace the star-forming gas directly, and the lowest energy transitions of these molecules are observed with the Expanded Very Large

Array (EVLA) and the 100-metre Green Bank Telescope (GBT) for galaxies above redshifts of  $z > 1.4$ . Current observations of the observable properties of these objects are being modelled by high quality numerical simulations, which include hydrodynamics.

The goal of the workshop was to bring together members of the Chilean and international astronomy communities to discuss the current state of models and observations of the gas in galaxies. The meeting was attended by more than 80 participants, including 25 students from the Chilean and international communities (see Figure 1). With early ALMA science due to commence later this year, and the deadline for cycle 0 falling in the week of the workshop, prospects for future observations with this facility were discussed, although this was not the main driver for the meeting. The conference programme was divided into six topics, and here we summarise the results of each of them.

### Gas in nearby galaxies

The meeting began with excellent talks by A. Leroy and S. Martin, who described the molecular gas in nearby galaxies, which can be directly involved in fuelling star formation activity. Except for early-type galaxies, the CO molecule directly traces star formation, even though the ratio of star formation rate (SFR) to CO luminosity can vary in different galaxies. The conversion factor between cold molecular gas mass and CO line luminosity can also vary between galaxies of different types, depending on factors such as metallicity. From an overview of molecular line surveys in nearby galaxies, S. Martin described some of the diagnostic applications of a few of the 54 molecular line species that have been detected in nearby galaxies to date, and gave us a preview for what will be learned from similar surveys of high-redshift galaxies, now that broad bandwidth receivers are available on sensitive submillimetre/mm telescopes like ALMA.

### Simulations and predictions for high- $z$ ISM properties

In order to place the observed gas properties of high-redshift galaxies in the context of models of structure and galaxy formation, most of the Monday sessions focused on simulations and semi-analytic models of galaxy formation. Review talks were given by D. Narayanan and F. Bournaud, and we learned that many of the observed ISM properties of disc galaxies, as well as massive starburst galaxies, can be reproduced by hydrodynamic simulations. The submm continuum flux densities of starburst galaxies are reproduced by galaxies before and during major mergers. Major merger galaxies are detected in the large (10–20 arcseconds) single-dish beams as single submm sources. The observed CO line properties we observe in many classes of high-redshift galaxies, from the broad linewidths of quasar host galaxies during reionisation to the star-forming galaxies studied at  $z \sim 2$  are reproduced by the models. Predictions of semi-analytic models of large-scale galaxy formation have also shown the evolution of properties such as the global star formation rate and the molecular gas mass function (talk by C. Lagos); predictions that will soon be tested by large ALMA surveys of molecular CO line emission (contribution by J. Gonzalez).

The Monday session finished with a great overview of the current status of ALMA commissioning by A. Peck. At the time ALMA had 15 antennas on the high site, and is preparing to begin early science operations toward the end of 2011. This talk prompted a discussion on ALMA proposal preparation, which was useful for both students and astronomers without previous experience of proposing for mm-array observations.

### Outflows and star formation at high redshift

Tuesday morning began with an excellent invited talk by R. Somerville on star formation and feedback in cosmological simulations, where it was shown that observations of the gas content in high-redshift galaxies are needed to break



Figure 1. The conference participants braving the winter temperatures in front of the ALMA building in Vitacura, Santiago.

some of the degeneracies in the predictions of cosmological simulations. S. Ellison compared the importance of galaxy mergers vs. bars in triggering central star formation, and showed how bars experience enhanced star formation in galaxies with  $\log(M_{\text{star}}/M_{\odot}) > 10$ . Results of  $H\alpha$  imaging of star-forming galaxies was discussed by K. Menendez-Delmestre and E. Nelson, and it was shown that starburst galaxies selected at submm wavelengths have SFR surface densities similar to luminous infrared galaxies, even when they contain an AGN. M. Rodrigues discussed the evolution of the ISM in intermediate-mass galaxies.

#### Molecular gas properties of high-redshift galaxies

The Tuesday afternoon talks focused on the molecular gas content of high-redshift galaxies, with extensive invited overview talks provided by K. Coppin, D. Riechers and A. Weiss. Direct interferometric imaging of the cold molecular gas as traced by the lowest energy transitions of the CO line are now possible

using the EVLA and the Australia Telescope Compact Array (ATCA), and we saw how this has led to a wealth of new submm data on starburst galaxies, quasar host galaxies and BzK-selected star-forming galaxies at  $z \sim 1.5$  (talks by D. Riechers, H. Dannerbauer, M. Aravena, B. Emons and J. Hodge). It has been found that the submm starburst galaxies and radio galaxies display extended reservoirs of cold molecular gas, while quasar host galaxies do not. The excitation of this molecular gas was discussed by A. Weiss, who showed that multiple molecular gas components are needed to fit the CO line spectral energy distributions at high redshift, similar to what is seen in the inner disc of the Milky Way. Surveys of structure formation at high redshift are now becoming possible due to the wide bandwidth receivers available on facilities like the EVLA or the IRAM Plateau de Bure Interferometer; these surveys trace structure through molecular CO line emission (contributions by M. Aravena and J. Hodge).

The conference dinner on Tuesday night was held at the locally owned and operated restaurant, Dona Tina. The night was enjoyed by all who attended, and traditional Chilean cuisine was accompanied by live music.

#### Atomic gas properties of high-redshift galaxies

With ALMA about to begin early science observations, it is timely to discuss the FIR properties of nearby galaxies being studied by Herschel, as these lines will be redshifted to the ALMA bands at high-redshift. G. Stacey gave an invited talk on the diagnostic potential of ionised species of carbon, nitrogen and oxygen with transitions in the FIR, where extinction does not impact line intensities as it does at shorter wavelengths. All three species have now been detected at  $z > 1$ , mostly with the Redshift ( $z$ ) and Early Universe Spectrometer (ZEUS). Large surveys of high-redshift [CII] line emission, which is the dominant cooling line in the ISM of galaxies, are now being conducted by submm-wavelength facilities, and the “[CII] line deficit” to the line luminosity observed in ultraluminous IR galaxies (ULIRGs) is also seen in the FIR luminous galaxies observed so far (talks by G. Stacey, E. Sturm, C. De Breuck, S. Gallerani). In E. Sturm’s review we saw how many FIR lines are observable in gravitationally-lensed galaxies with Herschel, and how we are able to study the high- $J$  CO emission lines in starburst galaxies and AGN.

The 2-cm transition of atomic hydrogen can be studied in absorption out to  $z < 1.8$  (presentation by N. Gupta), and this has permitted studies of the cold molecular gas over cosmic time. Detecting this line in emission from high-redshift galaxies is challenging with current facilities due to its faintness, but large surveys are planned for low frequency arrays like the Australian Square Kilometer Array Pathfinder (ASKAP), Murchison Widefield Array (MWA) and the South African radio telescope array MeerKAT, which are considered to be pathfinders for the Square Kilometer Array (SKA). A. Baker showed how deep surveys with the MeerKAT will detect H I in galaxies beyond a redshift of one.

### Metallicity, and the dusty ISM in high-redshift galaxies

The metallicity in galaxies tells us about their complete star formation history. An invited talk by G. Cresci showed how collisionally excited emission lines and faint recombination lines can probe the gas phase metallicity in high-redshift galaxies, where the measurement of stellar metallicities is more challenging. The VLT AMAZE and LSD surveys are providing the first metallicity maps at  $z \sim 3$ , showing evidence for massive infall of metal-poor gas feeding the star formation (talk by P. Troncoso).

Even in advance of the huge increase in submm/mm continuum sensitivity provided by ALMA, strong gravitational lensing of high-redshift galaxies has led to the discovery of significant samples of mm-bright galaxies in surveys by the South Pole Telescope and Herschel; their gas properties can be studied in detail with existing instruments, as described by T. Greve. The dust properties of submm-selected galaxies was discussed in an invited talk by A. Pope, who showed how polycyclic aromatic hydrocarbon (PAH) emission at mid-infrared wavelengths can distinguish between AGN and starburst dominance of the short submm-wavelength continuum emission, which is also evident in new observations of the FIR continuum emission properties of galaxies observed



Figure 2. The participants on the ALMA tour visiting the assembly hall of the European ALMA antennas at the Operations Support Facility (OSF).

with Herschel. The highest redshift submm starburst galaxies have been studied in the COSMOS field, as described by V. Smolcic, and we now know of such objects out to  $z = 5.3$ . Deep ALMA surveys of the continuum emission in star-forming galaxies will soon allow us to study the obscured star formation in galaxies similar to the Milky Way out to very high redshifts (talk by E. da Cunha).

On the final morning of the workshop we heard from A. Updike on how gamma-ray bursts (GRBs) can be used to probe the dust in distant galaxies, where silicates may have been the dominant form of dust. G. Brammer presented the results of the NEWFIRM photometric survey of the AEGIS and COSMOS fields, and showed that the density of massive, quiescent galaxies has grown since  $z = 2$ . A. Smette presented a magnitude-dependent bias in the number density of damped Ly $\alpha$  emitters which may not be caused by dust along the line of sight.

### Conference Summary

Rather than the standard meeting summary, we opened the floor to questions from the large number of students present at the meeting. A very lively discussion ensued on the long-term future of ALMA.

### ALMA and APEX tour

As part of the meeting, 16 of the participants made use of the option to visit the ALMA and APEX facilities near San Pedro de Atacama. After an introduction by the ALMA director, Thijs de Graauw, the group went up to the 5000-metre-high Chajnantor plateau. In the ALMA Array Operations Site building, the participants received a guided visit of the ALMA correlator and the air-conditioning facilities. The harsh observing conditions at Chajnantor (temperatures of  $-15^\circ\text{C}$ ) became obvious during the regular maintenance of the APEX bolometer arrays which was coordinated with the visit. After a lunch offered at the ALMA Operations Support Facility at 2900 metres, a tour was organised of the European ALMA antenna contractors' camp, which allowed the visitors to get close to one of the dishes being assembled (see Figure 2). After a visit of the ALMA control room and laboratories, the meeting was formally closed with an amazing *asado* (barbecue) at the APEX base camp in Sequitor.

### Acknowledgements

We thank Maria Eugenia Gomez and Paulina Jiron, without whom this meeting could not have taken place. We also thank the ESO IT and Facilities teams for their great assistance. The help from ALMA and APEX and in particular William Garnier, Thijs de Graauw and David Rabanus, was vital to the success of the ALMA tour.

## In memoriam Alan Moorwood

Alan Moorwood died on 18 June 2011 at the age of 66 after a short illness. He had recently retired from ESO as Director of Programmes, having played a leading role in instrumentation for many years.

There follows an obituary by Tim de Zeeuw and a joint tribute by three of his long-time ESO colleagues, Bruno Leibundgut, Bob Fosbury and Sandro D'Odorico.

### Obituary

Tim de Zeeuw<sup>1</sup>

<sup>1</sup> ESO

Alan, born in May 1945, was educated in the United Kingdom. After a few years at ESA in Noordwijk, he joined ESO as Infrared Astronomer on 1 October 1978, when the Organisation was still based in Geneva and had about 40 staff members. In an exemplary career spanning more than three decades, Alan pioneered the development of infrared instrumentation for La Silla and co-authored the VLT instrumentation plan. He ultimately oversaw ESO's entire instrumentation effort, while at the same time maintaining a very active research programme resulting in nearly 400 publications, which made him one of ESO's most-cited astronomers. Alan's research centred on using infrared imaging and spectroscopy obtained with space observatories and ground-based telescopes to understand star formation in galaxies, including the study of molecular hydrogen in starburst galaxies, the physics of active galactic nuclei and ultra-luminous infrared galaxies, and observations of high-redshift galaxies.

Alan developed the infrared instrumentation programme at ESO that resulted in some of the first infrared instruments on European telescopes. IRAC on the MPG/ESO 2.2-metre telescope, SOFI on the NTT and ISAAC on the VLT were built under his leadership. In October 2003 he was appointed Head of the Instrumentation Division. Under his successful leadership the Division commissioned many instruments including VISIR, SINFONI, CRIRES, HAWK-I and X-shooter,



upgraded several others and strongly engaged on the second generation instruments KMOS, MUSE and SPHERE.

From 1 February 2008 until his retirement on 31 May 2010, Alan was Director of Programmes, providing leadership, setting programmatic priorities and carrying out resource planning for three Divisions (Telescope, Technology and Instrumentation). In this role he gave strategic guidance for the planning and implementation of the entire optical-infrared programme,

and crucially influenced the design effort for the E-ELT and its instrumentation.

Alan generously served the scientific community. He was one of the most valuable mission scientists for the Infrared Space Observatory, was a sought-after collaborator, and one of the driving figures behind the very successful series of international SPIE instrumentation conferences and organised a number of other conferences, including the influential October 2007 Workshop, entitled

Science with the VLT in the ELT era. Alan was a role model for combining a high level of contribution to the Organisation with an active and high-quality research programme. He supervised numerous students, many of whom have gone on to become well-known astronomers themselves. He was a founding member of the Senior Faculty at ESO, and held the first Emeritus Astronomer position in recognition of his tremendous achievements (see Primas et al., 2010).

Alan was a key contributor to ESO's rise to its current world-leading position in astronomy. He will be remembered as a person of the utmost dedication, commitment and professionalism. His somewhat shy but open and friendly personality, his encyclopaedic knowledge of ESO and its history and his legendary dry humour were widely appreciated.

In the past year Alan had clearly made a transition into his new role as Emeritus,

and looked forward to many more enjoyable years. It was not to be, but even so Alan's legacy continues to grow, with the second generation instruments on the VLT coming online, those for the E-ELT to follow in the next decade, and many people's lives positively influenced by him.

#### References

Primas, F., Casali, M. & Walsh, J. 2010, *The Messenger*, 141, 50

## Tribute

Bruno Leibundgut<sup>1</sup>  
Bob Fosbury<sup>1</sup>  
Sandro D'Odorico<sup>1</sup>

<sup>1</sup> ESO

With the death of Alan Moorwood, ESO has lost one of its most prominent astronomers. Alan became a master in the art of combining his love for research with his dedication to the task of building the best possible instruments. He remained an active scientist until the very end. Less than a month before his death he gave a talk at a conference about the latest results on high-redshift galaxies detected with one of "his" instruments, HAWK-I. He proudly showed the results obtained on  $z > 7$  galaxies ("the only ones with real spectroscopic redshifts," as he pointed out). Alan also presented this result at the Science Day in Garching this past February.

Alan was always fully convinced of the need for active participation in advanced research for the astronomers who had project responsibilities, particularly for those in instrument development. With more than 160 refereed papers over 40 years he had one of the highest H-indices of all ESO astronomers. He made seminal contributions to many topics in infrared astronomy. His career started with

the mapping of infrared sources, and the list of his interests grew to include the Earth's atmosphere, HII regions, star-forming regions, supernova remnants, active galactic nuclei, starburst galaxies, ultra-luminous infrared galaxies and the high-redshift Universe. One of his favourite objects was the Circinus galaxy, a Seyfert 2 galaxy undergoing a massive starburst at a distance of only 4 megaparsecs. This is one of the closest active galaxies to our Milky Way but, because it is only 4 degrees from the Galactic Plane, it is heavily obscured and so best observed in the infrared.

In an undergraduate thesis at University College London (UCL), supervised by Mike Seaton, Alan predicted the flux expected to be emitted in the [CII] 158-micron fine-structure line from star-forming regions in the Galaxy. This was a topic that was to span his entire career, but only reach full maturity with the advent of Herschel, an ESA space mission in which Alan played an important role both before and after his retirement.

Alan started his career as an instrument builder/user as a student at UCL. He participated in balloon-borne experiments to measure far-infrared emission in the pioneering days where the payloads did not always follow a predictable trajectory. He then moved to ESTEC where, working for ESA, he perhaps felt that instruments

might enjoy a longer life expectancy. Eventually planting his feet firmly on the ground by joining ESO when it was based at CERN in Geneva, his career was set to see that Europe played a key role in the transformation of infrared astronomy, as ESO advanced to become the foremost astronomical observatory on the planet.

At the age of 34, Alan co-authored a major review article with John Beckman on infrared astronomy (Beckman & Moorwood, 1979), which summarised the state of this emerging field at the end of the 1970s. As they pointed out, infrared astronomy had then been evolving for a little more than a decade, but held great promise for "instruments outside the Earth's atmosphere". Consequently, Alan became strongly involved with ESA's Infrared Space Observatory (ISO).

Two years ago Alan presented some personal recollections of the ESO infrared instrumentation programme in a *Messenger* article (Moorwood, 2009). In his typical style he described the situation at ESO when he started as "[a]lmost state of the art". The development of infrared astronomy has been truly phenomenal. In Alan's words: "[T]he first infrared instruments offered by ESO had one pixel at the focus of a 1-metre telescope with an effective resolution of a few arcseconds." By now infrared instruments which "provide resolutions down

to the diffraction limit of an 8-metre telescope” and infrared cameras with “16 million pixels and a resolution of  $\sim 0.1$  arc-seconds over a field of  $7.5 \times 7.5$  arc-minutes<sup>2</sup>” have been deployed. Alan led this development over 30 years. He also mused in his article how the process of designing and building astronomical instruments has changed over the years: “It turned out we actually had to write down the specifications to remember them, use advanced design and failure mode and effects analysis software, have project plans and meetings and even reviews to check where we were.”

To the consternation of many of his colleagues and friends, even some of the native-English speakers, Alan would use his exquisitely-developed sense of irony

to make points with great effect. He could do this equally to cut through verbal obfuscation and reveal the naked truth or to light-heartedly diffuse a conflict. His aptitude for recalling past history and even the details of conversations was quite stunning and sometimes intimidating. He would recall one of your statements from years ago in order to reinforce a current point while you would struggle to remember that the conversation took place.

There are many more contributions that Alan made to ESO and its staff. He represented the ESO instrumentation programme in front of countless internal and external committees, always exhibiting a depth of knowledge and judgment that awed his audience. In front of bodies

such as the Scientific and Technical Committee and the ESO Council he was a convincing advocate of the need to keep part of the instrumentation development in house in order to serve as a link between the ESO community at large and the Observatories. As one of the key drivers of instrumentation at ESO, Alan was living proof that functional work and research can be successfully reconciled. Alan’s advice was sought by many people at ESO and he responded willingly and generously, particularly to those who posed well thought-out questions!

#### References

- Beckman, J. E. & Moorwood, A. F. M. 1979, Rev. Prog. Phys., 42, 87  
Moorwood, A. F. M. 2009, The Messenger, 136, 8

## In memoriam Carlo Izzo

Tim de Zeeuw<sup>1</sup>  
Michèle Péron<sup>1</sup>

<sup>1</sup> ESO

Carlo Izzo, a software engineer at ESO, died on 23 June 2011, at the age of 51 after fighting courageously a short illness.

Carlo, born in October 1958, was educated in Italy at the University of Padua where he studied astronomy. He started his career at ESA, Darmstadt in 1985 where he was involved in software development for the operation of the payload of the EXOSAT satellite. Following this he joined the Max-Planck Institute for Extraterrestrial Physics (MPE) in Garching on a Fellowship and then went on to be a software developer for X-ray astronomical data analysis within the MIDAS environment. He joined ESO in 1999 as a Scientific Applications Developer, where he

was involved in the development of the FORS and VIMOS pipelines. Later he became a main developer of the Common Pipeline Library and he was the ESO responsible for the KMOS pipeline.

Carlo was highly respected by his colleagues and customers for his expertise as an engineer and his strong astronomical background. Carlo was known for bringing innovative contributions to a wide range of projects including new pattern-matching methods for the FORS and VIMOS pipelines, scientific workflow and modular designs for multi-object spectroscopy, and science-grade improvements for the FORS Accurate Photometry project. He was dedicated, passionate and enthusiastic, and always had a positive approach to his work. He was excellent in communicating his enthusiasm to his peers and was a pleasure to work with. He will be remembered as a brilliant friend and colleague with a great sense of humour.



## New Staff at ESO

### Dimitri Mawet

I arrived from California with my wife Jessica and our cat Ishi on 1 April 2011 (not a joke!) to fill a position as VLT operations staff astronomer on UT4-Yepun, which hosts two adaptively-corrected instruments (NAOS–CONICA and SINFONI) and the wide-field camera HAWK-I. As an exoplanet hunter, coronagraphist and adaptive optics/wavefront control aficionado, my medium-term goal at ESO is to ensure a smooth “Paranalization” and subsequent operation of SPHERE, one of VLT’s second generation instruments. SPHERE is an extreme adaptive optics system feeding a suite of three instruments almost entirely dedicated to imaging and characterisation of extrasolar planetary systems. SPHERE is one of the most ambitious and complex facilities to arrive at the VLT, and so presents an extremely exciting challenge. SPHERE is filled with amazing technologies and has a science case aimed at answering some of the most fundamental questions confronting human kind!

My passion for science and technology and in particular for everything related to outer space, dates back to my childhood. My parents offered me my first astronomy book when I was aged five. I obviously couldn’t read then, but these were unique bedtime stories! I remember feeling totally overwhelmed by the amazing photos of the giant planets that had just been taken by the NASA *Voyager* and *Pioneer* probes, and fascinated by the (then) brand new Space Shuttle, to me the most beautiful spacecraft ever made. It was more than enough to imprint my subconscious for the rest of my life. Later on at school, I fell in love with science and mathematics, but astronomy or space science still seemed far away. I remember the pragmatism of some of my old and respectable high school teachers, who argued that astronomy would be a suicidal career choice (!). Guided by this, I therefore enrolled into engineering at the University of Liege. When I took my first proper astronomy course a couple years later, I was far from imagining that I would do a PhD and that the dynamic lecturer Professor Jean Surdej would be my future thesis advisor!

The fifth and last year of the engineer–physicist course required an original pro-

ject. One of the proposed subjects was the “four-quadrant phase-mask coronagraph (FQPM)”. The FQPM, invented in 2000 by Daniel Rouan, is one out of many different types of coronagraphs using the wave nature of light to perform its contrast-enhancing role, as opposed to Lyot-type coronagraphs which simply block the light. After being set on the track of FQPM with a sample of new ideas to explore, I was almost given *carte blanche* — definitely the kind of challenge and freedom that would get my 100% focus! In fact, this subject and its ramifications would keep me busy for the next ten years, PhD thesis included. In particular, I would invent my own coronagraph, and even give it the very esoteric name: the “vector vortex coronagraph”.

My first research years at the Institut d’Astrophysique et de Geophysique de Liege were fantastic, I studied and worked with amazing people and the company of many colleagues from the department of physics, and the Centre Spatial de Liege (CSL) where I met my wife Jessica. Thanks to a Marie Curie fellowship, I also spent a great deal of time in Paris, first at the Observatoire de Paris–Meudon, working with the FQPM team. There, I contributed to the development of the FQPM technology for various instruments: VLT–NACO, JWST–MIRI, and for SPHERE, which I consider one of my major contributions! I also spent half a year at the Institut d’Astrophysique Spatiale in Orsay working with Alain Leger and his team on nulling interferometry for Darwin/TFP-I, and on the very interesting subject of Ocean Planets.

So I fell early into the exoplanet science and technology cauldron. While technology has always fascinated me, it became clear very soon that it would be very hard to compete on the astronomy faculty job market with a profile as a pure technologist. Doubly motivated, I then worked very hard to take my technological inventions to telescopes in order to do unique science. But it took many years — a NASA postdoc followed by a permanent position at the Jet Propulsion Laboratory (JPL) at the California Institute of Technology — to do just that. The culmination of this effort, which involved many people, was the imaging of the extrasolar giant planets around HR8799 with a small 1.5-metre



Dimitri Mawet

portion of the 5.1-metre (200 inch) Palomar Hale telescope, using the coronagraph I invented; this involved the first on-sky tests of an extreme adaptive optics system and related high contrast imaging techniques. In parallel to these technical accomplishments, I started to get serious about observing programmes: my co-Is and I initiated extensive exoplanet hunt programmes using high contrast imaging at Palomar, Keck, VLT and Gemini. Our strategy has been to maximise the synergy between space and ground-based platforms: we use the output of survey missions such as Spitzer and WISE to form unique samples of identified extrasolar systems for ground-based follow-up.

At JPL-Caltech, I had the opportunity early in my career to be surrounded by prestigious colleagues from whom I learned a lot. I deeply enjoyed my 3.5-year stay at JPL. It was quite amazing to work at the very place that built the probes that took the fantastic images that had inspired me as a kid 25 years before! My wife and I totally blended in as Californians. But US budgets allocated to exoplanet research and in particular to the NASA Terrestrial Planet Finder (TPF) programme have been crumbling and so I started to look towards Europe and especially to ESO, which I still followed closely through my research and numerous contacts (I have been a user of the VLT for many years). So here I am, ready to close the loop with SPHERE, to which I first contributed almost ten years ago.

## Fellows at ESO

### Sergio Martin

I was born in Madrid, where the flag of the region consists of a plain crimson red background containing seven white stars representing the stars in the constellation of Ursa Minor (the Little Dipper). Even the flag of the city of Madrid shows the city's coat of arms where the seven stars of the constellation of Ursa Major (the Big Dipper) are depicted. Beautiful as it may seem, it may now be difficult to find someone who remembers the last time these stars could be clearly seen from the city, due to the light pollution related to modern living. It is thus difficult to understand how I chose to become an astronomer from such a star-deprived city! Actually I cannot remember the time when I took such a decision. At some point during high school I became intrigued by physics, and once I got to university I just knew that astronomy was the only way ahead for me. Perhaps my spending most of my childhood summers in a small town in one of the darkest spots in Spain, with an overwhelmingly star-crowded night sky, had something to do with my decision.

So there I was on my way to an astronomy career. After my degree in physics, I spent one year at the Observatorio Astronómico Nacional, where I first got in touch with the experience of real research. It was during this time that I observed with a professional telescope for the first time. That was the 30-metre radio telescope located at an altitude of almost 3000 metres on top of the Sierra Nevada, near Granada in southern Spain. This telescope was, and still is, the most powerful single dish telescope operating at millimetre wavelengths, and I was there using it for my own research project! I clearly remember the first time that I was allowed to access the computer controlling the telescope and how I ran outside the building to see how that massive antenna started to move under my first observing command. I was observing, and I loved it!

I was then given the opportunity to move to Granada, one of the most beautiful cities in the south of Spain, to start my PhD at the Instituto de Radioastronomía

Milimétrica (IRAM), an international research institute for radio astronomy that maintains the 30-metre telescope in Spain and the Plateau de Bure interferometer in the French Alps. I spent four years in Granada where, apart from carrying out my PhD research, I had to spend about a week per month as astronomer on duty at the observatory. There I helped visiting astronomers with their observations which allowed me to meet lots of people coming from institutes around the world and with a wide variety of science interests. Even though tiring at times, doing my PhD at an observatory was a great experience. On top of a great observing experience, I could also enjoy gorgeous mountain sunsets.

The main topic of my PhD was the study of the detailed chemical composition of the interstellar medium in the central region of galaxies. My aim was to understand whether the physical processes in these regions can be traced by measuring the abundances of different molecules. There are currently more than 50 molecules detected outside our Galaxy. If we manage to understand the origin of these molecules we can decipher valuable information about the regions where they formed.

My PhD years were over and it was time to move on. A couple of weeks after I defended my thesis I moved to the Harvard-Smithsonian Center for Astrophysics (CfA) in Cambridge (Massachusetts, USA), close to the lively city of Boston. The scientific life at the CfA, one of the biggest astronomy hot-spots in the world, was a whole new story compared with my previous experience. Hundreds of astronomers working on every field of astronomy resulted in dozens of science talks every week. Within the CfA, I joined the Sub-Millimeter Array (SMA) as a fellow. The SMA was the first interferometer operating at submillimetre wavelengths. The SMA interferometer combines the signal from eight 6-metre antennas to achieve high resolution astronomical images. Though located at an altitude of 4000 metres on top of Mauna Kea in Hawaii, we remotely controlled the array from Cambridge for the second half of the nightly observations.



Sergio Martin

Luckily, I had the opportunity of helping with the observations on site a few times a year. I have always felt the need to work close to the instrumentation and see this as key to keeping up with the daily operations. On top of that, I always tried to compensate a few days of intense night observation at high altitude with some time off in the amazing Hawaiian islands. During this time I extended my molecular studies to the very central region of our own Galaxy, where I studied how the molecular gas is affected by the harsh conditions around the central supermassive black hole. Even taking into account the extreme weather conditions of the US east coast, the time in Cambridge was scientifically and personally enriching.

But again, as part of this migrating job it was time to move on and I received the offer to work at ESO in Santiago, where I joined as an ALMA fellow. This was the opportunity to take part in the commissioning of the largest astronomy project ever undertaken on earth, the Atacama Large Millimeter/Submillimeter Array. At an altitude of 5000 metres in the middle of the Atacama desert, one of the driest

places in the world, hundreds of people are working hard to put together 64 large antennas working together as a unique and overwhelming instrument. Once ALMA is in operation, starting at the end of this year, we will be able to get a glimpse of the most distant galaxies formed in the early times of the Universe down to the planets forming around nearby stars. Being here in Chile during these exciting times, when ALMA is starting to peer into the Universe, is an extremely rewarding experience. We are indeed on the verge of the next revolution in astronomy and, as part of a worldwide astronomical community, I am keen to see what this amazing instrument will teach us about the origin of the Universe and the emergence of life.

It is actually difficult to figure out what will be the next step in my astronomy career: what one has to make sure is to enjoy every single step of the way.

#### Joana Ascenso

“Gastronomy, how very interesting!”  
“I agree, but I am actually an astronomer.”

It turns out that the idea of an astronomer evokes all sort of images, including those of the wacky astrologer, of the weatherperson, or even of a chef for the more distracted, and it takes some explaining to convince people that an astronomer is just “a scientist”. Describing what a scientist actually does, that takes another session altogether. In my case it’s relatively easy: I study how stars form.

It’s hard to identify a single event that led me to astronomy. Having grown up in Coimbra, Portugal where the sky was dark but not particularly spectacular, I cannot say it was the view from my window that decided my career. Maybe the rich tales of the stars from my grandparent’s village first made me realise that the Universe was not just stickers in the night sky, and I’m pretty sure that the big, heavy encyclopedia of the Universe in the living room had something to do with it too, since it was already missing a

piece of the spine from being opened too many times when I was still a teenager. The affinity for science must have done the rest, because when time came to choose a university degree, astronomy already sounded like the most interesting option. I did my undergraduate studies in mathematics, physics and astronomy at the University of Porto, during which time I also guided tours of the local planetarium, a very fulfilling experience that taught me the importance of communicating science. It’s remarkable how amazed people can be about even the simplest things in the Universe, especially the adults. Small children find it all normal, probably like learning that there are other cities besides their own, and I am sure I was more amazed by their replies than they were by my astronomical facts.

I continued in Porto for my Master’s thesis on the spectral properties of young T Tauri stars, after which I started my PhD. I had two thesis supervisors, who inspired me greatly: Teresa Lago in Porto, and João Alves, first at ESO in Garching, and then Granada, which meant I spent my time between these three cities. The experience of living abroad and working in different institutes (Centro de Astrofísica da Universidade do Porto [CAUP], ESO and Instituto de Astrofísica de Andalucía [IAA]), all of which have excellent conditions but somewhat different work cultures, widened my perspective of science and impressed me beyond expectation.

My PhD thesis was about young massive star clusters still embedded in their natal clouds. I went about it from the observational perspective, which provided me with one of the best experiences I’ve ever had: to observe with a “real” telescope. To see the near-infrared images of my first cluster taken at ESO’s La Silla Observatory in Chile with the dark desert as background was exhilarating. Those were images no one had ever seen before, and they were mine for the taking. They proved to be as scientifically relevant as beautiful, and I spent the following four years observing more clusters at the ESO telescopes, and studying their properties, namely mass function and morphology, and whether it was possible



Joana Ascenso

to actually detect and measure spatial segregation of stars of different masses in massive clusters.

My first post-doctoral fellowship took me to the Harvard-Smithsonian Center for Astrophysics in Cambridge, to work on Spitzer data of the Pipe Nebula, a nearby dark cloud. I ended up learning more about linear regression than I had ever intended, in a successful attempt to prove that the extinction law toward high-density cores was different from that of the low-density interstellar medium due to grain growth. This project, as well as the analysis of more data on some of the clusters I had studied in my PhD, was prolonged through my next postdoctoral position, back in Porto.

I am now back at ESO, eleven months into my fellowship, and enjoying every bit of it. Apart from doing science, I also work on the E-ELT (European Extremely Large Telescope) project assessing science goals, conditions for the use of different instruments, and whatever is necessary to help get the telescope going. The contact with other fellows, the varied and plentiful seminars and talks, and the proximity to the core of the observatory makes ESO a unique place for a post-doc.

## Personnel Movements

### Arrivals (1 July–31 September 2011)

#### Europe

Neumayer, Nadine (DE)	User Support Astronomer
Llopis, Elena (ES)	Internal Auditor
Pfrommer, Thomas (DE)	Laser Engineer
Krumpe, Mirko (DE)	Fellow
Galvan-Madrid, Roberto (MX)	Fellow
Tremblay, Grant (US)	Fellow
Pedretti, Ettore (IT)	Instrument Scientist
Wylezalek, Dominika (DE)	Student
Manara, Carlo Felice Maria (IT)	Student

#### Chile

Phillips, Neil Matthew (GB)	Test Scientist
Schuller, Frédéric (FR)	Operations Astronomer
Carlier, Arnaud (FR)	Head Of Engineering Department
Parra, Jose (CL)	Deputy Data Manager
Nakos, Theodoros (GR)	Test Scientist
Pizarro, Leonel (CL)	Administrative Clerk
Vera, Sergio (CL)	Telescope Instruments Operator
Mehner, Andrea (DE)	Fellow

### Departures (1 July–31 September 2011)

#### Europe

Schwarz, Joseph (US)	Software Manager
Sforna, Diego (IT)	Software Engineer
van Belle, Gerard (US)	Instrument Scientist
Correia Nunes, Paulo (PT)	Software Engineer
Eglitis, Paul (GB)	Head of Archive Department
Fox, Andrew (GB)	Fellow
Venemans, Bram (NL)	Fellow
Teixeira, Paula Stella (PT)	Fellow
Klaassen, Pamela (NL)	Fellow
Béchet, Clémentine (FR)	Optical Engineer
Nunez Santelices, Carolina Andrea (CL)	Student
Ricci, Luca (IT)	Student
Van Der Swaelmen, Mathieu (FR)	Student
Motalebi, Fatemeh (IR)	Student



The Spanish Minister for Science and Innovation, Cristina Garmendia Mendizábal visited Paranal on 1–2 August 2011. Minister Garmendia (third from left in the photograph) was accompanied by Carlos Martínez Riera, Director General for International Cooperation at the Ministry for Science and Innovation (MICINN), Xavier Barcons, Spanish delegate and Vice-president of the ESO Council, and Juan Manuel Cabrera, Spanish Ambassador in Chile. The

group was hosted at Paranal by the ESO Director General, Tim de Zeeuw, the ESO Representative in Chile, Massimo Tarengi, and the Director of Operations, Andreas Kaufer.

The minister visited the VLT control room and took part in the start of observations from the console of one of the VLT Unit Telescopes. The following day, the group traveled through the Atacama Desert to

ALMA, the Atacama Large Millimeter/submillimeter Array. Minister Garmendia visited the Operations Support Facility (OSF), where ALMA antennas are being assembled and tested, and then she continued to the 5000-metre-high plateau of Chajnantor to see the ALMA antennas that have been installed so far at the ALMA Operations Site. See Announcement ann11050 for more details.

ESO, the European Southern Observatory, is the foremost intergovernmental astronomy organisation in Europe. It is supported by 15 countries: Austria, Belgium, Brazil, the Czech Republic, Denmark, France, Finland, Germany, Italy, the Netherlands, Portugal, Spain, Sweden, Switzerland and the United Kingdom. ESO's programme is focused on the design, construction and operation of powerful ground-based observing facilities. ESO operates three observatories in Chile: at La Silla, at Paranal, site of the Very Large Telescope, and at Llano de Chajnantor. ESO is the European partner in the Atacama Large Millimeter/submillimeter Array (ALMA) under construction at Chajnantor. Currently ESO is engaged in the design of the European Extremely Large Telescope.

The Messenger is published, in hard-copy and electronic form, four times a year: in March, June, September and December. ESO produces and distributes a wide variety of media connected to its activities. For further information, including postal subscription to The Messenger, contact the ESO education and Public Outreach Department at the following address:

ESO Headquarters  
Karl-Schwarzschild-Straße 2  
85748 Garching bei München  
Germany  
Phone +49 89 320 06-0  
information@eso.org

The Messenger:  
Editor: Jeremy R. Walsh;  
Design: Jutta Boxheimer; Layout,  
Typesetting: Mafalda Martins;  
Graphics: Roberto Duque.  
www.eso.org/messenger/

Printed by Mediengruppe UNIVERSAL  
Grafische Betriebe München GmbH  
Kirschstraße 16, 80999 München  
Germany

Unless otherwise indicated, all images in The Messenger are courtesy of ESO, except authored contributions which are courtesy of the respective authors.

© ESO 2011  
ISSN 0722-6691

## Contents

### Telescopes and Instrumentation

E. Jehin et al. – TRAPPIST: TRAnsiting Planets and Planetesimals Small Telescope	2
M. Wittkowski et al. – CalVin 3 — A New Release of the ESO Calibrator Selection Tool for the VLT Interferometer	7
S. Ramsay et al. – A New Massively-multiplexed Spectrograph for ESO	10
M. Cirasuolo et al. – MOONS: The Multi-Object Optical and Near-infrared Spectrograph	11
R. de Jong – 4MOST — 4-metre Multi-Object Spectroscopic Telescope	14
L. Testi, M. Zwaan – ALMA Status and Science Verification Data	17

### Astronomical Science

E. Lelouch et al. – The Tenuous Atmospheres of Pluto and Triton Explored by CRIRES on the VLT	20
M. Wittkowski et al. – Molecular and Dusty Layers of Asymptotic Giant Branch Stars Studied with the VLT Interferometer	24
M. Petr-Gotzens et al. – Science Results from the VISTA Survey of the Orion Star-forming Region	29
C. Evans et al. – The VLT FLAMES Tarantula Survey	33
N. Förster Schreiber et al. – The SINS and zC-SINF Surveys: The Growth of Massive Galaxies at $z \sim 2$ through Detailed Kinematics and Star Formation with SINFONI	39

### Astronomical News

J. Wagg, C. De Breuck – Report on the Workshop “Multiwavelength Views of the ISM in High-redshift Galaxies”	46
T. de Zeeuw and B. Leibundgut et al. – In memoriam Alan Moorwood	49
T. de Zeeuw, M. Péron – In memoriam Carlo Izzo	51
New Staff at ESO	52
Fellows at ESO	53
Personnel Movements	55

Front cover: The first released image from the VLT Survey Telescope (VST) showing the Galactic H II region and star-forming complex M17 (NGC 6618), the Omega Nebula. The large area colour composite (pixel size 0.21 arcsecond) was formed from images taken with the 268 megapixel camera OmegaCam in the SDSS photometric system  $g$ ,  $r$  and  $i$  filters; an area 39 by 55 arcminutes is shown. The data were processed using the Astro-WISE software. See Release eso1119 for details. Credit: ESO/INAF-VST/OmegaCAM. Acknowledgement: OmegaGen/Astro-WISE/Kapteyn Institute